Characterizing multifaceted role of HtrA2 as a quality control protein

By

Ajay Rambhau Wagh
[LIFE09201304010]

Tata Memorial Centre (TMC),
Advanced Centre for Treatment, Research and Education in Cancer (ACTREC),
Kharghar, Navi Mumbai – 410210.

A thesis submitted to the
Board of Studies in Life Sciences
In partial fulfillment of requirements

For the Degree of

DOCTOR OF PHILOSOPHY

Of

HOMI BHABHA NATIONAL INSTITUTE

November 2019

STATEMENT BY AUTHOR

This dissertation has been submitted in partial fulfillment of requirements for an advanced degree at Homi Bhabha National Institute (HBNI) and is deposited in the Library to be made available to borrowers under rules of the HBNI.

Brief quotations from this dissertation are allowable without special permission, provided that accurate acknowledgement of source is made. Requests for permission for extended quotation from or reproduction of this manuscript in whole or in part may be granted by the Competent Authority of HBNI when in his or her judgment the proposed use of the material is in the interests of scholarship. In all other instances, however, permission must be obtained from the author.

Date: 26th June 2019

Place: Navi Mumbai

Ajay Rambhau Wagh

DECLARATION

I, hereby declare that the investigation presented in the thesis has been carried out by me. The work is original and has not been submitted earlier as a whole or in part for a degree / diploma at this or any other Institution / University.

Ajay Rambhau Wagh

List of Publications arising from the thesis

Journal:

- 1. Ajay R. Wagh & Kakoli Bose. "**Structural Basis of Inactivation of Human Counterpart of Mouse Motor Neuron Degeneration 2 Mutant in Serine Protease HtrA2**" Bioscience Reports. 2018 Aug 1. DOI: 10.1042/BSR20181072

Book/Book Chapter:

a. Ajay R. Wagh & Kakoli Bose. **"Emerging Roles of Mitochondrial Serine Protease HtrA2 in Neurodegeneration"** 2017, (Springer) DOI: 10.1007/978-981-10-2513-6_15

b. Ajay R. Wagh & Kakoli Bose. **"Apoptosis in cancer cell signaling and current therapeutic possibilities"** 2019, (Springer) DOI: 10.100/978-981-32-9816-3_5

Conference/Symposium

Poster Presentations:

- International conference on "***New Advances in X-ray Diffraction and Cryo - Electron Microscopy***" held in New Delhi 15-17 December 2014
- ***13th Asian Crystallographic Association Conference*** (AsCA) held in Kolkata, 5-8 December 2015
- ***31st Protein Society Meeting*** held in Montreal, Canada on 24th-27th July 2017in Enzymology
- ***Indo-US conference on Advances in Enzymology: Implications in Health, Disease and Therapeutics*** held at TMC-ACTREC on 15th- 19th January 2017

- ***Annual meeting of Society of Biological Chemists (I)*** – Mumbai held on 13th October 2018 at Institute of Chemical Technology, Mumbai
- ***Indo-US Conference on Sculpting the Future of Medicine-Gateway to Post Proteogenenomic Era*** held at TMC-ACTREC on 8th – 11th December 2018 (**Best Poster award**)
- ***7th Annual MPAI Conference*** **"***Precision Medicine is closer than you think"* held from 12th -13th January 2019, at ACTREC, Tata Memorial Centre, NaviMumbai.

Participation:

- ***TMC-Platinum Jubilee Conference "Healthcare: A commodity or Basic Human Need?"*** held at TIFR, Mumbai 27th – 29th January 2017

Date: 26th June 2019

Place: Navi Mumbai

Ajay Rambhau Wagh

Dedicated to my beloved parents

ACKNOWLEDGEMENTS

The completion of this work has dependent on a lot of people, and it could not have been completed without their constant support. First, I would like to acknowledge my advisor and mentor, Dr. Kakoli Bose, whose encouragement and ideas helped me complete the present work. These past six years in her laboratory have been a great experience and have prepared me for a bright future in this field. I am thankful for her patience and effort to help me become a better scientist. I have learned a lot from her, not only on the bench doing experiments, but also as a better presenter, lecturer, writer, thinker, and an all-rounder person. For all of this I thank her greatly.

The members of my doctoral committee have also been imperative in the completion of my work: Dr. S.V. Chiplunkar, Dr. Tanuja Teni, Dr. Dibyendu Bhattacharya and Dr. Prasenjit Bhaumik. I really appreciate their time, help and advice to guide me. I am grateful to former Directors' of ACTREC, Dr. Rajiv. Sarin and Dr. S.V. Chiplunkar and present Director Dr. Sudeep Gupta, Deputy Director Dr. Prasanna Venkatraman for providing research facility and excellent infrastructure. I am very grateful towards the Sam-Mistry, HBNI international travel fund and Biochemical Journal, Portland press UK for supporting me for my international conference visits during my PhD tenure. I also acknowledge CSIR for providing me the fellowship.

It was nice to have batch mates like Shalini, Asmita, Pravin, Shalaka, Ramchandra, Rajashree, Dhanashree, Burhan, Raikamal, Raghava, Mahalakshmi, Mythreyi, Raghupathi, Anuja, Vasudha and Rahul. Each one of them has made the life in ACTREC very lively and pleasant throughout my stay. I would reserve my heartiest thanks to a very special person of my life, Shalini, for being my pillar of strength through thick and thin and loving me for who I am.

It was an overall learning experience along with fun in Bose Lab. I would like to express my heartiest thanks to all the Bose lab family members especially my seniors Late Dr. Lalith Kumar

Chaganti, Dr. Nitu Singh, Dr. Raja Reddy Kuppili and Saujanya Acharya for their constant guidance, teaching and support which turned out to be very fruitful for my research tenure. Not only I learned many experiments from them in lab but also has acquired good ethics and lab practice as well. I am also thankful to other lab members, Mr. Padale ji, Ms. Snehal both being important helping hands in the lab and I am also thankful to Raghupathi, Aasna, Rashmi, Rucha, Sucheta, Shubham and other research fellows such as Mriganka, Jitesh and Shubhankar who helped me in innumerable ways during the entire period. I thank them all from bottom of my heart for their unconditional love and support. I am also immensely thankful to all trainees Anuradha, Amish, Apoorva, Bidya and Ankita who have worked with me sincerely without any complains.

I express my gratitude to the institute: Advanced Centre for Treatment, Research and Education in Cancer for providing common instrument facility, Macromolecular Crystallography and X-Ray Diffraction Facility, BTIS, library, IT, administration, accounts department and Students council of ACTREC for their constant help and support.

I will also cherish my stay during my PhD spent with my wonderful roommates Ajit, Kedar, Pravin, Sajad and Shubham making me feel, 'hostel room as home'. I am blessed with a friend circle outside ACTREC. I thank all of them for all their moral support and encouragement throughout this journey. Manish, Rajvi and Dr. Senthil need a special mention here for their unconditional support both morally and scientifically.

My appreciations are also to every other person who helped me directly or indirectly in this project.

I owe a lot more than I can express in words to my family; I say thanks and sorry to them for not taking their responsibility in these past years as a son in my selfish pursuit to finish Ph.D. I have no word that can suffice for their constant sacrifices in making my life beautiful and easy. I

immensely thank my elder brother (Vinay) and sisters (Asha and Varsha) for taking over my responsibilities during this period and who never made me feel guilty about anything. I know that I have reached so far only because you all believed in me. You all have been my source of strength and inspiration throughout my life. It would have been impossible to reach here without the support, love and affection of my family, this all what I have achieved is the outcome of seeds sown by clear thoughts of my parents and now I take it as my responsibility towards my nation and my family to get fruits out of this hard work.

Thank you all for your contributions.

And last but not the least, I thank Almighty God for everything ("Jay Shree Gajanan").

Ajay Rambhau Wagh

CONTENTS

Synopsis

Homi Bhabha National Institute

SYNOPSIS OF Ph. D. THESIS

1. **Name of the Student:** Ajay Rambhau Wagh
2. **Name of the Constituent Institution:** Tata Memorial Centre, ACTREC
3. **Enrolment No. and Date of Enrolment:** LIFE09201304010; 1st September 2013
4. **Title of the Thesis:** Characterizing multifaceted role of HtrA2 as a quality control protein
5. **Board of Studies:** Life Science

SYNOPSIS

Characterizing multifaceted role of HtrA2 as a quality control protein

Introduction:

The HtrA (High temperature requirement protease A) proteins belong to a unique family of oligomeric serine proteases that are conserved from prokaryotes to humans (1). The Human HTRA2 gene, consisting of eight exons, is localized at 2p13.1, and codes for a 50 kDa polypeptide of 458 amino acid residues. The full-length protein contains a mitochondrial targeting sequence (MTS) at its N-terminal end, a transmembrane domain (TM), the inhibitor of apoptosis protein (IAP)-binding motif (IBM), serine protease domain with dedicated catalytic triad Histidine (His198), Aspartic acid (Asp228) and Serine (Ser306), and one PDZ domain at the C-terminus. Following the translocation to mitochondria, HtrA2 undergoes maturation post processing at Ala133 that leads to removal of MTS and TM (Δ133) with concomitant exposure of the N-terminal IBM motif. The mature protein is primarily located in the inter membrane space of mitochondria. HtrA2 consists of 7 α-helices and 19 β-strands, which together form well-defined domains along with several functionally important loop structures (*1*). Amongst these loops, the active site serine residue (S306) resides in Loop 1 (L1; 302-306), while Loop 3 (L3; 275-285) harbors the mnd2 mutation.

A number of studies have shown that under normal physiological conditions, HtrA2 promotes cell survival by the maintenance of mitochondrial homeostasis implicating its role as a protein quality control factor in mitochondria. According to reports, disruption of this function of HtrA2 is associated with several neurodegenerative disorders including Alzheimer's and Parkinson's.

A first link between HtrA2 and neurodegeneration has been founded by the identification of its interaction with presenilin-1 protein in yeast two-hybrid assays. Mutations in presenilin-1 are

responsible for inherited forms of early onset Alzheimer's disease (AD). Further support for a possible role of HtrA2 in neurodegeneration was provided by the interaction between HtrA2 and AD-associated amyloid β.

First insight into the *in vivo* effects of HtrA2 dysfunction came from the characterization of motor neuron degeneration-2 (mnd-2) mutant mice in which a homozygous loss of function mutation (S276C) in the HtrA2 protein was identified in mnd2 mice leading to neurodegeneration, muscle wasting and early death (40 days) (13). Motor neuron degeneration 2 has been identified in the early nineties as a spontaneous mutation that is recessively inherited and exhibits altered gait, ataxia and slow muscle wasting. These mice show loss of a population of striatal neurons (11) suggesting possible failure of a protective mechanism and providing circumstantial evidence that the protease activity of HtrA2 might have a function in protein quality control akin to that of its bacterial homologues.

Taken together, the fact that the loss of catalytic activity in mnd2 results in increased sensitivity to stress, indicates that this protease might be essential for the transduction of mitochondria-related stress signals in cells not committed to apoptosis. Overall, the study emphasizes the physiological relevance of the protease activity of the protein. However, apart from the mouse model study, no further mechanistic characterization has been done on S276C mutant to delineate the structural basis of its inactivation. Therefore, the aim of this work was to understand how S276C point mutation that resides away from the catalytic triad completely abolishes the protease activity, which would indirectly shed light on HtrA2's mechanism of action.

Here, we dissected the structure of S276C HtrA2 mutant using multidisciplinary tools with an aim at understanding the conformational changes and structural perturbations that affect its overall protease activity which has helped us decipher the structural basis of mnd-2 disorder. In 2004,

Martins et al., generated a mouse model entirely lacking expression of HTRA2 and found that the phenotype was similar to Parkinsonism (9). They have observed that loss of HtrA2 is associated with accumulation of unfolded proteins in mitochondria, dysfunction of the mitochondrial respiration, generation of reactive oxygen species and cell death (4, 5). Since loss of HtrA2 causes neurodegeneration with parkinsonian features and due to its functional relevance in terms of mitochondrial homeostasis, Strauss et al., for the first time performed a mutation screen of the HTRA2 gene in German PD patients. In this study they reported that mutations in HTRA2 are associated with PD in German population by identifying two novel missense substitutions (c.1195G>A (p.Gly399Ser) and c.421G>T (p.Ala141Ser), located respectively in the PDZ domain and N-terminus of mature HTRA2) in PD patients and demonstrating a functional consequence of these variants *in vitro* (10). Both mutations were found to be associated with decreased *in vitro* activation of the protease activity with compromised mitochondrial function and morphology. However, the findings were not replicated in subsequent HTRA2 sequence analyses from different populations (11) (12). A mutation screen in Belgian PD patients also identified a novel missense mutation p.R404W (12). A multi-center study to evaluate the contribution of five high frequency SNPs (located in the regulatory region, 5′UTR region and intron) of HTRA2 to PD was performed recently and none of these SNPs were revealed to be related to the disease (13). Taken together, these independent sequence analysis studies on PD patients' HTRA2 gene from different countries identified few variants with good frequencies. These variants upon functional characterization have been found to be involved in affecting HtrA2's activity. Since HtrA2 has functional relevance in terms of mitochondrial homeostasis as well as its loss causes neurodegeneration with parkinsonian features, we decided to screen for mutations in the HTRA2 gene in a large sample of Indian PD patients and performed functional assays of identified mutations or variants.

Hypothesis:

Our central hypothesis is that understanding structural and functional basis of loss of HtrA2 protease activity in pathogenic variants might help correlate HtrA2's association with Parkinsonism and hence subsequently lead to better therapeutic outcome in future.

Results:

Objective 1: To understand the structural basis of inactivity of mnd2 mutant (S276C) HtrA2

Expression and purification of wild type human HtrA2 and hHtrA2 (S276C)

cDNA of histidine tagged HtrA2 was cloned in pET 20b vector. To introduce particular mutation in the WT. HtrA2, we employed PCR for site directed mutagenesis. Both His-tagged WT. HtrA2 and hHtrA2 (S276C) were expressed in bacterial strain BL21 DE3 and purified using two steps- Ni-NTA affinity chromatography and Gel filtration (FPLC) chromatography to get rid of additives as well as impurities.

Secondary structural organization and thermal stability of hHtrA2 (S276C) protein

Secondary structures of both WT. HtrA2 and hHtrA2 (S276C) were determined by Far-UV Circular Dichroism (CD) spectroscopy. It was observed that no significant secondary structural changes have occurred upon mutation. Thermal stability of the mutant protein was studied by thermal denaturation using CD and the melting point (T_m) of the protein was found to be around ~74°C, which is comparable to that of wild type HtrA2 as reported earlier (*2*).

- **Crystallization, Data Collection, Structure Determination and Refinement:**

The purified mutant HtrA2 was crystallized at 22^0C by the hanging-drop vapour-diffusion method using a protein concentration of 15 mg/ml in crystallization buffer (Mother liquor) by mixing 2 ul of protein and 1ul of mother liquor. The crystals typically grew to a size of 0.2 x 0.2 mm within 10 days. The crystal structure of hHtrA2 (S276C) was solved at 2Å resolution.

Structural basis of inactivation of hHtrA2 (S276C) mutant

A careful inspection of water molecules in the X-ray structure of HtrA2 (PDB: 1LCY) indicates that water (W) molecule no. 377, forms an interaction between side chains of S276 and I270* (distance 4.1Å) of the adjacent molecule. However, in case of the mutant hHtrA2 (S276C), where highly hydrophobic cysteine residue (CH2-SH) replaces the serine, W377 is absent suggesting abrogation of this water-mediated interaction might have adversely affected its activity. To eliminate the possibility of this observation being an artefact (as a consequence of different crystallization conditions), active site mutant HtrA2 S306A was crystallized under identical crystallization conditions as hHtrA2 (S276C). Superimposition of the structures of HtrA2 (S306A) and 1LCY (277 Cα atoms with RMSD value of 0.242Å) confirm that the same water molecule (W3777 in case of 1LCY) is present in the HtrA2 (S306A) as well with a stable *b-factor* (*temperature factor*) of 18.68 $Å^2$ thus highlighting its functional relevance.

Molecular dynamics simulation (MDS) study for identification of the water molecule

To further validate the importance of W377 molecule in stabilizing the protease structure in the dynamic loop region, MDS was performed. The coordinates of the structure used were those of the crystal structure of HtrA2 (S306A) (PDB: 1LCY) (*1*). The modeled structure of hHtrA2

(S276C) was created on the same template for further MDS analysis for 10ns. Upon analyzing the trajectories visually, and using water mediated hydrogen bonds with important residues, we observed that in case of hHtrA2 (S276C), there is no water-mediated hydrogen bonding with the cysteine residue. On the other hand, in HtrA2 (S306A), there is a stable water-mediated hydrogen bonding interaction with the serine residue thus reiterating the importance of the water molecule (W377) in its activity.

Chemical mutagenesis approach

To understand the importance of the serine residue at position 276 toward HtrA2 activity, site-directed mutagenesis was performed to replace it with a smaller and hydrophobic alanine residue. *In vitro* substrate cleavage assay using β-casein (both gel- and fluorescence-based) showed no activity in hHtrA2 (S276A) suggesting that the serine on loop L3 might be important for positively regulating the activity of the protease. With an aim at understanding the importance of loop L3 (on which S276 is located) for protease activity, the residues of the loop were scanned and the conserved residues were identified. Amongst some of the previously identified residues, Arginine 280 (R280) was found to be highly conserved across species. Crystal structure of liganded and unliganded DegS and HtrA1 (*3, 4*) demonstrate that upon substrate binding, this conserved arginine residue interacts with residues in LD*. This leads to conformational changes at and around the active site making it more conducive for substrate binding. To understand the importance of this arginine residue in HtrA2, we mutated it to alanine in wild type HtrA2 as well as in hHtrA2 (S276C) (double mutant). The protease activity using substrate β-casein was monitored as a function of enzyme concentration. For all the concentrations of HtrA2 (R280A) and HtrA2 (R280A, S276C), no activity was observed as opposed to wild type HtrA2**,** suggesting R280 is

important for HtrA2 activity. This also hints upon overall conservation of the structural determinants in loop L3 among DegS, HtrA1 and HtrA2 that modulate HtrA activity.

Summary:

This study reports the crystal structure of hHtrA2 (S276C) protease at 2Å resolution with intact catalytic triad. Comparison with wild type HtrA2 structure suggests that absence of a critical water-mediated intermolecular interaction between side chains of S276 of L3 and I270 from LD* (of adjoining monomer) might abrogate the relay of signal towards loop L1*, which includes residues of oxyanion hole and catalytic triad thus resulting in an inactive variant of the protease.

Objective 2: Characterization of HtrA2 variants associated with neurodegenerative disorders.

Mutation analysis of HTRA2 gene

Genetic result

To determine the frequency of HTRA2 mutations as a cause of familial Parkinsonism and to identify novel mutations in the gene, all 8 exons of HTRA2 gene from 170 (early and late onset) Parkinson disease patients and 160 controls (age, gender and ethnicity matched), were sequenced. Sanger sequencing under the specific conditions led to the detection of three exonic (c.421G>T, c.725C>T and c.1195G>A) sequence variations. The exonic sequence variations c.421G>T in exon 1 (leading to p.A141S) in a total of 2 PD patients (1.17%) and 3 neurologically normal control individuals (1.87%) and c.1195G>A in exon 7 (leading to p.G399S), in a total of two PD patients (1.17%) and four neurologically normal control individuals (2.5%), both were previously identified as a mutation associated with PD by Strauss et al (5). The c.725C>T variant, located in exon 3, which affects the second base of the codon results in the substitution of a Methionine for

a Threonine (T242M), was also detected in a single patient (0.58%) harboring its heterozygous state. Interestingly, this mutation was not found in any of the control chromosomes. The amino acid (Threonine 242) has been found to be evolutionary conserved across species making it an important mutation for further characterization.

Clinical result

The case carrying the c.725 C>T (p.T242M) variant was a 77-year-old woman. Patient's parents were from Karnataka region with no known consanguinity and no family history of Parkinsonism. Patient had modified Hoehn Yahr Scale of 3.0 that corresponds to a mild or moderate bilateral disease, some postural instability and physical independency. She had difficulty performing her regular working activities. There was also psychological disturbance, particularly anxiety. At the same time, sleep disturbances started and the patient felt depressed. Three months after the initial manifestation of the disease, the patient developed speech difficulties, especially with pronunciation.

In vitro functional assay of HTRA2 (T242M) variant

Effects of WT and mutant HtrA2 on the serine protease activity *in vitro*

To determine the effect of found mutation on the proteolytic activity, we generated recombinant HtrA2 (T242M) and compared the activity with the WT HtrA2 using previously described assays (*2, 6, 7*). Protease activity of the WT and HtrA2 (T242M) was measured both qualitatively and quantitatively using β-casein as a substrate. In the gel based protease assay (qualitative), at different concentrations of HtrA2 (T242M), there was no significant difference in the enzyme activity. However, comparing the basal activity of the proteins, in the quantitative fluorescence based *in vitro* protease (enzyme (HtrA2 (T242M)) – substrate (FITC-β-casein)) assay, significant

decrease (~1.8 fold) in the reaction rates (K_{cat}/K_m) were measured as compared to WT HtrA2. Our results also indicate that T242M HtrA2 has similar $k_{0.5}$ value suggesting, substrate binding is not affected and both the enzymes showed positive co-operativity.

HtrA2 (T242M) does not interfere in trimer formation

Functional protease activity of WT HtrA2 protein requires homotrimerisation (*2, 7*), which is primarily mediated by the N-terminal domain of HtrA2. According to the crystal structure of HtrA2 (*7*), Threonine 242 is located in the serine protease domain placed in the loop region in between β6 (harbors Aspartate 228 of the catalytic triad;) & β7 . To evaluate for possible effects of the HtrA2 (T242M) protein on trimer formation, size exclusion chromatography has been carried out. We observed HtrA2 (T242M) were eluted as a single peak at ~73.9ml of elution volume similar to the WT type HtrA2 as observed previously (*2*). This suggests that the mutation does not affect the oligomeric property of HtrA2 protein.

HtrA2 (T242M) mediates caspase-dependent cell death in neuronal cells

Since the mutation did not show any significant structural alteration, the role of T242M in HtrA2 functions was investigated. HtrA2 is a proapoptotic molecule and has been shown to relieve IAP inhibition on caspases, we investigated the effect of the T242M mutation on cell death via the canonical caspase-dependent pathway. SHSY5Y (thrice cloned subline of the neuroblastoma cell line SK-N-SH) cells were transiently transfected with WT as well as HtrA2-T242M. Caspase activation by Etoposide treatment was assessed by western blotting after 48hrs. Presence of activated (cleaved) caspase-3 in WT and HtrA2-T242M transfected neurons indicates caspase-dependent cell death in both the WT and variant**.** Further, cell viability was determined for both

WT as well as T242M transfected neuronal cells by MTT assay. Interestingly, the mutant protease transfected cell lines showed significant time-dependent reduction in the cell viability as compared to the WT transfected cells**.** To estimate the extent of cell death flow cytometry studies were performed with both WT and T242M transfected neuronal cell lines. The study revealed that there is a significant ~2.0 fold increase in Annexin V/PI (dual) positive cells in the HtrA2-T242M treated population as compared to WT and vehicle control population**.** Moreover, T242M transfected SHSY5Y cells showed 2.0 fold increase in the number of cells with sub-G1 DNA content as compared to the cells expressing WT HtrA2**.** All these observations point toward increased cell death and less cell viability induced by HtrA2-T242M in dopamine producing neuronal cells.

BAX up regulation induces increased cell death in HtrA2 (T242M) cells

A number of molecular factors such as Bcl-2 family members; Bad and Bax play key roles in the execution of apoptosis. We therefore investigated their expression pattern in SHSY5Y cells overexpressing HtrA2 (T242M). The Bcl-2 family of genes plays an important role in the regulation of apoptosis. Thus, to understand the molecular mechanism by which HtrA2 (T242M) induces caspase-dependent apoptotic cell death, we evaluated the expression levels of Bad and Bax proteins using western blotting. We observed a significant up-regulation in the expression of Bax protein in the HtrA2 (T242M)-transfected SHSY5Y cells as compared to vehicle control and WT HtrA2 cells. This observation indicates that over-expression of the mutant HtrA2 leads to increase in pro-apoptotic Bax level in the cell, which is significantly higher compared to its expression when mature HtrA2 is overexpressed.

Ultra structural changes induced by HtrA2 (T242M)

HtrA2 (T242M) induced severe ultra-structural abnormalities in transfected SHSY5Y cells. Using electron microscopy, we examined the morphology of HEK293T and SHSY5Y cells overexpressing WT and T242M mutant HtrA2 on an ultra-structural level. We have identified characteristic changes of mitochondria in a subset of cells. When compared with WT HtrA2, we observed abnormal mitochondrial morphology with disorganized cristae in cells overexpressing HtrA2 (T242M). Some of these mitochondria were filled with dense, lamellar structures. Numerous autophagic vesicles containing electron dense materials, protein inclusions and degenerating cellular organelles were readily visible throughout the cytoplasm. In our studies, observation of co-localization of mitochondria and lysosomes implies autophagy as a possible mechanism of cell death in those cells. Extensive cytoplasmic vacuolation was also apparent and intact mitochondria were not readily detectable. On the contrary, control cells exhibited numerous mitochondria (with intact inner and outer membranes and distinct cristae) and few cytoplasmic vacuoles.

HtrA2 (T242M) **induces mitochondrial membrane depolarization in neurons**

On the basis of morphological alterations, we next examined the effects of T242M HtrA2 overexpression on mitochondrial function. We therefore analyzed changes in mitochondrial membrane potential ($\Delta\Psi m$) by using JC-1 dye. Mitochondrial membrane potential is considered as a sensitive marker for mitochondrial health. As compared to the vehicle control, HtrA2 (T242M)-transfected SHSY5Y cells induced depolarization of the mitochondrial membrane. This is reflected by a significant increase in green to red fluorescence ratio of JC-1 dye. Increase in green fluorescence of JC-1 dye (due to formation of JC-1 monomers) indicates a drop in $\Delta\Psi m$

whereas increased red fluorescence (due to formation of JC-1 aggregates) corresponds to a stable ΔΨm and thus represents functional mitochondria. After treatment with 150µmol/L Etoposide (induces DNA damage by inhibition of Topoisomerase-II, and known to cause apoptotic cell death by different mechanisms including loss of mitochondrial transmembrane potential) for 6hrs (*8*), the mitochondrial membrane potential was decreased in all the samples investigated. However, this effect was more pronounced in cells overexpressing HtrA2 (T242M) as compared to WT.

HtrA2 physically interacts and gets phosphorylated by GSK3β

The identified mutant T242M is localized in the protease domain of HtrA2. Since the mutant was found to have negative effect on cell survival, we went through an analysis with several online servers that predicts serine, threonine or tyrosine phosphorylation sites in eukaryotic proteins using ensembles of neural networks viz. Scansite (http://scansite.mit.edu/) and NetPhos 3.1 server (http://www.cbs.dtu.dk/services/NetPhos/). These analyses identified T242 to be a part of the motif (QTKEPLPTLPLGRSA), where GSK3β phosphorylates the threonine residue. This prediction was further validated through a series of experimental studies. To elucidate direct interaction between HtrA2 and GSK3β if any, co-immunoprecipitation studies in HEK-293T cells were performed. Interaction between over-expressed C-terminal FLAG-tagged HtrA2 and endogenous GSK3β protein was confirmed by western blot analysis.

GSK3β Inhibits HtrA2 Serine Protease Activity in a Phosphorylation-dependent Manner

Since mature HtrA2 plays an important role in inducing programmed cell death at post-mitochondrial level (*9, 10*) (*11, 12*), we next examined whether anti apoptotic function of GSK3β is mediated by phosphorylation of HtrA2. Therefore, we transfected SHSY5Y cells (5×10^5) with

phosphomimic mutant (T242E) of HtrA2 and analyzed cell cycle using PI staining followed by flow cytometry. Interestingly, we detected remarkable increase in the survival of T242E transfected neurons (decreased sub G0/G1 population) relative to WT and HtrA2 (T242M) transfected neurons.

GSK-3β is essential for HtrA2 T242 phosphorylation with Apoptotic Stimulus

Growth factor withdrawal activates GSK-3 after inactivation of PI-3K/Akt pathway (*13, 14*). We employed flow cytometry to verify the involvement of GSK-3β signalling in SHSH5Y cells. Prior to that, to investigate the role of GSK-3β in phosphorylation-dependent HtrA2 inactivation, we inhibited GSK-3 by using a well-known potent inhibitor *SB415286* (Selleckchem Inc.). We transfected SHSY5Y cells (1×10^5) with T242M and WT HtrA2 with and without the inhibitor and subsequent serum withdrawal for 6hrs (so as to activate GSK-3β) and analysed the cell death using Annexin V/PI staining followed by flow cytometry. Interestingly, our flow cytometry data indicated that in presence of inhibitor, there is increase in cell death in both mutant and wild type HtrA2-transfected neurons as opposed to cells without inhibitor. In order to show inhibition by the specific inhibitor used, stability of β-catenin (Wnt signaling) was checked using western blotting. It is well known that in presence of inhibitor, GSK-3β-mediated destabilization of β-catenin was found to be inhibited.

Structure of the T242M Mutant of HtrA2

We further investigated whether the T242M mutation has some effect on the overall protein structure and in that quest, we solved the crystal structure of $HtrA2^{T242M/S306A}$ using x-ray crystallography at a resolution of 2.5A˚. The overall structure of the trimer of the mutant has been

found to be similar to that of the HtrA2 (S306A) (*1*, *7*), with root-mean-squares (rms) distance of 0.2A˚ between their equivalent Cα atoms. The structure of HtrA2 trimer contains a characteristic α/β fold that is conserved among members of the HtrA superfamily, with 19β-strands and 7α-helices. The mutation site, T242, is located in the loop connecting β6 and β7, on the surface of the trimer and far from the catalytic serine residue. This loop is quite stable in conformation, as indicated by the low thermal factors (23$Å^2$) in the wild-type (PDB: 1LCY) (*1*) as well as in the mutant structure. In addition, the sequences of this loop are highly conserved among the HtrA proteins. Therefore, no significant structural alteration has been found in the mutant protein.

Summary:

1. We carried out extensive sequencing of HTRA2/PARK13 gene (*10, 15, 16*) in a cohort of 170 early and late onset Indian PD patients and identified a novel, non-synonymous, heterozygous, substitution at position 242 in the protease domain.
2. Here, we provide evidence that the c.725 C>T; p.T242M variant is causative of an autosomal recessive form of late onset PD by genetic and functional data and may be a pathogenic mutation.
3. Based on the functional studies, our observation provides compelling evidence to support our finding that the T242M variant is detrimental for proper functioning of the protease as it disrupts mitochondrial function
4. Based on our findings on the molecular details of interaction between HtrA2 and GSK-3β, we speculate a general role for HtrA2 in cellr survival pathway under stress conditions. Our study opens up new areas of investigation on the role of HtrA2 in cellular homeostasis.

Significance of the study:

1. Collectively, using multidisciplinary approach, we provided the first structural insight into the mechanism by which inactivation of HtrA2 due to single point mutation occurs.
2. Our data support a role for HTRA2 in PD susceptibility in the Indian population
3. We have shown a direct and functional interaction between two proteins associated with Parkinson's disease and suggested that this novel pathway may also be relevant to sporadic forms of this disease
4. The characterization of the mitochondrial stress-responsive pathway involving HtrA2 and GSK-3β in neurodegeneration in humans will lead to an improved understanding of the

pathogenesis of Parkinson's disease, which might lead toward novel therapeutic approaches.

5. Our study suggests that phosphorylation of residues in the protease domain is an important mechanism by which the proteolytic activity of HtrA2 is modulated in response to stress.

References:

1. W. Li *et al.*, Structural insights into the pro-apoptotic function of mitochondrial serine protease HtrA2/Omi. *Nature structural biology* **9**, 436-441 (2002).
2. L. K. Chaganti, R. R. Kuppili, K. Bose, Intricate structural coordination and domain plasticity regulate activity of serine protease HtrA2. *FASEB journal : official publication of the Federation of American Societies for Experimental Biology* **27**, 3054-3066 (2013).
3. K. Zeth, Structural analysis of DegS, a stress sensor of the bacterial periplasm. *FEBS letters* **569**, 351-358 (2004).
4. C. Eigenbrot *et al.*, Structural and functional analysis of HtrA1 and its subdomains. *Structure* **20**, 1040-1050 (2012).
5. K. M. Strauss *et al.*, Loss of function mutations in the gene encoding Omi/HtrA2 in Parkinson's disease. *Human molecular genetics* **14**, 2099-2111 (2005).
6. P. R. Bejugam *et al.*, Allosteric regulation of serine protease HtrA2 through novel non-canonical substrate binding pocket. *PloS one* **8**, e55416 (2013).
7. A. R. Wagh, K. Bose, Structural Basis of Inactivation of Human Counterpart of Mouse Motor Neuron Degeneration 2 Mutant in Serine Protease HtrA2. *Bioscience reports*, (2018).
8. M. Marabese, M. Mazzoletti, F. Vikhanskaya, M. Broggini, HtrA2 enhances the apoptotic functions of p73 on bax. *Cell death and differentiation* **15**, 849-858 (2008).
9. S. Jamil, I. Lam, M. Majd, S. H. Tsai, V. Duronio, Etoposide induces cell death via mitochondrial-dependent actions of p53. *Cancer cell international* **15**, 79 (2015).
10. Y. Suzuki *et al.*, A serine protease, HtrA2, is released from the mitochondria and interacts with XIAP, inducing cell death. *Molecular cell* **8**, 613-621 (2001).
11. A. M. Verhagen *et al.*, HtrA2 promotes cell death through its serine protease activity and its ability to antagonize inhibitor of apoptosis proteins. *The Journal of biological chemistry* **277**, 445-454 (2002).
12. L. Cilenti *et al.*, Characterization of a novel and specific inhibitor for the pro-apoptotic protease Omi/HtrA2. *The Journal of biological chemistry* **278**, 11489-11494 (2003).
13. R. Hegde *et al.*, Identification of Omi/HtrA2 as a mitochondrial apoptotic serine protease that disrupts inhibitor of apoptosis protein-caspase interaction. *The Journal of biological chemistry* **277**, 432-438 (2002).

14. U. Maurer, C. Charvet, A. S. Wagman, E. Dejardin, D. R. Green, Glycogen synthase kinase-3 regulates mitochondrial outer membrane permeabilization and apoptosis by destabilization of MCL-1. *Molecular cell* **21**, 749-760 (2006).
15. R. Mishra *et al.*, Glycogen synthase kinase-3beta induces neuronal cell death via direct phosphorylation of mixed lineage kinase 3. *The Journal of biological chemistry* **282**, 30393-30405 (2007).
16. C. W. Gray *et al.*, Characterization of human HtrA2, a novel serine protease involved in the mammalian cellular stress response. *European journal of biochemistry / FEBS* **267**, 5699-5710 (2000).
17. S. Krick *et al.*, Mpv17l protects against mitochondrial oxidative stress and apoptosis by activation of Omi/HtrA2 protease. *Proceedings of the National Academy of Sciences of the United States of America* **105**, 14106-14111 (2008).

Publications in Refereed Journal:

a. **Published:**

- Ajay R. Wagh & Kakoli Bose. "**Structural Basis of Inactivation of Human Counterpart of Mouse Motor Neuron Degeneration 2 Mutant in Serine Protease HtrA2**" Bioscience Reports. 2018 Aug 1. DOI: 10.1042/BSR20181072

b. **Accepted:** NA

c. **Communicated:**

- Ajay R. Wagh, Vasudha Mishra, Rajiv Sarin, S. S. Kulkarni, Pramod B. Gai and Kakoli Bose. **"Novel variant T242M in HTRA2 induces apoptosis of dopaminergic neurons and contributes to Parkinson's disease: An Indian case-control study"** manuscript ready for submission.

d. **Other Publications:**

Book/Book Chapter:

c. Ajay R. Wagh & Kakoli Bose. **"Emerging Roles of Mitochondrial Serine Protease HtrA2 in Neurodegeneration"** 2017, (Springer) DOI: 10.1007/978-981-10-2513-6_15

d. Ajay R. Wagh & Kakoli Bose. **"Apoptosis in cancer cell signaling and current therapeutic possibilities"** 2019, (Springer) communicated

e. **Conference/Symposium**

Poster Presentations:

- International conference on "***New Advances in X-ray Diffraction and Cryo - Electron Microscopy***" held in New Delhi 15-17 December 2014

- ***13th Asian Crystallographic Association Conference*** (AsCA) held in Kolkata, 5-8 December 2015
- ***31st Protein Society Meeting*** held in Montreal, Canada on 24th-27th July 2017in Enzymology
- ***Indo-US conference on Advances in Enzymology: Implications in Health, Disease and Therapeutics*** held at TMC-ACTREC on 15th- 19th January 2017
- ***Annual meeting of Society of Biological Chemists (I)*** – Mumbai held on 13th October 2018 at Institute of Chemical Technology, Mumbai
- ***Indo-US Conference on Sculpting the Future of Medicine-Gateway to Post Proteogenenomic Era*** held at TMC-ACTREC on 8th – 11th December 2018 (**Best Poster award**)
- ***7th Annual MPAI Conference*** **"***Precision Medicine is closer than you think"* held from 12th -13th January 2019, at ACTREC, Tata Memorial Centre, NaviMumbai.

Participation:

- ***TMC-Platinum Jubilee Conference "Healthcare: A commodity or Basic Human Need?"*** held at TIFR, Mumbai 27th – 29th January 2017

Signature of Student: Date: 26/03/2019

Doctoral Committee:

S. No.	Name	Designation	Signature	Date
1.	Dr. S.V. Chiplunkar	Chairman		12/4/19
2.	Dr. Kakoli Bose	Guide & Convener		12/4/19
3.	Dr. Tanuja Teni	Member		12/4/19
4.	Dr. Dibyendu Bhattacharya	Member		30/3/19
5.	Dr. Prasenjit Bhaumik	Invitee		28/3/19

Forwarded Through:

15/4/19

Dr. S.V. Chiplunkar
Chairperson,
Academic &Training Program, ACTREC

(Prof. Dr. S. V. Chiplunkar)
Chairperson, Academic &
Training Programme , ACTREC

16/4/19

Dr. S. D. Banavali
Dean, Academics
T.M.C.

PROF. S. D. BANAVALI, MD
DEAN (ACADEMICS)
TATA MEMORIAL CENTRE
MUMBAI – 400 012.

To,
Dean,
Homi Bhabha National Institute
BARC

Encl: as above

List of Abbreviations

BSA	Bovine Serum Albumin
CD	Circular dichroism
DMEM	Dulbecco's modified Eagle's medium
DMSO	Dimethyl sulfoxide
E.coli	*Escherichia coli*
EDTA	Ethylene diamine tetraacetic acid
FITC	Fluorescein isothiocyanate
HEK	Human embryonic kidney
HtrA2	High temperature requirement A2
IBM	IAP-binding motif
IGFBP	Insulin growth factor binding domain
IMS	Intermembrane space
IP	Immunoprecipitation
IPTG	Isopropyl β-D-1-thiogalactopyranoside
ITC	Isothermal titration calorimetry
KDa	Kilodalton
mM	Millimolar
MBP	Maltose binding protein
MD	Molecular dynamics
MRE	Mean residual ellipticity
Ni-NTA	Nickel-nitriloacetic acid
PCR	Polymerase chain reaction
PDB	Protein Data Bank
PDZ	Postsynaptic density protein 95- *Drosophila* disc large tumor -Zona occludens1
PEA-15	Phosphoprotein enriched in astrocytes-15
PAGE	Polyacrylamide Gel Electrophoresis
RMSD	Root mean square deviation
RMSF	Root mean square fluctuation
RT	Room temperature
RU	Response units
SDM	Site-directed mutagenesis
SEC	Size-exclusion chromatography
SPR	Surface plasmon resonance
SDS	Sodium Dodecyl Sulphate
TM	Transmembrane domain
TBST	Tris Buffered Saline with 0.1% Tween-20
TEMED	N,N,N',N' Tetramethyl Ethylene Diamine
XIAP	X-linked inhibitor of apoptosis protein
XDS	X-ray Detector Software

List of Figures

List of Tables

CHAPTER 1:

Introduction and review of literature

- ***Protein quality control:***

Misfolded or damaged proteins formed due to defective quality control function represent a serious hazard to the cell as they might accumulate as large aggregates, a process associated with neurodegenerative disorders. The accumulation of such misfolded or damaged proteins obstructs essential biological processes and can lead to cellular malfunctions. To prevent the formation of possibly toxic protein aggregates all cells have developed a sophisticated system of molecular chaperones and proteases to reduce the amount of unfolded or aggregated protein that formed during the stress conditions (*17*).

Out of these two, proteases are having specific importance in this protein quality control mechanisms because they protect as well as regulates the functional part at the same time; they are protective when they remove problematic polypeptides through degradation, and regulatory when they activate, for example, the unfolded protein response (UPR) by proteolytic inactivation of negative regulators ***(Figure 1.1)***. One such heat shock induced serine protease essential for cell survival at higher temperature in bacteria belongs to family of HtrA.

- **High temperature requirement A: general overview**

The HtrA (high-temperature requirement protease A) family of serine proteases was initially identified in bacterium *E. coli* as a heat shock-induced serine proteases [71]. At low temperatures it behaves as a molecular chaperone, while, at higher temperature, it displays the proteolytic activity [72, 73]. An additional characteristic of this family members is about its protease activity which is unlike other proteases is exceptionally regulated such as it can be turn on and off, reversibly.

In humans, HtrA proteases are found to be associated with several cellular processes, such as maintenance of mitochondrial homeostasis, cell death, maintenance of mitochondrial morphology etc.

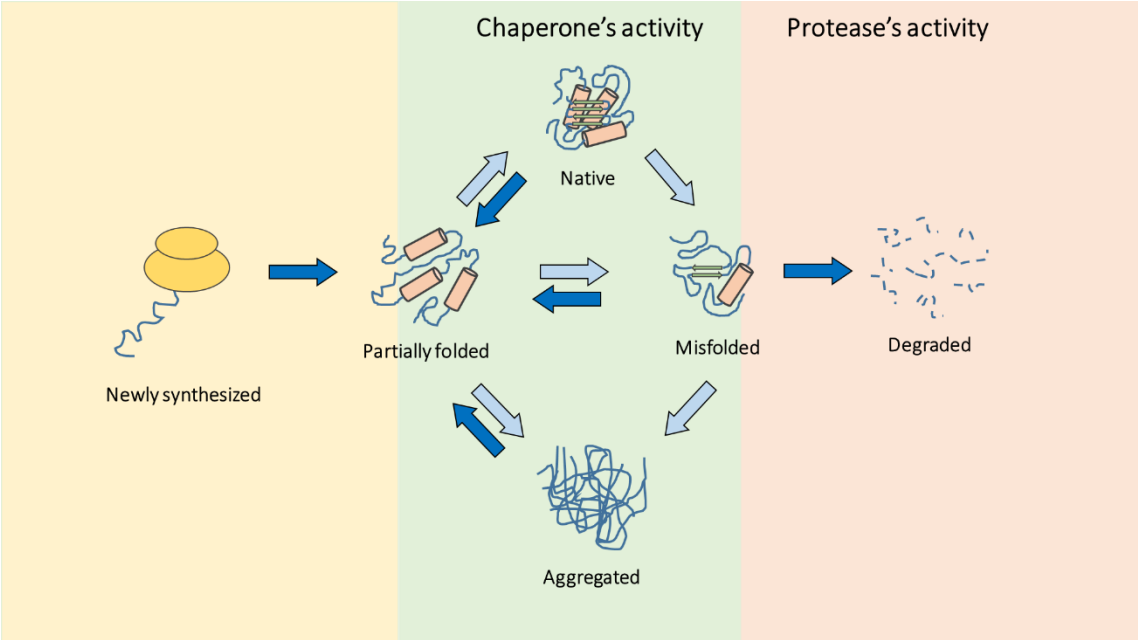

Figure 1.1: Schematic diagram showing chaperone and proteases' activities in protein quality control mechanism.

There has been several confirmations that supports the role of human HtrAs in multiple pathways that lead to programmed cell death and chemo-therapy-induced cellular toxicity. This multidimensional capability associates them with major pathological conditions such as cancer and neurodegenerative disorders hence making them therapeutically important [2, 74-76].

These family of proteins are all oligomeric serine proteases with chymotrypsin-like domain structures [77]. Till now, four human homologues of bacterial HtrA have been identified: HtrA1 (L56 or PRSS11) [78], HtrA2/Omi [79], HtrA3 [80] and HtrA4 [81]. All these

mammalian HtrA proteins share a highly conserved chymotrypsin like serine protease domain and one PDZ domain. HtrA2s N-terminal domain decides their cellular localization and functionality.

Strikingly, the N-terminal regions of mammalian HtrA1, 3 and 4 are much variable from that of HtrA2/Omi. The N-termini of HtrA1, 3 and 4 contain predicted signal peptides as well as domains that are recognized as IGF binding and protease inhibitor domains, which include an N-terminal signal peptide (SP), an insulin growth factor binding domain (IGFBP) and a kazal-type S protease inhibitor domain (KI) [82]. Mammalian HtrA2 lacks all these N-terminal domains but has a transmembrane segment or regulatory domain (TM) ***(Figure 1.2)***.

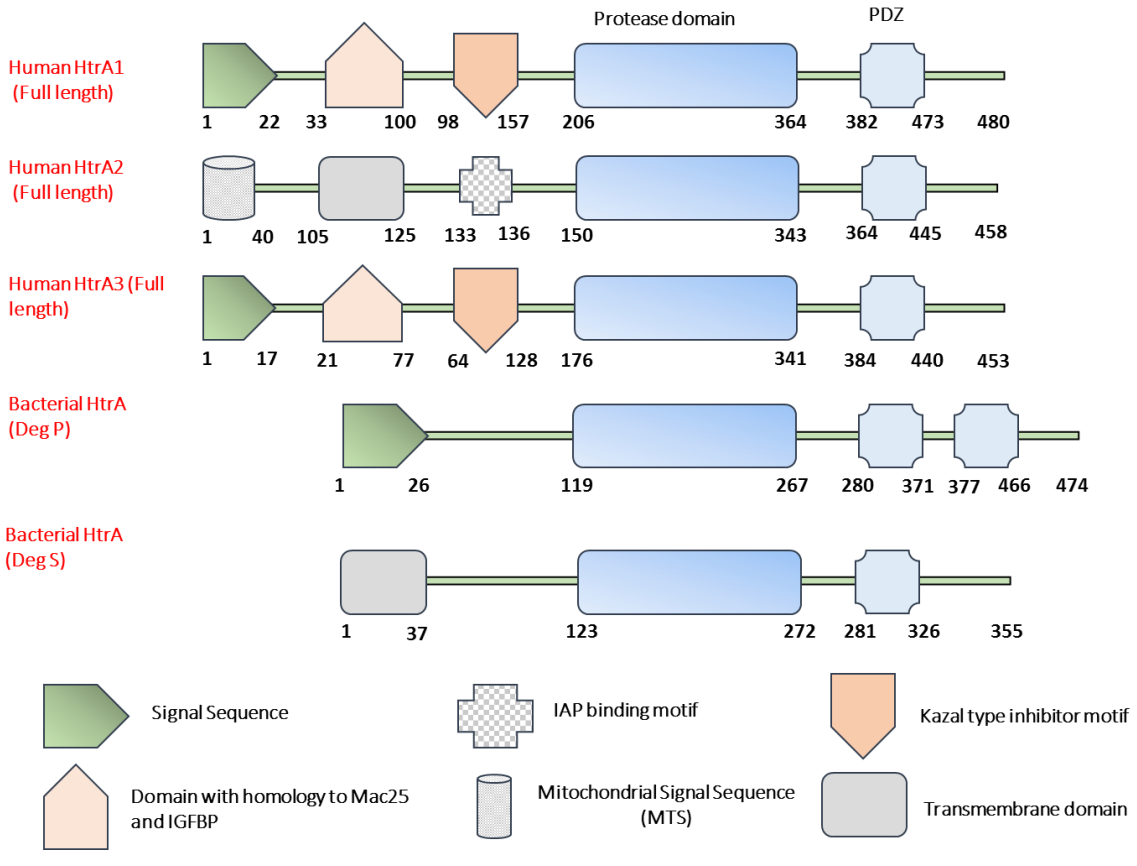

Figure 1.2: Domain association of HtrA family members.

- ***HtrA2: a mitochondrial serine protease***

The mitochondrial serine protease high-temperature requirement protein A2 (akas Omi) is a member of the HtrA family in eukaryotes (*11*). It is expressed from a nuclear gene as a proenzyme of 49 kDa with an N-terminal mitochondrial localization signal that mediates its translocation into the mitochondrial intermembrane space (IMS) (*12, 18*). In eukaryotes, along with HtrA2, there are other paralogues of this family are present, HtrA1/L56, HtrA3/PRSP and HtrA4, which are all homologous to the bacterial HtrA endoprotease, a proteolytic enzyme that removes damaged and denatured proteins at elevated temperatures (*19*). HtrA2 is synthesized as a precursor at 458 amino acids and is processed in the mitochondria to its mature form through the removal of the first 133 amino acids, exposing an 'AVPS' tetra peptide motif (*20*).

Unlike the other members of the HtrA family, HtrA2 is not secreted and it is exclusively located in the IMS of the mitochondria under normal conditions (*11, 21, 22*). HtrA2, like the rest of HtrA proteins, contains a catalytic domain as well as a PDZ domain (postsynaptic disk large and zonula occludens 1) known to be involved in protein-protein interaction *(refer figure 1.2)* (*19*). This mammalian enzyme shares sequence and structural homology with the *Escherichia coli* serine protease HtrA/DegP (*1, 20, 23*). HtrA/DegP is localized in the periplasmic space, where it controls bacterial thermal and oxidative tolerance by acting as a chaperone at normal temperatures. At elevated temperatures, the chaperone transforms into an active endoprotease that degrades damaged and misfolded proteins (*24-26*). Evidence for an evolutionary conservation of this function is provided by the observation that the expression of HtrA2 is up regulated following heat shock of human neuroblastoma SH-SY5Y cells (*15*). Moreover, the proteolytic activity of recombinant HtrA2 is significantly elevated upon heat shock (*27*).

- ***HtrA2 location on Chromosome***

The HTRA2 gene consists of eight exons (covers around 4565 bases) and it is located on chromosome at 2p13.1 position ***(Figure 1.3)*.**

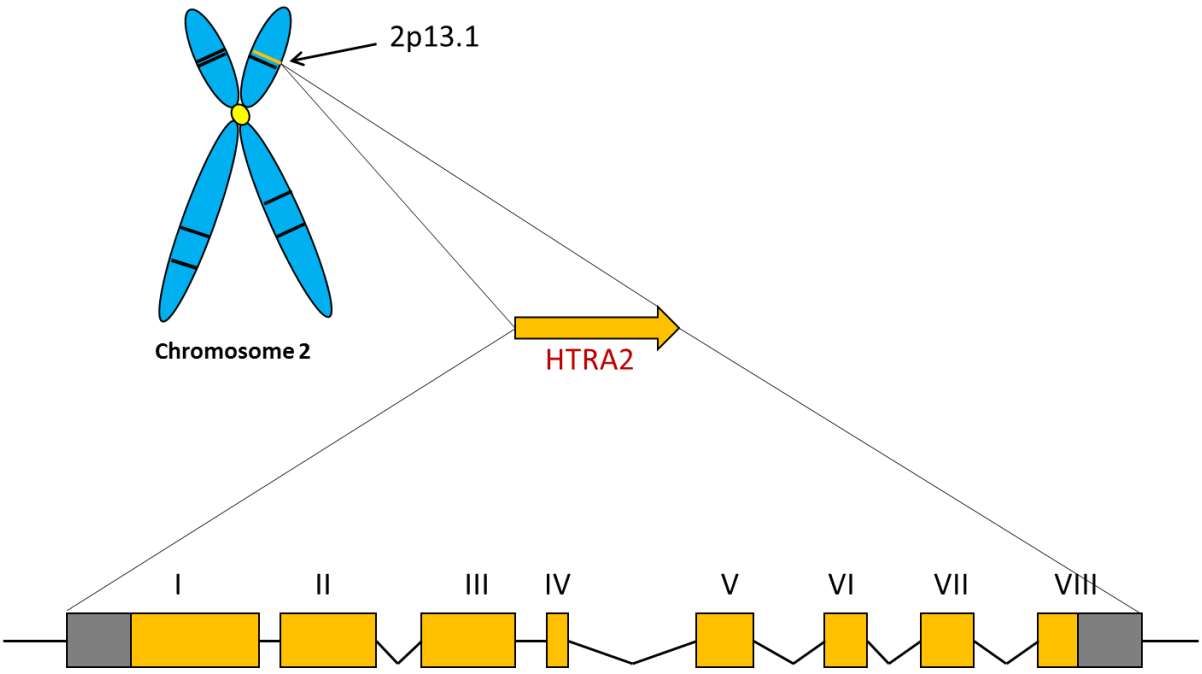

Figure 1.3: Representation of the HTRA2 gene. Exons are shown in *yellow colour*.

The gene codes for a 49 kDa polypeptide of 458 amino acid residues. After complete translation, the full length protein is targeted primarily to the intermembrane space (IMS) (*9*), where it is attached through its N-terminal transmembrane anchor to the inner membrane of mitochondria. During maturation, the first 133 amino acids from the N-terminus get cleaved and upon apoptotic stimulation, it is released from IMS into the cytosol as a 36 kDa mature protease (*9, 10, 12, 18*) ***(Figure 1.4)*.**

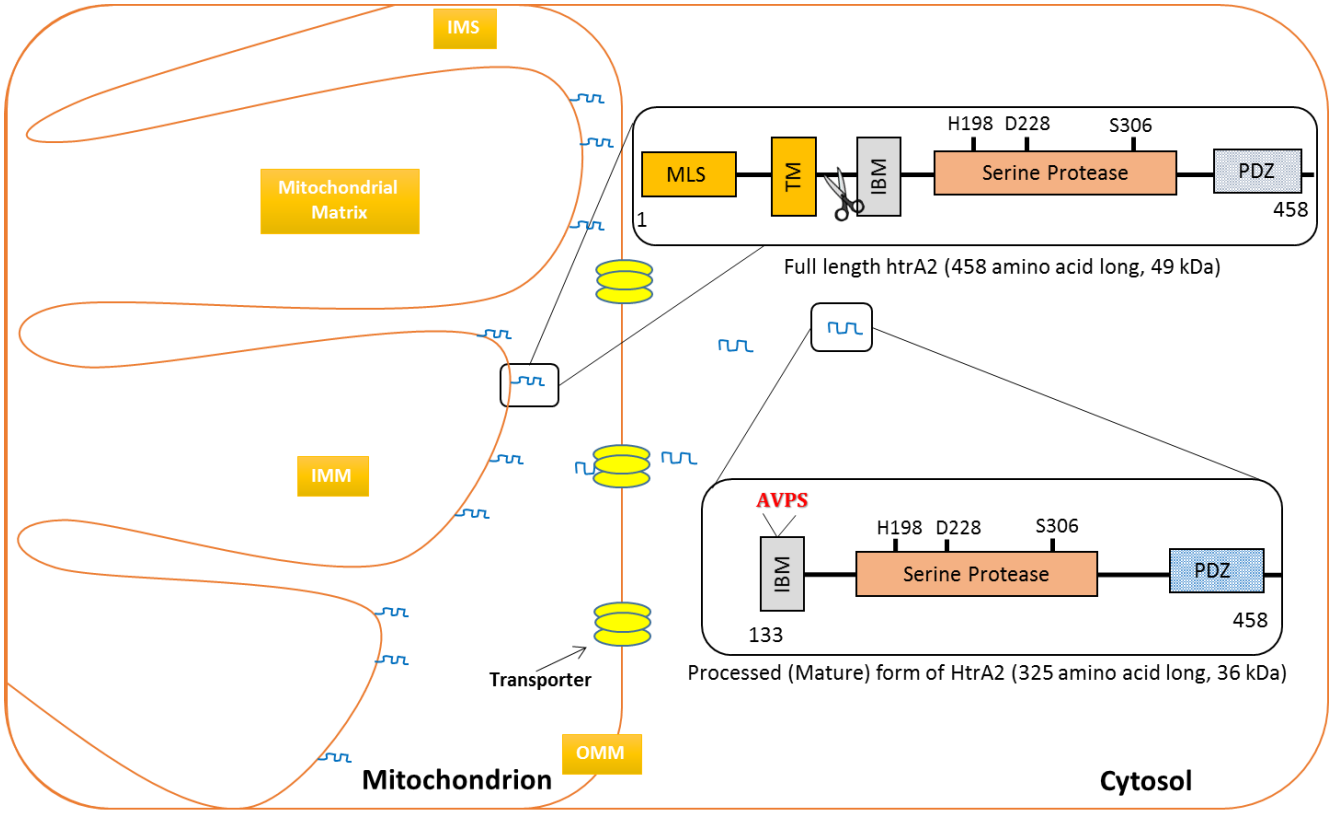

Fig. 1.4: HtrA2 and its maturation process.

- **Structural details**

Crystal structure of mature HtrA2 (133 - 458 residues) in a substrate unbound form was solved at 2.1 Å [14], which provides a broad overview of the global structural organization of the inactive protease. It has trimeric pyramidal architecture with the short N-terminal region at the top and PDZ domains residing at the base of the pyramid. Trimerisation is mediated through extensive intermolecular hydrophobic and van der Waals interactions involving aromatic residues primarily from the N-terminal region ***(Figure 1.5)***. The domain contains several loop structure that are, LA (residues 37-41), L1 (169-173), L2 (190-196), L3 (residues 142-162), and LD (residues 126-140)

[9]. The active-site pocket surrounded by the regulatory loops is buried in the hydrophobic core of the protease domain and is arranged 25 Å above the base of the pyramid. This arrangement along with its trimeric architecture restricts entry of substrate molecules to the active site thus leading to low protease activity. PDZ domains have a canonical binding site comprising highly conserved ‗G-Φ-G-Φ motif', where Φ denotes hydrophobic residues. The first Gly residue is highly variable among PDZ domains while second and fourth residues are hydrophobic (Val, Ile, Leu, or Phe) [117]. This recognition sequence is represented by YIGV in HtrA2, which is highly buried in the intimate interface between the PDZ and the protease domains [14].

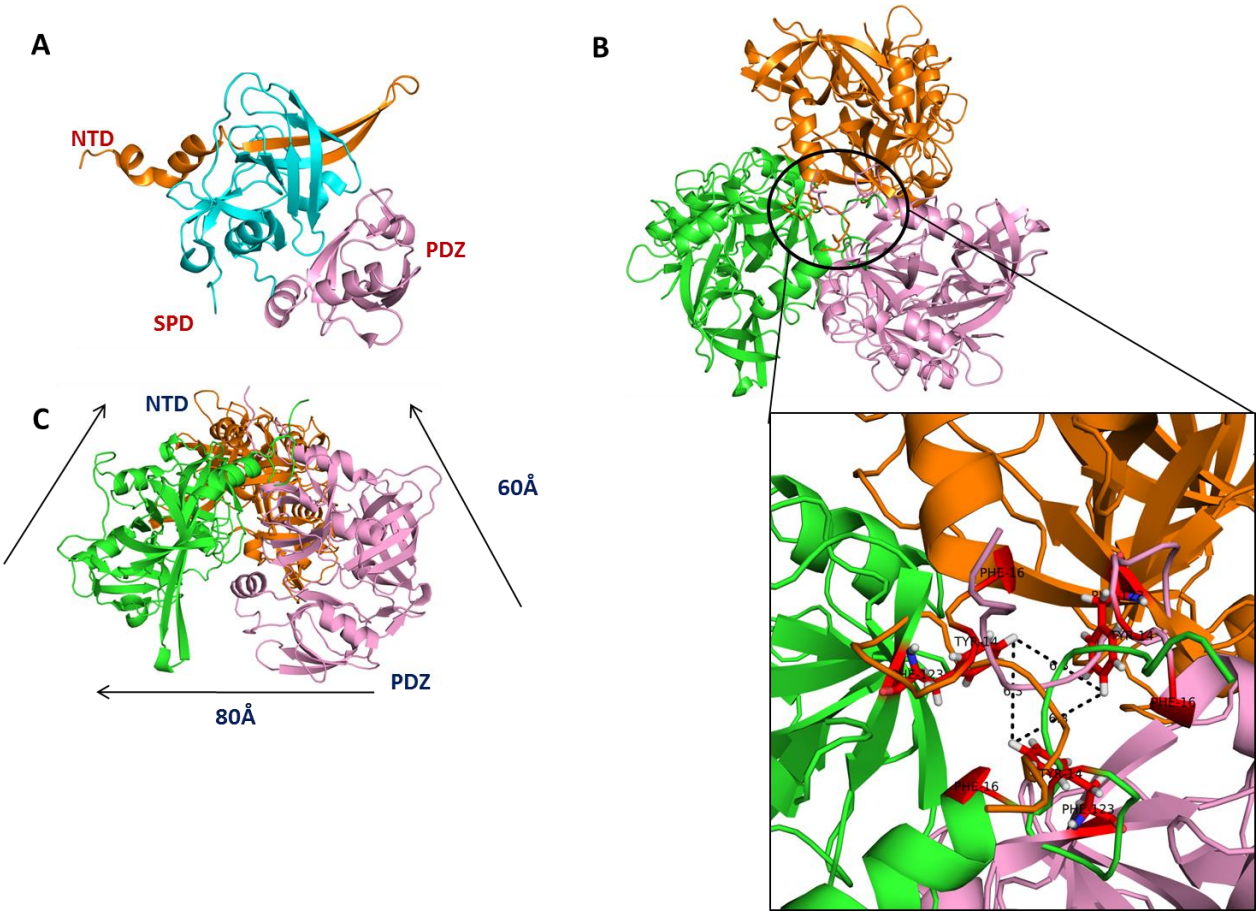

Figure 1.5: Crystal structure of HtrA2 (134-458 amino acids). A**)** Li et al 2002 given crystal structure, PDB: 1LCY has 7α helix and 19β sheets; PDZ (Pink colour) Post Synaptic of 95kDa, Disk Large, Zonula occludens; SPD (orange colour) Serine Protease Domain; NTD (Black colour) N-Terminal Domain. B) After maturation, residues involved in trimerisation of HtrA2, Y14, F16 and F123 from each monomer, C) the three-fold symmetry axis. HtrA2 trimer forms a pyramid like shape, N-terminal domain situated at the top of the pyramid and PDZ at the base. *All the images were generated using PyMol.*

HtrA2 and its Association with Neurological Disorders

- ***Parkinson's disease (PD)***

It is the most common neurodegenerative disease after Alzheimer's that affects 1-2% of the population over the age of 60. It is mainly considered by an death of dopamine producing neuronal cells present in the specific region (*substantia nigra pars compacta)* in the brain (*28*). Numerous information proposed that environmental factors, genetic sensitivity, and aging are important components, which lead to the progression of this disorder (*29-31*).

Basically, the overall the whole thoughtful (pathogenesis) behind this disorder came from the documentation genes found to be associated with PD (*32*) (*33*, *34*). About 18 genes also known as *PARK genes* found to be associated with pathogenesis of PD (*35-42*).

Table 1: Parkinson's disease associated genes and their role in PD.

Symbol	Gene locus	Name of Gene	Role in PD
PARK 1	4q21-22	SNCA	Confirmed
PARK 2	6q25.2-q27	parkin	Confirmed
PARK 3	2p13	Unknown	Unconfirmed
PARK 4	4q21-q23	SNCA-triplication	----
PARK 5	4p13	UCLH1	Unconfirmed but possible
PARK 6	1p35-p36	Pink1	Confirmed
PARK 7	1p36	DJ1	Confirmed
PARK 8	12q12	LRRK2/ Dardarin	Confirmed
PARK 9	1p36	ATP13A2	Confirmed
PARK 10	1p32	Unknown	Confirmed

PARK 11	2q36-27	Unknown	Unconfirmed
PARK 12	Xq21-q25	Unknown	Confirmed
PARK 13	2p12	HtrA2	Confirmed
PARK 14	22q14.1	PLA2G6	Confirmed
PARK 15	22q12-q13	FBX07	Confirmed
PARK 16	1q32	Unknown	Confirmed
PARK 17	16q11.2	VPS35	Confirmed
PARK 18	3q27.1	EIF4G1	Unconfirmed

- ***HtrA2 Variants and PD Pathogenesis***

Most PD cases are due to sporadic mutations (i.e., cause not known). A strong genetic predisposition toward Parkinson's in this subgroup has been observed since 15–20% of these patients have a family history of the disease. Due to insufficient information on the mechanism of molecular pathogenesis of sporadic PD as well as selective dopaminergic neuron loss, it is unclear whether gene mutations are involved in sporadic PD patients. Several single nucleotide

polymorphisms (SNPs) of the HTRA2 gene have been identified and their relevance in PD has been studied. **(Figure 1.6)**.

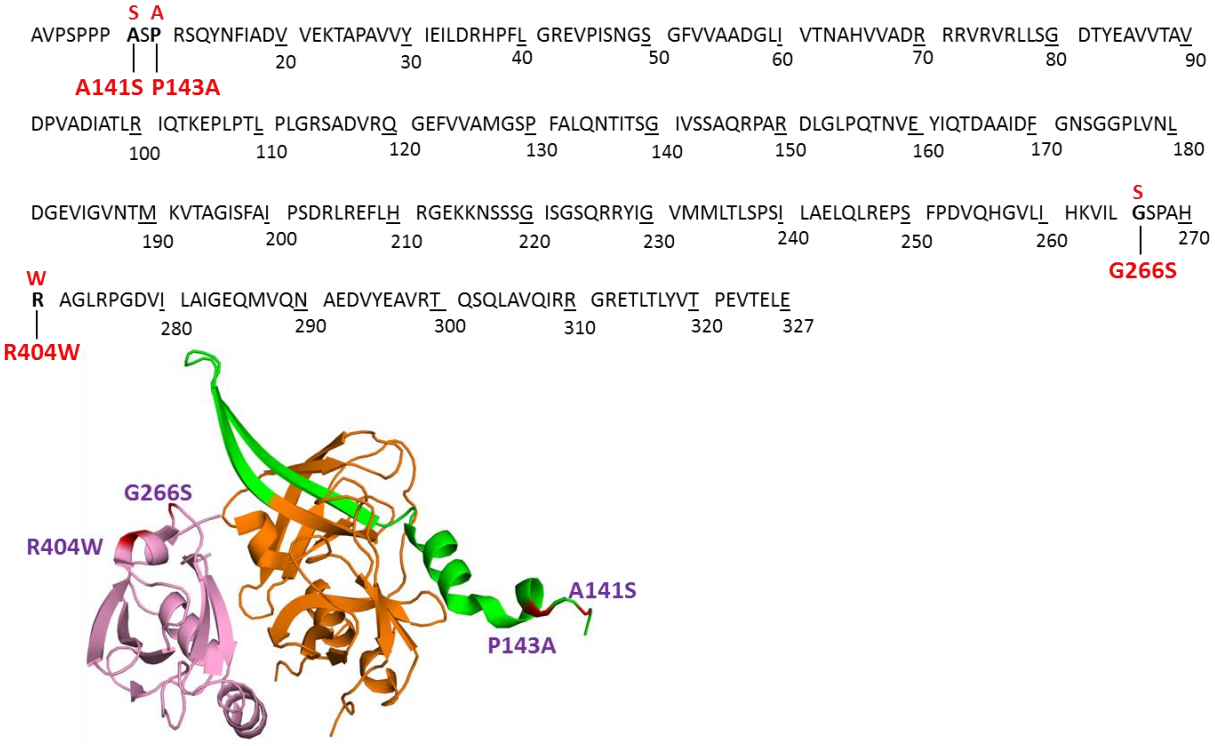

Figure. 1.6: Pathogenic Mutations positions in HtrA2 protease.

Collectively, these independent sequence analysis studies on PD patients' HTRA2 gene from different countries identified few variants with good frequencies. These variants upon functional characterization have been found to be involved in affecting HtrA2's activity. Since HtrA2 has functional relevance in terms of mitochondrial homeostasis as well as its loss causes neurodegeneration with parkinsonian features, we screen for variants in the HTRA2 gene Indian PD patients and performed functional assays of identified mutations or variants

Aims and objectives of the study

Earlier studies indicated that HtrA2 could also induce cell death, either apoptosis (*10*, *27*, *43*) or necrosis (*44*), in a caspase-independent manner through its protease activity, and XIAP has been shown to be a proteolytic substrate in vitro. In contrast to this assumption, mice with either mutant or knocked out HtrA2 suffer from neurodegeneration due to progressive mitochondrial damage (*45-47*). This suggests that HtrA2 is not involved in neuronal apoptosis and fully functional HtrA2 protein is required for preventing mitochondrial damage and ultimately to neurodegeneration.

Mice with mnd2 mutation suffer a great loss of neuronal cells, this led us for the first time in understanding the primary function of HtrA2, i.e. maintenance of the mitochondrial homeostasis. Our main focus was to understand the effect of single point mutation on the overall conformational change in the protein structure using multidisciplinary tools that would ultimately help understand the cause behind inactivity in the protease and its association with neurodegeneration.

Objective 1:

To understand the structural basis of inactivity of mnd2 mutant

Specific aims:

1a. Biophysical study of mnd2 mutant (hHtrA2 S276C) protein using spectroscopy

1b. Structural analysis of mnd2 mutant (hHtrA2 S276C) protein using X-ray crystallography

Objective 2:

Characterization of HtrA2 variants associated with pathogenesis

Specific aims:

2a. Sequence analysis of HTRA2 gene from Indian Parkinson's disease (PD) patients

2b. Biophysical, structural and functional characterization of HtrA2 variants associated with PD

CHAPTER 2:

Materials & Methods

2.1 Materials

2.1.1 Antibiotics:

A. Ampicillin *(Sigma Aldrich)***:** Used for bacterial as well as mammalian clone selection. [Storage 4°C]; final concentration used 100mg/ml

B. Chloramphenicol *(Sigma Aldrich)***:** Used for bacterial clone selection. [Storage 4°C]; final concentration used 100mg/ml

2.1.2 Buffers:

A. Buffers made in Laboratory:

i. **3X Lamellae loading dye:** For SDS-PAGE sample loading. [Storage RT]

TRIS	150mM
SDS	6%
Glycerol	30%
BME	3%
Bromophenol Blue	0.012%

ii. **6X Gel Loading dye for DNA:** [Storage RT]

Xylene Cyanol FF 0.25% (w/v) (migrates at 4160 bp with TAE)

Bromophenol blue 0.25% (w/v) (migrates at 370 bp with TAE)

Glycerol 30% (w/v)

iii. **10X HEPES Buffer** HEPES 10mM, pH 8.0 NaCl 100mM

iv. **10X SDS Running Buffer:** (pH-No need to adjust) [Storage RT]

TRIS	250mM
Glycine	1920mM
SDS	1%

v. **50X TAE:** For Agarose electrophoresis. [Storage RT]

TRIS	2M
Acetic acid	114.2mL (for 1Ltr)
EDTA	50 mM

(pH was adjusted to 7.5 with NaOH and autoclaved)

vi. **Immunoprecipitation Buffer:** [Storage 4°C]

TRIS 50mM (pH 7.5)

NaCl 150 mM

NP-40 0.4-0.6%

Protease inhibitor 1X

vii. **NP-40 Lysis Buffer:** For Mammalian cell lysis. [Storage 4°C]

TRIS	50mM (pH 7.5)
NaCl	150 mM
NP-40	1%
DTT	1mM
Protease inhibitor	1X

NaF	10mM
Na3VO4	1mM
β-Glycerophosphate	10mM

B. Protein Purification buffers: [Storage 4°C]

i. 1X HEPES Buffer HEPES 10mM pH 8.0, NaCl 100mM, Imidazole 10mM

ii. *Ni-NTA Binding/Washing Buffer*

Glycerol	1%
TritonX-100	0.1%
Protease inhibitor	1X (in lysis buffer only)

iii. TBST: For western blots washing. [Storage RT], TRIS 25mM, pH 7.5, NaCl 150 mM, Tween-20 0.1% (w/v)

C. Commercially available Buffer:

10X Fast Digestion Buffer *(Thermo)*

10X Pfu Polymerase Buffer *(Thermo)*

10X Taq-polymerase Buffer (*Thermo)*

2.1.3 Reagents:

Antibodies:

[Storage -20/4°C] Primary antibodies;

Anti-HtrA2 1:1000 (Rabbit monoclonal, *Sigma*)

Anti-FLAG 1:8000 (mouse monoclonal, *Sigma*),

Anti-BAX 1:1000 (mouse monoclonal, *cell signaling technology)*

Anti-BAD 1:1000 (mouse monoclonal, *cell signaling technology)*

Anti-GSK3β 1:1000 (rabbit polyclonal, *cell signaling technology*),

Anti-β-catenin 1:1000 (rabbit monoclonal, *cell signaling technology*),

[Storage 4°C] Secondary antibodies;

Anti-mouse-HRP *(GE-healthcare),*

Anti-rabbit-*HRP (GE-healthcare),*

Bradford Reagent (*BioRad*)**:** Used for protein estimation

Imidazole *(Sigma)***:** For His tagged protein elution 250mM. [Storage 4°C]

IPTG (Isopropyl-D-thiogalactoside) *(Sigma)***:** For bacterial protein induction.

Luria-Bertani (LB) medium: For bacterial culture.

2.1.4 Plasmids:

Mammalian expression vectors:

pCDNA3-WT type HtrA2/ HtrA2 S306A-Flag was a kind gift from Dr. L.M. Martins (Leicester).

Bacterial expression vectors:

pET20b HtrA2-6x His was used for recombinant protein expression.

2.1.5 Primers and Oligos *(Sigma)*

Table-2.1: List of site directed mutagenesis primers

HtrA2 Variant	Forward primer (5'- 3')	Reverse primer (5' - 3')
S276C	CGGCATTGTT**TGT**TCTGCTCAGC	GCTGAGCAGAACAAACAATGCCG
S276A	CGGCATTGTT**GCC**TCTGCTCAGC	GCTGAGCAGAGGCAACAATGCCG
R280A	CTCTGCTCAGCGTGCA**GCC**AGAGACC	GGTCTCTGGCTGCACGCTGAGCAGAG
S306A	TGATTTTGGAAAC**GCT**GGAGGTCC	GGACCTCCAGCGTTTCCAAAATCA
T242M	TAAGGAGCCTCTCCCC**ATG**CTGCCTC	GAGGCAGCATGGGGAGAGGCTCCTTA
T242E	TAAGGAGCCTCTCCCC**GAG**CTGCCTC	GAGGCAGCTCGGGGAGAGGCTCCTTA

2.1.6. SDS-PAGE:

Gel electrophoresis apparatus (BIORAD®)

A. Resolving gel (12%): 10 ml
    a. Autoclaved distilled water – 3.3 ml
    b. 30% acrylamide mix – 4 ml
    c. 1.5 M Tris HCl (pH 8.8) – 2.5 ml
    d. 10% SDS *(sodium dodecyl sulphate)* – 100 µl
    e. 10% APS *(ammonium persulphate)* - 100 µl
    f. TEMED *(tetramethylene diamine)* - 10 µl
B. Stacking gel (5%): 4 ml
    a. Autoclaved distilled water - 2.7 ml
    b. 30% acrylamide mix - 0.67 ml

c. 1M Tris (pH 6.8) - 0.5 ml

d. 10% SDS - 40 µl

e. 10% APS - 40 µl

f. TEMED - 8 µl

C. 1X Running Buffer (pH 8.3): 1L

a. Glycine - 72 gm

b. Tris-base - 15 gm

c. SDS - 5 gm

D. Acrylamide solution:

30% (w/v) containing acrylamide: bis-acrylamide in ratio 29:1

Dissolve in 60 mL of MQ water.

Heat the solution to 37ºC and adjust the volume to 100 mL.

Filter the solution by filtration through 0.22 µm Millipore filter membrane.

Confirm that the pH of the solution is 7.0 or less

E. 10% SDS: (For 100 mL)

10 gm of SDS (Sodium dodecyl sulphate or Sodium lauryl sulphate FWM 288.38)

Dissolve in 100 mL of MQ water.

F. 5X Loading Buffer: 10 ml

a. 0.5 M Tris (pH 6.8) - 4 ml

b. DTT - 0.77 gm

c. 10% SDS - 1 gm

d. Glycerol - 5 ml

e. Bromophenol blue - 0.0025 gm

G. Staining solution: 1L

   a. Commassie Brilliant Blue R250 - 2.5 gm

   b. Methanol - 400 ml

   c. Acetic acid - 100 ml

   d. Double distilled water - 500 ml

H. Destaining solution: 1L

   a. Methanol - 450 ml

   b. Acetic acid - 100 ml

   c. Double distilled water - 450 ml

2.1.7. Crystallization:

   a. Cover slips (16x16 mm)

   b. Crystallization plates (24-well Laxbro®)

   c. Silicon Grease

   d. Siliconization solution (1% Dichlorodimethyl silane in toluene)

Freezing of the crystals:

a. Liquid Nitrogen (77K)

b. Canisters

c. Cryovials and loops

d. Cryoprotectant solution (25% Glycerol in reservoir solution)

Miscellaneous:

i. Nanodrop® Spectrophotometer V3.5.2

ii. Leica® MZ 16 Inverted Microscope

iii. THERMO Scientific - Snake Skin® Pleated Dialysis membrane (10 kDa cutoff)

iv. MILLIPORE® Amicon® Ultra-15 Centrifugal filter unit (15 mL capacity, 10 kDa cutoff)

v. Home Source single crystal X-ray Diffractometer

vi. QIAgen QIAprep® / Sigma Spin-Miniprep Kit

Buffer P1 –

a. 50 mM Tris-Cl (pH 8.0)

b. 10 mM EDTA

c. 100 µg/mL RNAse A32

Buffer P2 –

a. 200 mM NaOH

b. 1% SDS (w/v)

Buffer N3 –

3.0 M Potassium Acetate (pH 5.5)

vii. Circular Dichroism Spectropolarimeter (JASCO® - J 815)

2.2. Methods (Experimental methodologies):

2.2.1. Molecular cloning

For the current study, various plasmids, constructs were either designed and prepared in-house or procured from outside labs. For cloning following materials and Methodologies were followed.

2.2.2. Competent cells preparation

For plasmid transformation *E Coli*, strains like DH5α and BL21 were used and the competent cells of these strains were prepared by following Methodology.

2.2.2.1. Reagents:

i. **SOB** (Supra-Optimal Broth) **Media (100mL):** For optimal growth of bacteria. (2% Bacto tryptone, 0.5% Bacto-yeast extract, 0.05% Sodium chloride, 2.5 mM KCl, 10 mM MgCl2) 10mM MgSO4 and 50mM KCl were prepared separately, autoclaved and added to the incomplete autoclaved SOB.

ii. **Transfer Buffer (pH 6.7) 50mL:** (PIPES, MnCl2, CaCl2) Transfer buffer was prepared in autoclaved Milli-Q, pH was adjusted by adding 1N HCl and filter sterilized by 0.22µm syringe filter.

iii. **DMSO:** Acting as a cryopreserving agent for competent cells.

iv. **Liquid Nitrogen:** For snap freezing the freshly prepared competent cells.

2.2.2.2. Methodology:

Glycerol stock of *E. coli* bacteria strain was streaked on a LB-agar plate and incubated at 37ºC/180rpm for overnight. Single colony was picked up and inoculated in 100mL of autoclaved complete SOB media and incubated at 18ºC/180rpm till the OD reaches up to 0.35 to 0.4.

Note: DO NOT exceed the OD beyond 0.4.

After the OD reaches bacteria culture were centrifuged at 4ºC/5000rpm for 10min. Cell pellet was dislodged and washed with 20mL of chilled sterilized transfer buffer twice, by intervenient centrifugation of 4ºC/5000rpm for 10min. The washed pellet was reconstituted in 10mL of chilled transfer buffer. To this suspension 700µL of DMSO was added drop-wise by intervenient mixing

on ice. This bacterial suspension was aliquoted (100µL) in MCT, snap-freezed in liquid nitrogen and stored at -80ºC.

2.2.3. PCR amplification:

For different gene plasmid constructs preparation the particular gene was PCR amplified from either cDNA library or from another plasmid constructs, using different primer set containing required restriction enzyme sites.

2.2.3.1. Reagents

i. 10X Pfu/Taq Polymerase Buffer
ii. Forward and Reverse primers (10pmol)
iii. dNTPs (10mM) (Working: 200µM)
iv. MgCl2 (25mM) (Working: 500µM)
v. DNA template (~100ng)
vi. Pfu Polymerase enzyme.

2.2.4. Site directed Mutagenesis:

For the expression of mutant gene of HtrA2 site directed mutagenesis Methodology was followed.

2.2.4.1. Reagents

a) 1X HF (High Fidelity) buffer *(Thermo)*

b) Forward and Reverse primer (10pmol)

c) dNTPs (10mM)

d) MgCl2 (25mM)

e) DMSO

f) Wild type Plasmid constructs (100ng)

g) High Fidelity polymerase enzyme *(Thermo)*

h) DpnI restriction Digestion enzyme *(Fermentas/Thermo)*

i) Competent cells

j) LB broth and Agar

k) Plasmid isolation Kit (Mini/Maxi prep) *(Sigma/Quiagen)*

2.2.4.2. Methodology:

Point mutations or deleted mutations were incorporated in the forward and reverse primer of the specific gene. PCR amplification (50µL reaction volume) was carried out using the primers and the specific wild type template by following PCR programme.

Initial denaturation at 95ºC for 5min, Denaturation at 95ºC for 1min, Annealing at 48ºC for 1min Extension at 72ºC for X min (X= size of the vector/2) Total cycle no. 18

Then the PCR mixture was put for restriction digestion with DpnI enzyme at 37ºC for overnight in water-bath.

Then the digested mix was transformed into the DH5α competent cells following the transformation Methodology (Described earlier).

2.2.5. Plasmid isolation (Mini prep):

For selection of positive recombinant plasmid constructs and for transfection of mammalian cells plasmid isolation was performed.

2.2.5.1. Reagents

Miniprep Plasmid Extraxtion Kit *(Sigma)*

2.2.5.2. Methodology:

After overnight incubation (from the Transformation step) the bacteria colonies were picked up, inoculated in (10mL for miniprep/500mL for maxi-prep) LB broth containing ampicillin (100µg/mL of media) and incubated incubated at 37ºC/180rpm for 14-16hr. Then the bacteria culture were pelleted down and proceed for plasmid extraction following the Kit manufacture Protocol.

3. Protein Expression and Purification

One of important application of recombinant DNA technology is to facilitate expression and purification of huge amount of proteins. One of the factors affecting the level of expression of a cloned gene is the strength of promoter. An efficient expression vector system can convert bacterial cells into a protein production system with yields as high as 10-20% of total cellular protein. Since foreign protein can be toxic to host cells, genes must be under very stringent promoter control. The expression vectors generally contain inducible promoters that can be controlled by an inducing agent, e.g. Lac operon is induced by addition of IPTG. In the absence of lactose in the growth medium, the lac promoter is repressed by Lac repressor protein. Induction or turning on of the Lac promoter is achieved by the addition of either Lactose or its analogue, IPTG (isopropyl-β-D-thioglactopyranoside) to the medium. Either of these substances prevents the Lac repressor from binding to the Lac operator, thereby enabling transcription to occur.

In BL21 (DE3), the T7 polymerase is under the control of lacUV5 promoter. BL21 (DE3) carries the Lac I gene in its chromosome. Lac I represses the expression of T7 polymerase. Consequently

the expression of T7 polymerase is induced by IPTG. Adding IPTG to the culture of BL21 (DE3) strain containing expression vector will induce the expression of T7 polymerase which in-turn will transcribe the gene of interest into corresponding protein.

3.1. Requirements:

Sterile LB broth containing Ampicillin (100 mg/ml), IPTG, micropipette with sterile tips, sterile 10 ml pipette, table-top centrifuge.

3.2. Methodology for protein expression:

A single transformed colony from antibiotic resistant LB agar plate was inoculated in 10 ml LB broth containing required amount of antibiotic. The culture was allowed to grow overnight on shaker incubator at 37^{o}C and 180rpm. After 16hrs of incubation, the scaling up of protein expression was carried out by inoculating 10 ml of starting culture to 1000 ml (~1:100 ratios) of autoclaved LB broth containing required antibiotic. The culture was grown at 37 °C till the OD_{600} reaches between 0.6-0.8 i.e. mid-log phase; A_{600} between 0.6-0.8. The protein was induced by adding IPTG (at a concentration of 0.2 mM). The culture flasks were incubated at 18°C for 16-18 h under constant shaking of 200 rpm. Cells were then harvested by centrifugation at 5,000 rpm for 10 min at 4°C. The pellet obtained was stored at -80^{o}C until further use.

3.3. Recombinant Protein Purification:

Protein purification is a sequence of practices projected to isolate a particular type of protein from a complex mixture. Highly pure protein is essential for the characterization of the structure, function and interactions of the protein with ligand, protein, DNA and RNA. The precursor

substance is usually a microbial culture or biological tissue. The various steps during protein purification method may free the protein from undesired substances, separate the protein from debris of the mixture, and finally isolate the desired protein from the whole matrix. Separation of desired protein from all others is usually the most difficult aspect of purification. Purification steps may utilize differences in physiochemical properties such as (for example) protein size, binding affinity and biological activity.

Generally, a purification procedure contains one or more chromatographic separation steps. The fundamental procedure in chromatography is to stream the medium containing the proteins through a packed column with various substances such as agarose. Different proteins interact in a different way with the column matrix and undergo separation during passage through the column. Regularly, proteins are detected as they elute from the column by their absorbance at 280 nm. Many different chromatographic methods exist including,

- Size exclusion chromatography: Separate the molecules on the basis of size
- Hydrophobicity chromatography: Separate the molecules on the basis of hydrophobicity
- Ion exchange chromatography: Separate the molecules on the basis of charge
- Affinity chromatography: Separate the molecules on the basis of affinity towards a tag

Affinity chromatography provides the highest specificity and selectivity for the purification of bio-molecules. Protein molecule has a three dimensional structure, and ligands having ability to recognize one of the structural motifs of a protein is used in affinity chromatography. This interaction can be exceptionally specific and the ligand molecule interacts only with the engineered molecule, or the ligand can be designed in such a way so that it recognizes a group of structural analogous. Ligand on the solid support should possess excellent avidity for its target selection; however, it should be reversible. If the adsorption of target bio-molecule(s) is too strong

it will make it difficult to separate it from bound ligand. If the affinity ligand is a peptide or protein, special care needs to take to keep them physiologically active during the process of purification. Since affinity chromatography is highly specific, it is considered as a powerful tool in purifying proteins from a complex mixture.

3.3.1. Purification of recombinant proteins:

Reagent

a) LB media and LB agar Plate

b) Ampicillin (100mM): Working Concentration: 100µM

c) IPTG (100mM): Working Concentration: 100µM

d) Ni-NTA agarose beads (Genetix)

e) Imidazole (Sigma)

Materials and Methods

f) Ni-NTA Lysis Buffer

g) Ni-NTA Binding/Wash Buffer

j) His-tagged elution buffers

Methodology

Escherichia coli BL21 (DE3) strain cells were transformed with pET20b-HtrA2 (Wt and its mutants) following the standard transformation protocol. Next day single Colony was picked up and inoculated in 10 ml LB medium containing 100µg/ml ampicillin as starter culture and incubated at 37ºC /180rpm shaker condition. After 18hr of growth the starter culture was inoculated into 1ltr sterile LB-amp medium and incubated at 37ºC/180 rpm shaker condition till

the OD reach at 0.6-0.8. OD was checked at 600nm in spectrophotometer. At 0.6-0.8 OD (After ~3-4hr of starter culture inoculation) 100µL of 100mM IPTG was added for protein induction and was incubated at 18ºC/180 rpm shaker condition for 18hr. (Separated flask was kept for uninduced culture). After completion of 18hr growth the bacterial cells were pelleted down by centrifugation at 5000 rpm for 15min at 4ºC then proceed for protein purification methodology.

His tagged Protein Purification methodology

The cell pellet from 1ltr culture was resuspended in ice cold 20mL Ni-NTA lysis buffer purification lysis buffer. Cell suspension was sonicated on ice at 70% amplitude for 60 sec (in each 60 sec sonication with break of 60 sec) 3-5 cycles. Note: The no. of cycle may vary depending on the PCV (Pack cell volume) and till the suspension became comparatively clear. (DO NOT sonicate for a longer time.). The cell lysate was then centrifuged at 13000 rpm for 55 mins, and the supernatant was collected. (Note: Before proceed towards protein purification procedure, small scale cell lysis (From 10mL uninduced and induced bacterial culture) followed by protein induction was checked on SDS-PAGE. 4-5 mL of Ni-NTA agarose bead was added to a 50mL ECONO column (Bio-Rad) and washed twice with Ni-NTA wash buffer. Then the 20mL supernatant lysate was added to the column, mixed properly and kept at 4ºC with rotation for binding for 1hr. After binding the bead was allowed to settle down and the lysate was drained out from the bottom of the column. The bead was washed with 50mL Ni-NTA wash buffer thrice and the flow through was discarded. Note: The flow through can be collected for analysis. Then the bound His tagged protein was eluted from the bead by 5mL elution buffer containing 250mM imidazole. Elution buffer was added to bead 1mL each time followed by 2 minutes incubation. Note: The concentration of imidazole can be standardised depending on the purity of the eluted

protein fractions. The eluted fractions were analysed in SDS-PAGE and quantitate for further purification process.

4. Mammalian Cell Culture and reagents:

4.1. Routine maintenance of cell lines

Cell line used: HEK293T cells (Human Embronic Kidney cells) and Human SH-SY5Y neuroblastoma cells.

HEK293T and SH-SY5Y culture: Both the cell lines were grown on culture dish *(BD-Falcon)* in DMEM *(GIBCO)* supplemented with 10% and 15 % FBS *(GIBCO) respectively*, 37ºC, 5% CO2 and in humid condition.

4.1.1. Reagents

a. Culture Medium (DMEM):

[Storage 4°C] Dulbecco's Modified Eagle Medium (DMEM) containing high glucose, pyridoxine hydrochloride and sodium pyruvate (Invitrogen) was prepared as per the manufacturer's Protocol. Powdered medium was reconstituted in 800 ml autoclaved Milli-Q water under sterile conditions. 3.5 g sodium carbonate was added and pH was adjusted to 7.2 using 1 N HCl. The volume was made up to 1 L was filtered by a sterile filter assembly and stored at 4°C. 1.5mM HEPES, 10% FBS *(GIBCO Invitrogen)*, and 1X antibiotic mixture (of 100IU of penicillin per ml, and 100µg of streptomycin per ml and amphotericin) *(Himedia)* was added to prepare the complete medium.

b. 1X sterile PBS [Storage 4°C].

c. 1X sterile trypsin made in 1X PBS [Storage 4°C].

d. DMSO *(Sigma)* [Storage RT].

4.2. Revival of cryo-freeze cells

i. The vial of cryo-freeze cells was removed from liquid nitrogen and incubated in a 37ºC water bath. The cells were closely monitored until completely thawed.

Note: Maximum cell viability is dependent on the rapid and complete thawing of frozen cells. **IMPORTANT:** Do not vortex the cells.

ii. As soon as the cells were completely thawed, the outside of the vial was disinfected with 70% ethanol and proceeded immediately to the next step.

iii. In a laminar flow hood, the cells were transferred to a sterile 15 mL conical tube and onto that 5 mL of complete DMEM media (pre-warmed to 37ºC) was added drop wise.

IMPORTANT: Do not add the whole volume of medium at once to the cells. This may result in decreased cell viability due to osmotic shock.

iv. The cell suspension was gently mixed by slow pipetting up and down twice to avoid introducing any bubbles. **IMPORTANT:** Do not vortex the cells.

v. The tube was centrifuged at ~1000 rpm for 2-3min to pellet the cells.

vi. Then the supernatant was decanted as much of as possible. **Note:** Steps iii – vi are necessary to remove residual cryo preservative (DMSO).

vii. The cells were resuspended in a total volume of 8 mL of complete DMEM media (pre-warmed to 37ºC).

viii. The above 8mL cell suspension was added onto the culture plate (10 cm); that was pre-incubated in the 37ºC incubator.

ix. Then the cells were incubated at 37ºC in a 5% CO2 humidified incubator.

x. The next day, the medium was exchanged with fresh complete DMEM Medium (pre-warmed to 37ºC).

4.3. Sub-culturing/Passaging of cells, trypsinization and sub-culturing

i. Carefully remove the medium from the culture plate containing the confluent layer of SH-SY5Y cells.

ii. Rinse the plate once with 1X PBS. Note: Add the PBS slowly from the side to avoid detaching the SH-SY5Y cells.

iii. Aspirate the PBS.

iv. Apply 3-5 mL (10 cm plate) of 1X pre-warmed trypsin and aspirate within 30 seconds. Note: Sh-SY5Y cells were trypsinized very fast.

v. Apply 5 mL of complete DMEM Medium (pre-warmed to 37°C) to the plate.

vi. Gently mix the cell suspension. Transfer the dissociated cells to a 15 mL conical tube.

vii. Centrifuge the tube at 1000 RPM for 2-3 minutes to pellet the cells.

viii. Discard the supernatant.

ix. Apply 2 mL of complete DMEM Medium to the conical tube and resuspend the cells thoroughly. Note: Do not vortex the cells.

x. Count the number of cells using a haemocytometer.

xi. Plate the cells to the desired density into the appropriate fresh complete DMEM Medium. It was recommended that ~1.5 million cells be plated at on 90mm plate.

xii. The next day, exchange the medium with fresh complete DMEM Medium. The cells should be ready for passaging or harvesting 2 to 3 days after this step.

4.4. Freezing down the cells

i. The medium was carefully removed from the culture plate containing the 80% confluent layer of SH-SY5Y cells. **Note:** For freezing 70-80% confluence was recommended.

ii. The plate was rinsed once with 1X PBS. **Note:** Add the PBS slowly from the side to avoid detaching the SH-SY5Y cells.

iii. 3-5 mL of 1X pre-warmed trypsin (for 10 cm plate) was added to the plate and aspirated within 30seconds. **Note:** SH-SY5Y cells were trypsinized very fast.

iv. Then 5 mL of complete DMEM Medium (pre-warmed to 37ºC) was added to the plate.

v. Cell suspension was then gently mixed and transferred to a 15mL conical tube.

vi. The tube was centrifuged at 1000 RPM for 2-3 minutes to pellet the cells; the supernatant was discarded and kept on ice.

vii. Freezing media was prepared by adding 10% DMSO in FBS.

viii. 2 mL of freezing media (10% DMSO in FBS) was added to the conical tube slowly and the cells were resuspended thoroughly. **Note:** Do not vortex the cells.

ix. The cell suspension was aliquot into 2 cryo-vials and kept at -80ºC for overnight.

x. Next day the vials were transferred into liquid-N2 for longer storage. **Note:** cells remain viable for more than 10 years in this condition.

4.5.Transient transfection

4.5.1. Reagents

a) Calcium phosphate method (CaCl2 0.5M, 2XBBS).

b) Lipofectamine 2000/3000 *(Invitrogen)*

4.5.2. **Methodology** (Calcium phosphate method):

i. ~1 million SH-SY5Y cells were seeded on a 60mm plate in complete DMEM media and allowed to grow for 24hr at 37ºC, 5% CO2 (for transfection 50-60% confluent plate was the optimum condition).

ii. The media was replaced with fresh complete media.

iii. 4-5hr of media change transfection procedures starts.

iv. 10µg of DNA+Milli-Q was made upto 100µL; 100µL of 0.5M CaCl2 was added, and then 200µL of 2X BBS was mixed with the DNA-CaCl2 mix.

v. Then the solution was kept for 30min at RT.

vi. After the incubation the DNA-mix was added onto culture plate drop wise and was mixed properly.

vii. Or Cells were transfected by lipo-based techniqe according to manufacturer's protocol.

4.6. Mammalian cell lysis

4.6.1. Methodology:

i. Cell were grown in culture till 80-90% confluent

ii. Then the media was completely aspirated and plate was washed with 4mL 1X PBS.

iii. 500µL chilled NP40-lysis buffer was added to the plate (90mm), cells were scrapped from the plate and collected in a MCT.

iv. Then the suspension was vortexed for 10 seconds and incubated on ice for 30min.

v. After the incubation the suspension was again vortexed for 20 seconds.

vi. Then it was centrifuged at 13000 rpm for 30 min at 4ºC.

vii. The supernatant was collected and kept on ice; that is cell lysate.

viii. The protein concentration of the cell lysate was measured by Bradford protein estimation method following the manufacturer protocol and Bradford reagent.

4.7. Live cell confocal imaging

4.7.1. Reagents:

i. Optimum Minimum Essential Media (Opti-MEM), buffered with HEPES and sodium bicarbonate,

ii. 35 mm glass-bottomed dishes (Cell E&G, USA)

4.7.2. Methodology:

i. Cells were grown in the glass-bottomed dishes and were transfected at the confluency of 40-50 % with the desired plasmids.

ii. Post 24-30 h of transfection, the complete medium was replaced with minimally fluorescent Opti-MEM.

iii. To monitor co-localization, confocal imaging was performed with Zeiss LSM 510 META equipped with 100× or 63× 1.4 NA (numerical aperture) objectives. Single- or dual-colour images were obtained using separate excitation in 12-bit format and with line averaging of two.

iv. GFP fluorescence was excited with a 488 nm argon laser and collected between 495 and 550 nm.

v. Transmitted light images were captured in the blue channel. Z-stacks were collected at intervals of 2–4 seconds and laser illumination was minimized to limit photo damage.

vi. Images acquired were further processed using LSM 510 image examiner software.

4.8.Sodium dodecyl sulfate- Polyacrylamide gel electrophoresis (SDS-PAGE)

4.8.1. Reagents:

i. 30% Acrylamide (29.2% acrylamide (w/v) and 0.8% bis acrylamide(w/v)),

ii. 1.5 M Tris-HCl pH 8.8, 1 M Tris-HCl pH 6.8, 10% SDS, 10% APS, TEMED and 6X SDS sample buffer (62.5 mM Tris-HCl pH 6.8, 25% Glycerol, 2% SDS, 0.5% bromophenol blue),

iii. Electrode buffer (5X): 15.1 g Tris base, 94 g glycine and 5 g of SDS were dissolved in deionized water to a final volume of 1 litre.

iv. **Molecular weight markers –** Fermentas page ruler prestained protein ladder-SM 0671

v. **Coomassie staining solution –** 0.25% coomassie brilliant blue R 250, 45% methanol and 10% acetic acid in distilled water

vi. **Destainer –** 45% methanol (v/v) and 10% acetic acid (v/v) in distilled water

4.8.2. Methodology:

The samples were separated on 12% SDS-PAGE depending on the molecular weight of the proteins being analyzed with 5% stacking gel.

4.9. Immunoprecipitation

4.9.1. Reagent:

i. Protein-G sepharose beads/ anti-FLAG-M2 Agarose beads *(GE Healthcare)*

ii. Antibodies (preferably polyclonal)

iii. Mammalian cells (Minimum 10 million cells)

iv. NP-40 lysis buffer

v. IP buffer

4.9.2. Methodology:

i. 1mL of chilled wash buffer (Wash buffer was NP-40 lysis buffer without NP-40) was added into 20µL of Protein-G sepharose beads.

ii. The beads were washed twice by gently inverting the tubes 4-5 times and then beads were pelleted down by centrifugation at 1000rpm for 2 min at 4°C.

iii. The wash buffer was discarded and the beads were esuspended in 1mL of wash buffer.

iv. 2-4µg of Ab/IgG isotype was added into 20µL of Protein-G sepharose beads and kept for binding for 2h/overnight at 4°C on a rotator. (**IMPORTANT**: Do not follow this step for M2-agarose bead and anti-HA-beads).

v. Next day the cells wrew harvested from the culture plates by trypsinization and lysed by NP-40 Lysis Buffer.

vi. Pre-clear cell lysate was prepared by adding required amount of cell lysate into 20µL of Protein-A sepharose beads and keeping it for binding for 1h at 4°C on a roter. (**IMPORTANT**: Do not follow this step for M2-agarose bead and antiHA-beads)

vii. Then pre-clear cell lysate was collected by centrifugation and was added into previously prepared Ab/IgG bound Protein-A sepharose beads.

viii. The total volume was made upto 1mL with lysis buffer and kept it for binding for 2h at 4°C on a roter.

ix. After binding the bead suspension was centrifuged at 1000 rpm for 2 min at 4°C and the supernatant was carefully separated.

x. The beads were washed (4 times) with chilled wash buffer by gently inverting 3-4 times and centrifugation at 1000 rpm for 2 min at 4°C.

xi. Finally the beads were resuspended with 20µL of wash buffer and 10µL of 3 X lamellae buffer (**Importantly without BME**) and boiled at 100°C for 5 mins.

xii. Then the IP-suspensions and 5-10% input (cell lysate) were loaded on a SDSPAGE and the proceeded towards the methodology of western blot.

4.10. Western Blotting

4.10.1. Reagents:

i. Cell lysate

ii. 3X lamellae dye

iii. SDS-PAGE

iv. 1X SDS-running buffer

v. PVDF membrane

vi. 1X transfer buffer

vii. Antibodies

viii. Luminiscence reagent (ECL-prime, GE-Healthcare)

4.10.2. Methodology:

i. Cell lysates were prepared in NP-40 lysis buffer mixed in 1X lamellae dye and boiled for 10 min at 100ºC dry bath.

ii. Then the samples were loaded and separated on SDS-PAGE in 1X SDS-running buffer (150V, 300mA and for 90min). **Note:** Run out the dye front from the gel.

iii. After a complete separation the samples were transferred onto a PVDF membrane in 1X transfer buffer at cold condition (120V, 300mA for 90min). **Note:** Avoid overheating.

iv. Membrane was then put in 3% BSA/5%milk for blocking for 1h at RT or O/N at 4ºC.

v. Appropriate primary antibody dilution (in 1%BSA in TBST) was used for probing.

vi. For membrane washing 1X TBST was used and at least 4 washes were given for time period of 10 minutes each on rocker.

vii. HRP conjugated secondary Ab was used for probing the membrane for 1h at RT.

viii. Then membrane was washed in TBST and detection was done by following manufacturer protocol of ECL-prime.

ix. Various exposures were taken in X-ray film for analysis.

4.11. Immunofluorescence

4.11.1. Reagents:

i. TritonX-100

ii. 3% Paraformaldehyde

iii. TBST

iv. 5%BSA-TBST

v. 1X PBS

vi. Poly-Lysine and Laminin

vii. Chamber-slides and Glass coverslips

viii. Antibodies (primary & fluorophore labelled secondary) and DAPI

ix. Mounting Media; Vectashield *(Vectorlabs)*

x. Nail paint

4.11.2. Methodology:

i. SH-SY5Y cells were grown on sterile glass coverslips or in chamber slide according to the protocol described earlier. **Note:** For better imaging cells should not be grown beyond 80% confluence.

ii. For HEK293T cells, coverslips were coated with 0.1mg/mL of poly-L-Lysine for 1h at RT inside the hood. Then washed with 1XPBS twice.

iii. For hNPCs chamber-slides or glass coverslips were coated with Laminin according to the protocol described previously.

iv. Culture media was removed from the monolayer cells carefully and immediately fixed with 4% paraformaldehyde (pre-warmed at 37ºC) for 20 min at RT.

v. Then the fixed cells were washed with 1X PBS (2mL for 35mm dish or 500µL for 4 well chamber-slides) for 2-3 times very carefully. (Washing time varies 2-3 min). **IMPORTANT:** Do not give vigorous washing or do not agitate the plate or slide.

vi. Cells were then permibilized with 0.3% TritonX-100 in 5% BSA-TBST for 2h at RT. **Note:** After permibilization 1 PBS wash can be given (but optional).

vii. Appropriate primary antibody dilutions (1:50 to 1:100) were prepared in above 5% BSA-TBST solution.

viii. Then the coverslip/chamber-slide was placed on parafilm layered moist chamber.

ix. The antibody dilution was apply on the cell monolayer carefully so that to cover the whole coverslip/well properly and were incubated for 1h at RT or overnight at 4ºC in

a moist chamber. **Note:** For 1cm X 1cm coverslip 100µL and for 4-well chamber-slide 50µL antibody dilutions are enough to cover the cells.

x. After incubation the antibody was decanted carefully and coverslip was placed back to the 35mm dish containing 2mL 1X PBS. The cells were then washed with 1X PBS for 2-3 times very carefully.

xi. Appropriate dilutions of secondary antibody (1:200 to 1:400) were prepared in 5% BSA-TBST solution. **Note: DO NOT** expose the secondary antibody to bright light and further steps should be done in dim light area.

xii. Then coverslip/slide was placed in moist chamber and cells were probed with fluorophore labelled secondary antibody for 1h at RT in dark then washed with PBS slowly as in step-x.

xiii. After the washing, PBS was aspirated carefully and the cells were then probed with 100µL/50µL of DAPI (1µg/mL) solution made in Milli-Q water, for 1min in dark. **Note:** This step was done in the 35mm dish only.

xiv. 2mL 1X PBS was then applied to cells (in 35mm dish).

xv. Finally coverslips were took out from PBS, extra PBS can be decanted to paper towel and mounted on a glass slide containing mounting media (20µL for 1cm X 1cm coverslip). **Note:** The mounting procedure for the chamber-slide was followed from the manufacturer protocol.

xvi. The coverslips were fixed permanently on glass slide by applying nail-paint to the four sides and proceeded for imaging immediately or kept at 4ºC dry and dark place for future use. **Note:** For long storage slides can be placed at -20ºC dry place, but in long storage the intensity of fluorophore gradually decreases.

xvii. Images were taken by laser confocal microscope (Nikon Meta510). A minimum of 5 fields from one coverslip were selected for imaging. The fluorophore intensity and the co-localization of proteins were measured by the software "Zeiss LSM Image Browser".

5. Cell viability assay

5.1. MTT assay

Cell viability was quantified by its ability to reduce tetrazolium salt 3-(4, 5-dimethylthiazole-2ϒ)-2, 5-diphenyl tetrasodium bromide (MTT) to colored formazan products (Sigma# m-2128) as per manufacturer's protocol. MTT reagent (5mg/ml in PBS) was added to the cells at $1/10^{th}$ volume of the medium to stain only viable cells and incubated at 37°C for 4hrs. MTT solubilisation buffer (0.01M HCl, 10% SDS) of two fold volume was added to cells, followed by incubation in the dark at 37°C for 24hrs. The absorbance values were measured on a micro plate reader at 570 nm and 630 nm. Cell viability was expressed as the percentage of absorbance obtained in control cultures.

6. Protein-Protein Interactions

Protein–Protein Interactions (PPI) studies are very important to understand biological functions of complex molecules. Molecular processes in the cell system are approved by molecular mechanism of large pool of proteins organized by their protein–protein interactions. e.g. signal transduction in the cell is accomplished by protein–protein interactions of the signaling molecules and these processes play a fundamental role in many biological activities and several diseases such as cancer and neurodegenerative diseases. PPI is central to virtually every process in a living cell. The PPIs

help us to understand the bioactive core located at the complex interface and design of inhibitor or provide leads for new therapeutic approaches.

There are several techniques by which these PPIs can be studied; however, the requirements of each of these methods are unique and dependent on many properties of the ligand and analyte. Usually a combination of techniques is necessary to validate, characterize and confirm protein interactions. In our study following were the techniques used for measurement of protein-protein interaction:

6.1. Co-Immunoprecipitation

Co-immunoprecipitation (co-IP) is similar in methodology to pull-down assays because of the use of beaded support to purify interacting proteins. The difference between these two approaches, though, is that while pull-down assays use a bait protein to purify any proteins, co-IP uses antibodies to capture protein complexes in a lysate. In a typical experiment, cells are lysed and a whole cell extract is prepared under non denaturing conditions. **Note:** It is essential to use non-denaturing conditions in order to maintain any interactions that occur. An antibody specific to the bait is then added to the extract, forming a primary complex. This complex is then immobilized on protein A or protein G sepharose beads. Proteins that do not bind are removed by a series of washes. The protein complex is then eluted from the beads and dissociated by SDS sample buffer. Samples are then evaluated by SDS-PAGE followed by western blotting with specific antibodies against the binding partners.

Reagent:

a) Protein-G sepharose beads (GE Healthcare)

b) Antibodies (preferably polyclonal)

c) Mammalian cells (Minimum 10 million cells)

d) NP-40 lysis buffer

e) IP buffer

Methodology:

- 1mL of chilled wash buffer (Wash buffer was NP-40 lysis buffer without NP-40) was added into 20µL of Protein-G sepharose beads.
- The beads were washed twice by gently inverting the tubes 4-5 times and then beads were pelleted down by centrifugation at 1000rpm for 2 min at 4°C.
- The wash buffer was discarded and the beads were resuspended in 1mL of wash buffer.
- 2-4µg of Ab/ IgG isotype was added into 20µL of Protein-G sepharose beads and kept for binding for 2h/overnight at 4°C on a rotator.
- Following day the cells were harvested from the culture plates by trypsinization and lysed by NP-40 Lysis Buffer.
- Pre-clear cell lysate was prepared by adding required amount of cell lysate into 20µL of Protein-A sepharose beads and keeping it for binding for 1h at 4°C on a rotor.
- Then pre-clear cell lysate was collected by centrifugation and was added into previously prepared Ab/IgG bound Protein-A sepharose beads.
- The total volume was made up to 1mL with lysis buffer and kept it for binding for 2h at 4°C on a rotor.
- After binding the bead suspension was centrifuged at 1000 rpm for 2 min at 4°C and the supernatant was carefully separated.
- The beads were washed (4 times) with chilled wash buffer by gently inverting 3-4 times and centrifugation at 1000 rpm for 2 min at 4°C.

- Finally the beads were resuspended with 20µL of wash buffer and 10µL of 3X lamellae buffer (Importantly without BME) and boiled at 100°C for 5 min.
- Then the IP-suspensions and 5-10% input (cell lysate) were loaded on a SDS-PAGE and the proceeded towards the methodology of western blot.

7. Biophysical characterization

7.1. Circular dichroism spectroscopy

Circular Dichroism (CD) spectroscopy measures differences in the absorption of left-handed versus right-handed polarized light which arise due to structural asymmetry. Once the protein molecule differentially absorbs the left and right handed light, the emerging light is elliptically polarized. CD spectra in the far UV range (260-180 nm) can be analyzed for the different secondary structural components of the protein such as alpha helix, parallel and antiparallel beta sheet, turn, and others. Absorption minima at λ 208 nm and 222 nm indicate α-helical structure, whereas a minimum at λ 218 nm is a characteristic of β-sheets. The disordered secondary structural elements or random coil protein are characterized by a low ellipticity at 210 nm and negative band near λ 195 nm. Based on the high agreement between secondary structures derived from CD and X-ray crystallography, several algorithms have been developed to provide an estimation of the secondary structure composition of proteins from CD data. Widely used algorithms include SELCON (self-consistent), VARSLC (variable selection), CDSSTR, K2D and CONTIN. An online server DICHROWEB that provide flexibility of analyzing data by various algorithms and databases as well as using several reference sets is used for the data analysis. CD spectra therefore can rapidly determine the overall folding and secondary structural elements of the protein. The method is also very reliable for monitoring changes in the conformation of proteins

under different conditions such as denaturation studies, unfolding experiments, mutational analysis, etc.

7.1.1. Secondary structural analysis

Material: Phosphate buffer (20mM Na_2HPO_4/NaH_2PO_4 buffer pH 8.0, Quartz cuvette (1 mm), CD Polarimeter (Jasco, J815)

Protocol: Far-UV CD data of 10 μM protein in phosphate buffer were collected between λ 250 and 190 nm (Settings: Scan speed 20 nm/s, accumulation-3, data pitch 0.1, and temperature 25 ^oC).

Data analysis

CD data from at least three independent experiments were used for data analysis. The spectra were plotted as ellipticity (θ) on Y-axis and wavelength (nm) on X-axis. Data is represented in the form of the Mean Residual Ellipticity (MRE or [θ]) given as $deg.cm^2.mol^{-1}$, since the value is concentration independent and constant for a protein.

Ellipticity was converted to mean residue ellipticity using the formula,

$$[\theta]MRE = \frac{\theta * MRW}{10 * c * d}$$

, where, MRW (Mean residue weight) = Molecular weight / (number of amino acids -1), 'c' is concentration of protein (mg/ml), d is the pathlength in cm

The data is then saved in Dichroweb format and subsequently analyzed by Dichroweb server (http://dichroweb.cryst.bbk.ac.uk).

7.1.2. Thermal Denaturation

Thermal stability of protein is an index of its overall stability. It can be assessed by monitoring the CD spectrum with increasing temperature. Far-UV CD region can be used to evaluate the secondary structural changes in proteins. The co-operative nature of melting curve shows that the protein is well folded.

Reagents: Phosphate buffer (20mM Na_2HPO_4/NaH_2PO_4 buffer pH 8.0

Protocol: Thermal denaturation of wild-type and mutant proteins was done simultaneously using multi-cell cuvette holder. A Far-UV CD spectrum (λ 260 to 195nm) was collected in a temperature range of 20ºC to 85ºC with an increment of 2ºC/min. At each data point, the sample was equilibrated for 5mins.

Data analysis

Ellipticity corresponding to 222nm at different temperatures was obtained for calculation of melting temperature (T_m). Firstly, ellipticity of fully folded (θ_f) and unfolded forms (θ_u) were estimated using nonlinear regression (GraphPad Prism). This was then used to calculate fraction folded at any temperature (α) with the following formula:

$$\alpha = \frac{[F]}{[F]+[U]} = \frac{\theta i - \theta u}{\theta f - \theta u}$$

, where [F] and [U] are concentration of folded and unfolded forms respectively, and θ_t is the observed ellipticity at a given temperature. To calculate the Tm, the fraction folded at given temperature was further analysed using nonlinear regression (Igor Pro).

8. Protein oligomerization and size characterization

Oligomerization is a common property found among disordered and exposed hydrophobic patch containing proteins. Such protein may form several oligomeric species which may or may not have biological significance. An oligomer is usually referred to a macromolecular complex formed by mostly non-covalent bonding of macromolecules like proteins. Homo-oligomerization takes place when few identical molecules assemble together, whereas, hetero oligomer involves three or more different macromolecules. Protein oligomerization can be detected and characterized using different methodologies. Each technique has its own advantages and disadvantages, and therefore confirmation should be drawn by combining several approaches. The number of techniques available are analytical ultracentrifugation, size exclusion chromatography, scattering techniques, NMR spectroscopy and mass spectrometry to detect and quantify oligomerization.

8.1. Size-exclusion chromatography

Size-exclusion chromatography (SEC) is an analytical technique that separates dissolved macromolecules based on their size and shape (hydrodynamic radius). There are two basic types of size exclusion chromatography. One is gel permeation chromatography, which uses a hydrophobic column packing material and a non-aqueous mobile phase (organic solvent) to measure the molecular weight distribution of synthetic polymers. The other is gel filtration chromatography, which uses a hydrophilic packing material and an aqueous mobile phase to separate, fractionate, or measure the molecular weight distribution of molecules soluble in water, such as polysaccharides and proteins. Separation is carried out by means of a porous separation matrix with different sized cavities. Completely solvated polymer chains diffuse according to their hydrodynamic volume into the cavities of the separation matrix and are sorted in terms of their

size. The molecular weight of an unknown protein is calculated based on the time taken to move through the gel column (Superdex 75 or 200) as compared to the time by the mixture of standard known proteins such as alcohol dehydrogenase, bovine serum albumen, lysozyme, and MBP. The proteins with the higher molecular weights travel faster as they are excluded from the gel compared to low molecular weight proteins.

- Elution volume (V_e)/void volume (V_0) vs. log of molecular masses of standards was plotted to generate the calibration curve.
- The molecular weight of the unknown protein was determined from plot of the log molecular weight of the standard proteins versus k_{av} ($k_{av}=V_e-V_0/V_c-V_0$), where V_e is elution volume of the protein, V_c is the volume of the column, and V_0 or void volume calculated by determining the elution volume of blue dextran (1 mg/ml).

8.2. Dynamic light scattering

Dynamic Light Scattering (Photon Correlation Spectroscopy) is one of the most popular technique for measuring the size and distribution of molecules and particles typically in the submicron region. The Brownian motion of particles or molecules in suspension causes laser light to be scattered at different intensities. Analysis of these intensity fluctuations yields the velocity of the Brownian motion and hence the particle size using the Stokes-Einstein relationship. Most of the "particle size analyzed" operate at 90° and use red light of wavelength 675 nm. DLS is also capable in measurements of several parameters such as molecular weight, radius of gyration, translational diffusion constant etc.

The molecular size estimation in the present work was done using Wyatt technology DynaPro particle size analyser.

Reagents:

Protein solution (1 mg/ml) in phosphate buffer

Methodology:

Protein and buffer solution was filtered (0.45 µm pore size) and degassed prior to measurement. 1mg/ml protein in 10 mM Na_2HPO_4/NaH_2PO_4 buffer (pH 8.0), 100 mM NaCl was used. Histogram analyses of DLS results were carried out using the software DYNAMICS v.6.0

8.3. Native poly acryl amide gel electrophoresis (PAGE)

Native PAGE is one of the most powerful techniques for studying the composition and structure of proteins in its native form, since the conformation and the biological activity of proteins remain intact during this technique. It is occasionally used for molecular weight (MW) measurements; however, SDS-PAGE is easier and in most cases are reliable than native PAGE.

9. In-vitro serine protease enzymatic assay

9.1. Qualitative and Quantitative enzyme substrate (β-casein/ FITC- β-casein)

In quantitative enzyme substrate cleavage assay, the protease activity of wild-type HtrA2 and its variants were determined using a generic substrate for serine proteases, FITC (fluorescein isothiocyanate) labelled β-casein (Sigma). FITC fluorescence was monitored in a multi-well plate reader (Berthold Technologies) using excitation and emission wavelengths of 485 and 535 nm respectively. Reaction rates (v_0) were calculated using linear regression analysis. The steady-state kinetic parameters were calculated from the reaction rates by fitting the data to Hill form of Michaelis-Menten equation:

$$Velocity = Vmax/(1 + \left(\frac{K0.5}{[substrate]}\right)n)$$

On other hand, in qualitative assay which is also referred as gel based assay, in that enzyme and substrates are incubated and catalysis is observed using SDS PAGE.

10. Crystallization

Three-dimensional structural analysis of a protein is highly crucial for understanding how a protein's function(s) is regulated. In a globular protein, polypeptide chain(s) fold to generate a compact structure whose function depends on the arrangement of polypeptide chain in three dimensional space, termed as tertiary structure. Proteins tend to crystallize when provided with appropriate conditions, and in order to achieve crystallization, purified protein undergoes slow precipitation from an aqueous solution. The individual protein molecules assemble and align on each other in the form of lattice held together by non-covalent interactions, and made up of smallest "unit cells" by adopting a dependable orientation. Protein crystallography is commonly used to determine protein's three-dimensional structure via X-ray diffraction method.

X-ray diffraction data cannot be obtained unless a well-ordered crystal appears which provide a diffraction pattern when exposed to X-rays. The diffraction pattern can then be processed to derive the three-dimensional structure of the protein. However, protein crystallization is essentially very tricky due to highly fragile nature of protein crystals. Protein crystals are highly occupied with large channels due to irregularly shaped surfaces, therefore, the non-bonding interaction that grip the lattice usually are formed through solvent molecule layers. In order to grow a well formed crystal, sufficient homogeneity with purity of the protein is required at an optimal pH conditions, as different pH's can result in different crystal packing (*48*). For crystallization, protein should be present in appropriate buffer system and precipitants.

Several factors affect crystallisation of proteins which includes: Sample purity, concentration, temperature, pH, ionic strength and volume of crystallization solution, etc.

Process of crystallization is differentiated into two steps: Nucleation process and crystal growth

Nucleation and growth can occur within the supersaturated regions as depicted in phase diagrams (**Figure 2.1**). The diagram mainly comprises of three regions; unsaturated region, saturated region, and supersaturated region. Growth can occur in saturated or supersaturated region while nucleation most often start in supersaturated region. The major focus of crystallization process is to obtain sufficiently large crystals having dimension between 0.1-0.5 mm. However, it is an extremely challenging task to obtain a diffraction quality crystal. The best approach to get crystallization is through systematic exposure of the protein solution to varieties of buffers which have different combinations of precipitants, such as salts, poly ethylene glycols. For successful crystallization, the protein-precipitant mixture must approach nucleation phase very slowly to provide sufficient time for crystal growth. Most commonly used precipitants in crystallization trail are salts ($(NH_4)_2SO_4$, NaCl, KH_2PO_4), organic polymers (PEG) and alcohols (methanol, ethanol, propanol, acetonitrile). Salt usually maintain the ionic strength of the solution while organic polymers reduce protein solubility by lowering the dielectric constant of solvent. Solubility of a protein is found lowest at its isoelectric point (pI) since protein carries a net zero charge.

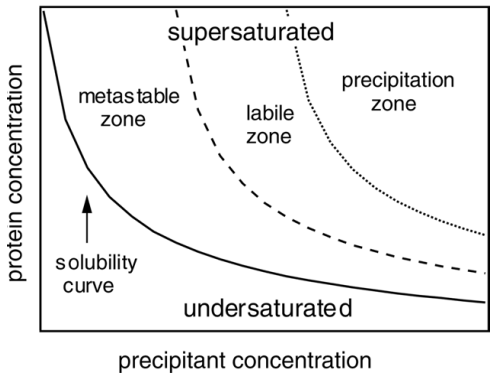

Figure 2.1: The phase diagram of crystallization.

10.1. Methods of crystallization:

Different methods have been developed to crystallize functionally important proteins. Some of the more frequently used methods are vapor diffusion, micro-batch, dialysis and liquid–liquid diffusion method technique.

A. Vapour Diffusion method:

Subcategories into hanging drop and sitting drop. In both the methods a droplet of purified protein, buffer and precipitant is present in a closed system and allowed to equilibrate with a reservoir solution containing the same precipitant in higher concentrations. In the beginning, protein and precipitant concentration in the droplet is different, but as the system equilibrate the diffusion starts from higher concentration to lower concentration which in turn leads to nucleation, a level optimal for crystallization.

Vapor diffusion is a simple and powerful method since it consumes less protein, and several crystallization conditions can be explored with a limited amount of protein. It is also convenient for crystal growth monitoring, crystal manipulation and harvesting.

B. Microbatch:

The problem of microcrystals can be overcome by using a low density paraffin oil (0.87 mg/ml) which float on the surface of protein-precipitant mixture, thus reduces the rate of evaporation (*49*). In this method, a mixture of paraffin and silicon oil can also be used. This is an excellent method for refining the known crystallization condition and optimization of crystal growth (*50*).

C. Dialysis:

The dialysis method employs slow diffusion of inorganic molecules through a semi permeable membrane which results in the formation of supersaturated state of protein solution. The system tries to maintain equilibration between precipitant and solute molecules by allowing selective

passage of water and precipitant. The dialysis bag is kept in a chamber containing the reservoir solution with a precipitant (*51*).

D. Liquid–liquid diffusion method:

In this method, protein and precipitant solution maintain direct contact keeping the dense solution at the bottom. A concentration gradient is generated due to the diffusion of protein and precipitant and crystallization may occur at appropriate protein and precipitant concentration. Free interface diffusion is a method of choice for fine-tuning the crystallization conditions.

10.2. X-Ray Diffraction:

In an X-ray diffraction method, a crystal is exposed to X-ray beam, and diffractions are measured over a suitable detector. There are two kinds of X-ray sources used in protein crystallography:

a. The conventional laboratory X-ray generator (home source) and
b. The synchrotron radiation source.

The high energy X-rays source generates the X-ray of wavelength 0.3-2Å and used in the determination of three dimensional structures of proteins. The crystal is mounted usually in a loop which is attached with goniometer head. The goniometer allows proper centering of the crystal in the X-ray beam so that during rotation crystal remain focused to X-ray beam. Commonly used detectors includes Image Plate, CCD and Pixel Array Detectors.

The electrons present on the periodically arranged macromolecules inside the crystal interact with the X-rays during exposure and diffract X-ray in certain directions. Diffracted rays are captured on the detector as discrete spots called as reflections. The directions of these reflections are given by Bragg's law which states that a reflection is produced only when difference in the path length

for rays reflected from successive planes is equal to an integral number of wavelength of the incident X-rays.

$$2dhkl\ Sin\theta hkl = n\lambda$$

,where λ is the wavelength, θhkl is the angle of incidence or reflection, n is an integer and d is the distance between the parallel lattice planes with Miller indices h,k,l. hkl are the indices for the Bragg reflections. All the Bragg reflections contain information about any given atom in the three dimension structure, and every atom in the structure contributes to intensity of all the Bragg reflections. A Bragg reflection consist sets of parallel planes series and diffracted ray, as reflections from these atomic planes generate constructive interference. In all other cases, reflected waves from successive planes of the crystal become out of phase due to destructive interference and no diffracted beam emerges from the crystal. Intensities of several Bragg diffraction spots need to be collected to solve a protein three dimension structure. This can be achieved by using the rotation method, where the crystal is rotated by small angles and a series of diffraction images generated in which each image contains several reflections collected at a defined angles.

Diffraction data of mounted crystal can be collected either at room temperature or at ultralow temperature (100K) with the crystal bathed in a jet of liquid nitrogen. Room temperature data is generally collected to see the diffraction pattern but due to radiation damage mounted crystal become highly prone for damage. Data collection at cryogenic temperature significantly overcome this problem and X-ray induced radiation damage become minimal. To prevent the formation of crystalline ice and crystal disorderness, cryo-protectant can be applied at the surface of crystal by flash cooling the crystal in liquid nitrogen. Glycerol is the most commonly used cryo-protectant followed by PEG and other organic substances.

In the present work, initial X-ray diffraction data was collected at 100K at home source facility ACTREC. Crystals were equilibrated briefly in cryoprotectant solution of 30% glycerol. A total of 227 frames were collected each for an oscillation angle of 1º and exposure time of 10 min.

Conditions: concentration: 10-25 mg/ml, Temperature: 22 °C, Crystal screen: Hampton

Protocol:

1. Protein of concentration 10-25 mg/ml is spinned in a refrigerated centrifuge at 13,000rpm, for 10 minutes.
2. This protein is then transferred into a fresh eppendorf and neatly labelled.
3. Add around 1ml of the buffer in each well.
4. Take cover slips and put them in a row.
5. Pipette out 1ul of protein in each of the cover slips.
6. Carefully invert the coverslips and place them on the well and ensure that they are properly sealed.

Put the tray in a temperature controlled environment where it won't be disturbed and the tray is observed under the microscope at regular intervals.

11. Molecular Dynamics (MD) simulation:

It is a computer simulation that allows interaction of atoms and molecules for a period of time, providing a view of their physical movements. The trajectories of atomic and molecular motion are determined by considering forces between the particles and potential energy as defined by molecular mechanics force fields. MD simulation use numerical methods to find the properties of molecular systems. In simulation of docking process, the protein and the ligand are physically separated, and then ligand is allowed to find its position into the protein's active conformation. The moves incorporate internal changes to the ligand's structure, translations and rotations. The

advantage of docking simulation is that it more accurately models reality, and ligand flexibility is easily incorporated.

11.1. General steps for MD simulation:

1. Crystal structures retrieval from Protein Data Bank (PDB) (http://www.rcsb.org/pdb/) which can be used as a model template.
2. Model energy minimization: Energy level is the most basic property of molecules that can be calculated using three major theoretical methods, (i) molecular mechanics, (ii) semi-empirical (quantum mechanics), (iii) ab-*initio (*quantum mechanics) approach, Energy minimization is the first step carried out for geometry optimization of the molecular structure.
3. Dynamics simulation and conformation search: Integration of molecular dynamics (solving Newton's law of motion for the nuclei) for all atoms in the system generates molecular trajectories. Conformation search of bio-molecules is carried out by repeating the procedure of rotating dihedral angles to achieve lowest energy conformations of molecular systems.
4. Calculation of molecular properties: Some physicochemical properties such as thermodynamic quantities, solubility, molar volume, heat capacity, molar refractivity density, dipole moment, magnetic susceptibility, partial atomic charge, ionization potential, electrostatic potential, solvent accessible surface area and van der Waals surface area are computed.
5. Structure superposition and alignment: It involves comparison of series of homologous molecules to get the best energy minimized model, which requires superposition or alignment of structures.

CHAPTER 3:

HtrA2 in protein quality control

3.1. *Introduction*

HtrA and Protein quality control function

In our cells, HtrA2 help maintain normal mitochondrial function by maintaining a control over misfolded proteins which formed in the intermembrane space during stress conditions. It is assumed that the key role of HtrA2 is to take care of mitochondria and its homeostasis. The premature demise of rats with knockout of HTRA2 corroborates the crucial role of HtrA2 protease (*47*).

A surprising and unexpected new function of HtrA2 was uncovered when it was found that its inactivation is responsible for the mnd2 (motor neuron degeneration 2) phenotype in mice These animals carry a spontaneous mutation on Ser276Cys located in the protease domain, and homozygous animals exhibit Parkinsonism phenotype a shortened life span, typically dying by 40 days of age (*7, 46, 52, 53*).

The phenotype of HtrA2 KO animals suggests that this protease has two different and opposite functions based on its subcellular location. In the mitochondria, HtrA2 has a cytoprotective function; whereas once it is released to the cytoplasm, it has a pro-apoptotic role. Most of the studies so far have focused on its pro-apoptotic function and very little if anything is known about what it does in the mitochondria. Its bacterial homologue DegP is a molecular chaperone under low temperatures which helps fold proteins and assemble oligomers, but in high temperature environments, it acts as a protease (*20*).

Since DegP acts as a chaperone, it has been assumed that HtrA2 has some sort of similar function while in the mitochondria.

3.2. Experimental Procedures

3.2.1. Purification of recombinant proteins –

Processed and/or mature (Δ133) HtrA2 and all required mutants (S173A, S143C, S143A, R147A) having 6x His-tag in pET-20b were expressed and purified as described previously (*6*). The mnd2 mutant (S143C) was generated by SDM using PCR and were expressed in *E. coli* strain BL21 (DE3). Following are the primers were used during site directed mutagenesis.

Variant	Forward primer (5'- 3')	Reverse primer (5' - 3')
S276C	CGGCATTGTT**TGT**TCTGCTCAGC	GCTGAGCAGAACAAACAATGCCG
S276A	CGGCATTGTT**GCC**TCTGCTCAGC	GCTGAGCAGAGGCAACAATGCCG
R280A	CTCTGCTCAGCGTGCA**GCC**AGAGACC	GGTCTCTGGCTGCACGCTGAGCAGAG
S306A	TGATTTTGGAAAC**GCT**GGAGGTCC	GGACCTCCAGCGTTTCCAAAATCA

Table 3.1: List of primers used in this work. (Mutation is shown as bold and underlined)

Cells were grown at 37°C till the OD_{600} reaches 0.6-0.8 and was then induced with 0.2 mM IPTG. Mutant proteins were purified by affinity chromatography using Nickel-Nitrilo triacetic acid (Ni-NTA) resin (Novagen, MA, USA) in buffer 20 mM Na_2HPO_4/NaH_2PO_4, pH 8.0 containing 100 mM NaCl. Purity of protein was assessed by SDS-PAGE.

3.2.2. Native PAGE assay

Purified proteins (wild type and hHtrA2S276C) in native-PAGE sample buffer (62.5mM Tris-Cl, pH 6.8, 15% glycerol, 0.01% Bromophenol Blue) were separated on a 7.5% native-PAGE. Samples were run along with the standard protein ladder of molecular weight ranging from 40 to 150 kDa (NativeMark™ Unstained Protein Standard, Thermo Fischer. Inc.).

3.2.3. Gel Filtration chromatography

Gel filtration chromatography was performed in a buffer comprising 10 mM HEPES (pH 8.0), 100 mM NaCl referred to as *buffer-B* hereafter. Highly concentrated (~20 mg/ml) purified mutant proteins (S276C and S306A) were separately applied to a Superdex S200 HR 10/300 column (GE Healthcare, Uppsala, Sweden) that was pre-equilibrated in *buffer-B*. Proteins were then eluted in the same buffer at a flow rate of 0.2 ml/min. The standards used for calibration were as follows: bovine serum albumin 66 kDa, Alcohol dehydrogenase 150 kDa, *β*-amylase 200 kDa. Elution volume (*Ve*)/void volume (V_0) *vs.* log of molecular masses of standards was plotted to generate the calibration curve from which molecular weights of hHtrA2 and its variants were calculated as described earlier (*2*).

3.2.4. Dynamic light scattering

Experiments were carried out on DynaPro-MS800 instrument (Watt Technology USA)). The mutant hHtrA2S276C protein and buffer solutions were filtered (0.22µm pore size) and degassed prior to measurement. 3mg/ml protein in *buffer-A* was loaded into a 45µl quartz cuvette. Experiments were performed at 25°C and at least 20–30 measurements each of 10secs duration were collected.. Histogram analyses of dynamic light scattering (DLS) results were carried out using the software DYNAMICS v.6.0. The molecular size estimation in the present work was done using Wyatt technology DynaPro particle size analyzer. From the correlation function, the diffusion coefficients (D_T) of the molecules were calculated by fitting the data. Finally the hydrodynamic radius (Rh) of the particles and molecules were determined:

$$D = \frac{kT}{6\pi\eta 0Rh} \quad \text{---------- (1)}$$

$$Rh = \frac{kT}{6\pi\eta 0Rh} \quad \text{---------- (2)}$$

Here, k: Boltzmann-constant, T: temperature in Kelvin and η_0: viscosity of solvent**.**

3.2.5. Far-UV Circular Dichroism (CD) Spectropolarimetry

Far-UV CD measurements were made using a JASCO J-815 spectropolarimeter (JASCO, Easton, MD, USA) with a 1-mm cell at 25°C in a thermostatted cell holder at a concentration of 10μM in *buffer A*. CD spectra of wild type hHtrA2 and purified hHtrA2S276C were recorded in the far-UV region (260 nm to 195 nm). All spectra were recorded at least thrice and the average blank-corrected data has been plotted.

The *mean residue ellipticity* [θ]mrw, λ in units of *deg.cm2.dmol-1* is given by:-

$$[\theta]mrw, \lambda = \frac{MRW\theta}{10d.c} \text{ ---------- (3)}$$

, where θ is the observed ellipticity (degrees), *d* is the path length (cm), λ is the wavelength (nm), and *c* is the concentration (in units of g/ml). For thermal denaturation studies, far-UV CD experiments were performed between 25 and 100°C at 2°C intervals to measure melting point temperatures (Tm) of wild type and hHtrA2S276C. The mean residue ellipticity was computed as reported previously (*54*).

3.2.6. In vitro enzyme substrate cleavage (protease) assay –

The protease activity of wild-type and its variants were determined using FITC (fluorescein isothiocyanate) labelled β-casein (Sigma, St. Louis, USA) substrate as described earlier (*6*). The cleavage of fluorescent substrate was measured by incubating respective concentration of enzymes with increasing concentrations (0 – 20 μM) of β-casein at 37°C in reaction buffer (20 mM Na_2HPO_4/NaH_2PO_4, pH 8.0 containing 100 mM NaCl, 0.1 mM β-mercaptoethanol (ME)). FITC-fluorescence was monitored in a multimode plate reader using excitation wavelength of 485 nm

and emission at 535 nm. Reaction rates (v_0) were calculated using linear regression analysis. The protein activation curves were fitted to the following equation:

$$Velocity = Basal + max/(1 + \left[\frac{Kact}{substrate}\right]n)$$

, where 'K_{act}' is half maximal activation constant and 'n' is the Hill constant (*55*). The steady-state kinetic parameters were calculated from the reaction rates by fitting the data to Hill form of Michaelis-Menten equation,

$$Velocity = Vmax/(1 + \left(\frac{K0.5}{[substrate]}\right)n)$$

, where 'V_{max}' is the maximum velocity and $K_{0.5}$ is substrate concentration at half maximal velocity using KaleidaGraph (Synergy software). All the experiments were done in triplicate and the mean ± S.E.M. values are shown in the results.

3.2.7. Protein crystallization:

FPLC purified hHtrA2S276C protein at a concentration of 25 mg/ml was used for setting up crystallization trials as described in materials and methods. Crystallization trials were set using commercially available crystallization kits (Hampton Research, Inc) using sitting (initial trials) and hanging drop methods. Initial crystallization drop volume of 3 µl containing 2 µl protein and 1 µl mother liquor mixture was equilibrated through vapour diffusion against 0.5 ml of precipitant solution in the reservoir at 22°C. This crystallization conditions were observed at different time points, and further optimised by varying the pH as well as concentration of precipitant and salt. The crystals were confirmed as protein crystals by staining with Izit dye from Hampton Research. Initially, crystals-like particles were observed in one of the wells containing **formulation no. 21 (0.1M MES pH 6.5 (buffer), 2M NaCl (Precipitant), 0.1M KH_2PO_4 and 0.1M NaH_2PO_4)** from

Crystal Screen 2 (Hampton research). For the crystallization of catalytically inactive mutant HtrA2S173A, same condition was followed. Further finer optimization of crystallization conditions led to formation of larger crystals.

3.2.8. Diffraction data collection and processing:

The hHtrA2S276C crystals (with a biggest dimension of 0.3 x 0.2 x 0.2 mm) obtained after 2 weeks were cryo-protected using 30% (v/v) glycerol as cryo-protectant prepared in mother liquor solution, and thereafter crystals were flash frozen in liquid nitrogen before exposure to X-rays. Initial diffraction data were collected using rotating anode X-Ray Generator (Bruker) and Image plate (MAR Research), operated at 50 kV and 100mA (Macromolecular X-ray diffraction facility at ACTREC). The crystal diffracted to about 2.05 Å resolution. A total of 180 oscillation frames were collected at 100 K with the detector set at a distance of 250 mm. The diffraction data were processed using iMOSFLM (*56*) software, and scaled using SCALA program from CCP4 suite (*57*). V_M and filling map was calculated and solvent content was estimated (*58*). Later on, for the actual data collection of the single-crystal of hHtrA2S276C mutant protein crystals were carried out on the protein crystallography beam line (PX-BL21) at the 2.5 GeV Indus-2 synchrotron radiation facility RRCAT, Indore, India (*59*). The crystals were soaked in a cryo-protectant solution (reservoir/well solution with 30% glycerol). A total of 131 diffraction images for S276C crystals were collected on a MAR225 CCD (Rayonix) detector from a cryo-cooled crystal (100 K) by using 1° oscillation and X-rays of wavelength 0.97947 Å. Similarly, for hHtrA2S306A, multi-wavelength X-ray data were collected at the beamline BM30 (FIP), ESRF Grenoble. All data sets were collected using the single, flash-frozen crystal of hHtrA2S306A of size 0.35 x 0.45 x 0.2 mm.

Data were indexed and integrated using software **X**-ray **D**etector **S**oftware (XDS) and were subsequently scaled using the software AIMLESS from the CCP4 suite (*60*).

3.2.9. Structure Solution of hHtrA2 S276C structure:

Crystal structure of the mutant HtrA2 was solved by Molecular Replacement (MR) using Phaser program (*61*). The hHtrA2S306A structure (PDB ID-1LCY) was acquired from the Protein Data Bank, and was processed for removal of water and ligand molecules from the coordinate file, and was thereafter used as the search model (*62*). The rotational and translation searches were carried out using PHASER software (*63*) and the MR solution was further refined by REFMAC 5 of CCP4 suite (*57, 64*). Initially the model was refined as rigid body, and later rounds were of restrained refinement (*64*).

3.2.10. MD simulation and analysis

The coordinates of the initial structure used in this study were from the crystal structure of hHtrA2S306A (1LCY) (*1*) procured from the protein data bank (PDB) (*65*). The crystal structure of already available HtrA2 (1LCY) was having disappeared N-terminal residues (AVPSP) and two flexible regions (^{344}RGEKKNSSSGISGSQ^{358} and ^{282}ARDLGLPQT^{290}) therefore, we modelled and refined the missing loop regions using Prime 3.0 (Schrodinger, LLC, New York, 2011). Accordingly, we created S276C on the same template for our further MDS studies. We subjected both the proteins (wild type HtrA2 and hHtrA2S276C) to molecular dynamics simulation run for 10 ns each using GROMACS suite where, AMBER99sb-ILDNP force field (OPLS-AA) was used to generate topology and parameter files (*66-68*). For each structure, all water molecules (TIP3P water model) within 3.0 Å of a nitrogen or an oxygen atom were included in the search. To bring the net charge of the system to zero, each of them underwent neutralization process through the

replacement of solvent molecules with ions. 1500 steps of steepest- descent minimization was performed for each system where the Lennard-jones interaction cut-off was kept at 10Å and the electrostatic interactions were treated using particle-mesh Ewald method (PME)[4,5]. All calculations were run under periodic boundary conditions using an orthorhombic (minimum distance between protein and cell faces was initially set to 10 Å) cell geometry.

Results:

Determining oligomeric property of hHtrA2S276C

According to the crystal structure of catalytically inactive mutant (Ser306Ala) of hHtrA2 (PDB: 1LCY) shows that Serine 276 is positioned near one of the residues involved in trimerisation (Phe 256), as shown in **Figure 3.1A** (*1*).

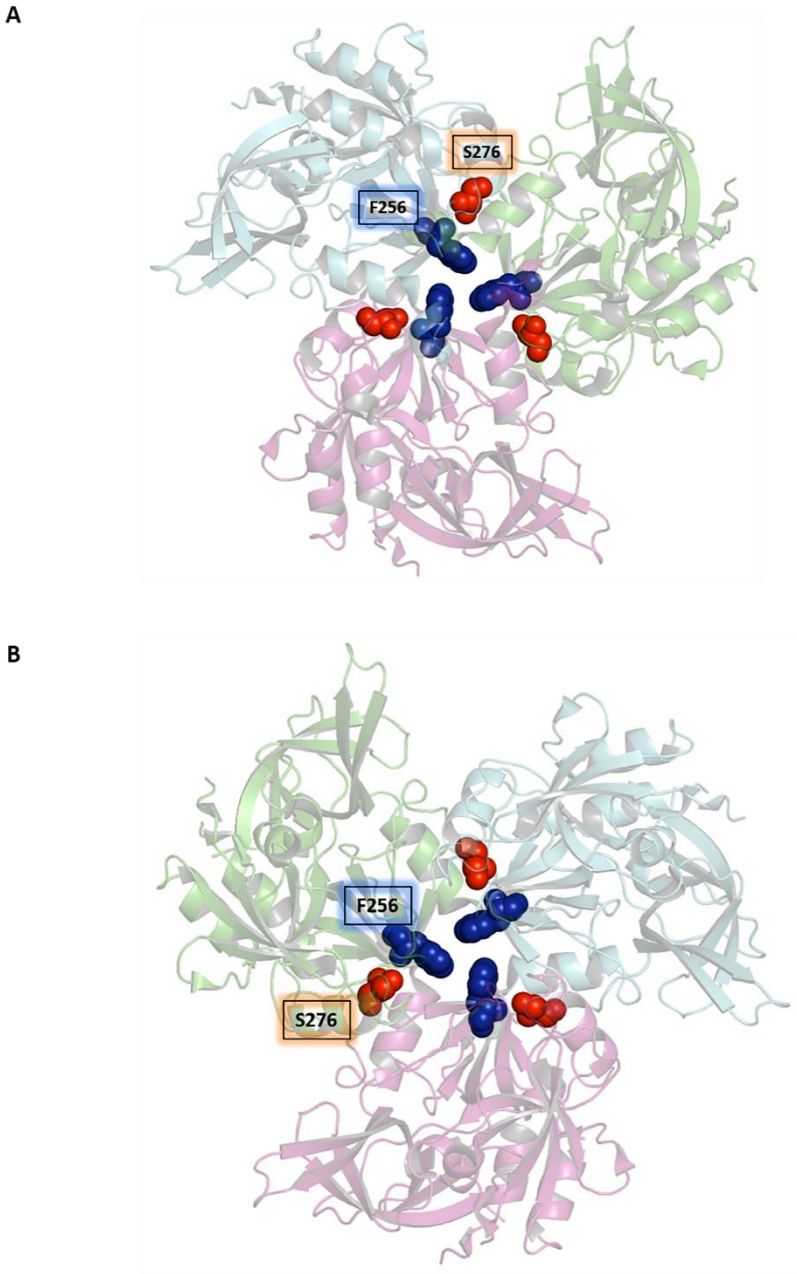

Figure 3.1A. Location of S276C in the crystal structure. (A and B) Top and Bottom view of Cysteine 276 (Red-spheres) is located in the vicinity of, F256 (Blue spheres) which is one of the crucial residues involved in the homotrimerisation of hHtrA2, three different colored subunits with circle showing F256 interconnection. The arrows represent the residue.

To inspect whether S276C mutation impacts the trimeric structure of the protein, we determined its apparent molecular weight (MW) using native-polyacrylamide gel electrophoresis (Native-PAGE), size exclusion chromatography (SEC) and dynamic light scattering (DLS).

In the native PAGE, comparison of mobility of both the bands (wild type & mutant) with the standard markers depicted that the proteins are of equal molecular weight **(Figure 3.2B)**. However, native PAGE separates proteins depending upon the charge they have, wild type hHtrA2 bands displaced slightly down relative to hHtrA2 S276C. Likewise, to validate the results of native PAGE experiment, quantitative approaches have been used such as SEC and DLS. In SEC, both the wild type and mutant hHtrA2 were eluted at detected as single peaks at ~70ml of elution volume **(Figure 3.2C**), similar oligomeric status for wild type hHtrA2 has been observed previously (*2*), suggesting the mutation does not affect the oligomeric property of hHtrA2 protein. Our DLS data also showed that mutation did not affect the overall conformation as the hydrodynamic radii of both wild type hHtrA2 and hHtrA2S276C were found to be very similar (*69*). Furthermore, DLS analysis also provided average polydispersity of 12.5% at 25°C for hHtrA2S276C indicating its homogeneity **(Figure 3.2D)**

B

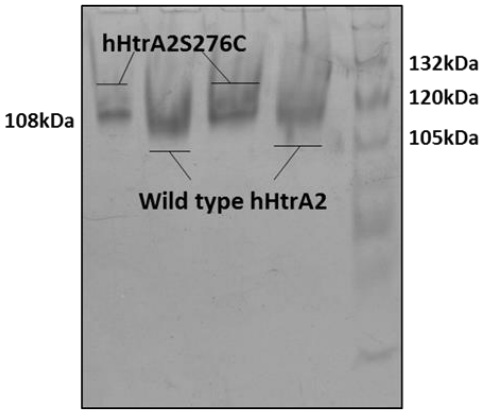
hHtrA2S276C
132kDa
120kDa
108kDa
105kDa
Wild type hHtrA2

C

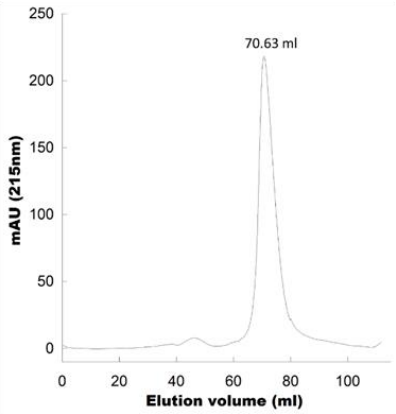
70.63 ml
mAU (215nm)
Elution volume (ml)

D

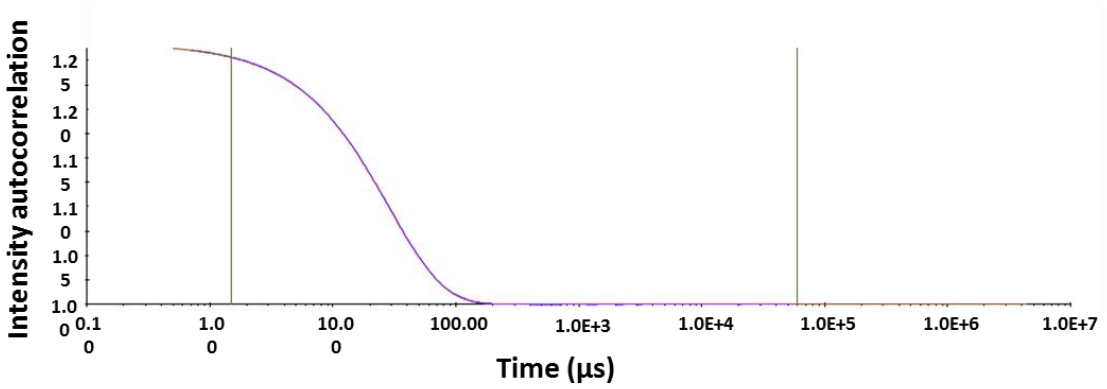
Intensity autocorrelation
Time (µs)

E

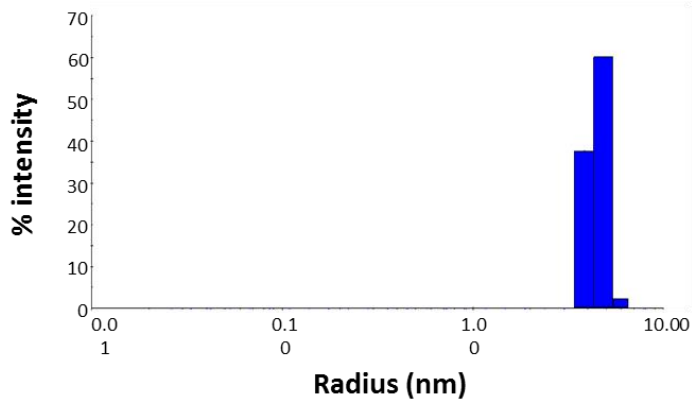
% intensity
Radius (nm)

F

	Radius (nm)	%PD	Mw-R (kDa)	%intensity	% mass	% number
Peak 1	4.5	12.3	114	100	100	100

Figure 3.2. Effect of S276C mutation on the overall conformation of hHtrA2 protease (B) 7.5% native PAGE resolving gel visualized by staining with coomassiae brilliant blue shows similar band size for both the proteins, (C) Size exclusion chromatography showing elution peak of hHtrA2S276C at ~70ml that corresponds to ~108kDa as described under Materials and Methods section, (D) **Dynamic light scattering data analysis.** Correlation function graph which indicates intensity fluctuations of scattered light with respect to time (μs) to determine how rapidly the intensity fluctuates, which is related to the diffusion behavior of macromolecules, (E) Particle size distribution of hHtrA2S276C particles in histogram format. (F) Table showing average hydrodynamic radius of hHtrA2S276C particles and polydispersity index

Secondary structural organization and thermal stability of hHtrA2S276C protein

To investigate whether S276C mutation results in alteration in the protein or its stability, far-UV CD spectroscopy was performed on purified wild type and hHtrA2S276C as observed in **Figure 3.3A.** (*54*). The spectra that are typical for proteins with α-helical and β-stranded structure (*2*) overlap on each other suggesting no significant secondary structural changes has occurred in presence of mutation.

Furthermore, to conclude whether S276C mutation has affected thermal stability of hHtrA2, both wild type and the mutant were subjected to thermal denaturation conditions. Change in ellipticity

at 208 nm as a function of temperature has been represented in **Figure 3.3B**, which show a T_m value of hHtrA2S276C to be □74°C, which is comparable to that of wild type hHtrA2 as reported earlier (*2*). This study indicates that hHtrA2 retains its stability upon S276C mutation and it caused neither destabilizing nor stabilizing effect on the overall structure of protein.

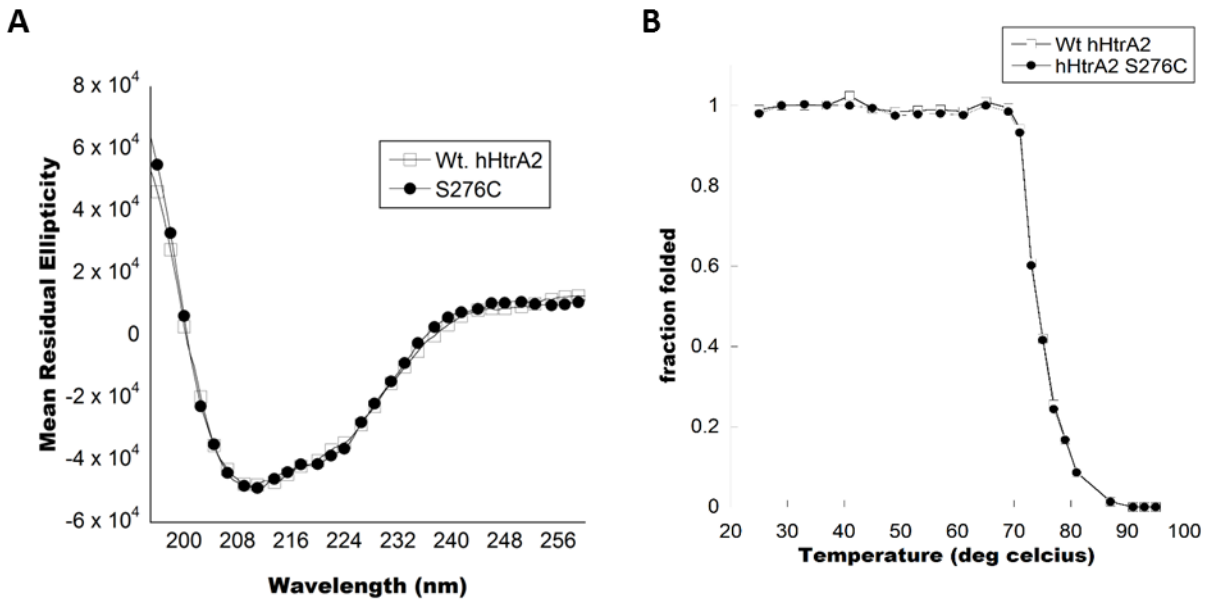

Figure 3.3. Effect of S276C mutation on the overall conformation of hHtrA2 protease (A) CD study of hHtrA2S276C mutant. CD spectra of wild type hHtrA2 and hHtrA2S276C between 195 nm and 260 nm show very similar secondary structural architecture. The plots are average of data obtained from experiments done in triplicate. (B) Thermal denaturation experiment of wild type hHtrA2 and hHtrA2S276C using far-UV CD spectroscopy within the temperature range of 20° to 100°C.

In summary, CD analysis of the both Wt and S276C HtrA2 established that their secondary structure and thermal stability were not significantly changed when compared to each other. Thus, we consider that our deductions based on the analysis of the Wt. HtrA2 and its variant are effective,

and the experiential and conferred changes in proteolytic activity of hHtrA2S276C must be due to the subtle changes in the overall tertiary and, probably, quaternary, structure.

Important L3 loop residues important for hHtrA2 activity

To know the importance of the serine residue at position 276 toward hHtrA2 activity, site-directed mutagenesis was performed to replace it with a smaller and hydrophobic alanine residue. *In vitro* substrate cleavage assay using β-casein (both gel-based and fluorescence-based) showed no activity in hHtrA2S276A **(Figures 3.4 A and B)**, suggesting that the serine on loop L3 might be important for positively regulating the activity of the protease. Since both the mutants (hHtrA2S276C and S276A) were found to be inactive, we could not calculate the reaction rate of

catalysis, however we have presented the kinetic parameters for the wild type hHtrA2 as shown in **table 3.2**, which is comparable to previous literature reports (*2*).

A

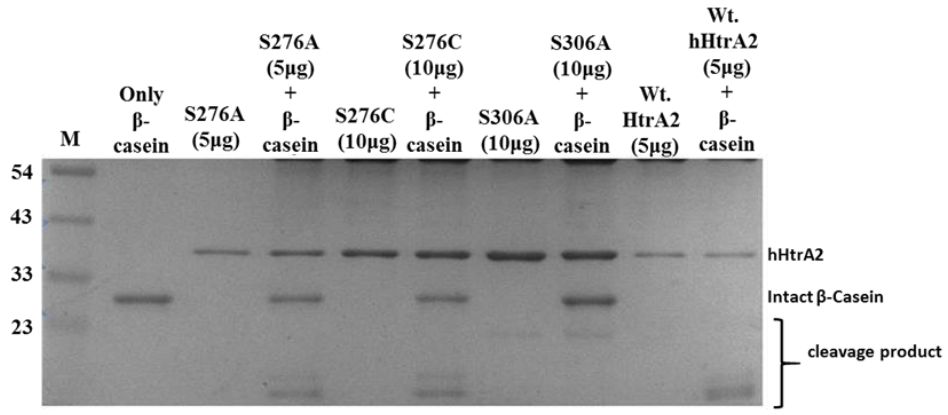

B

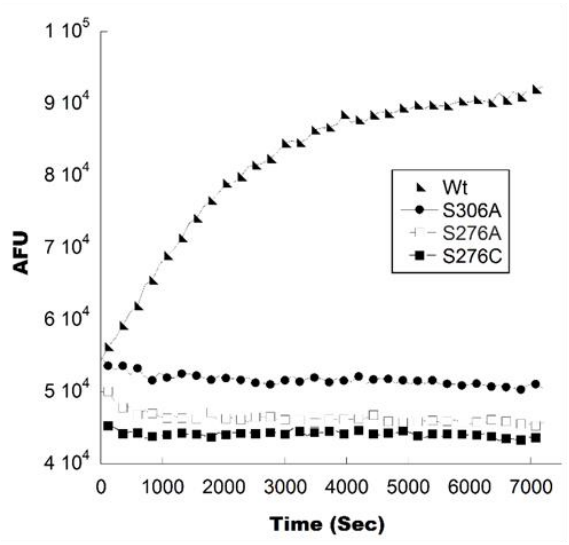

C

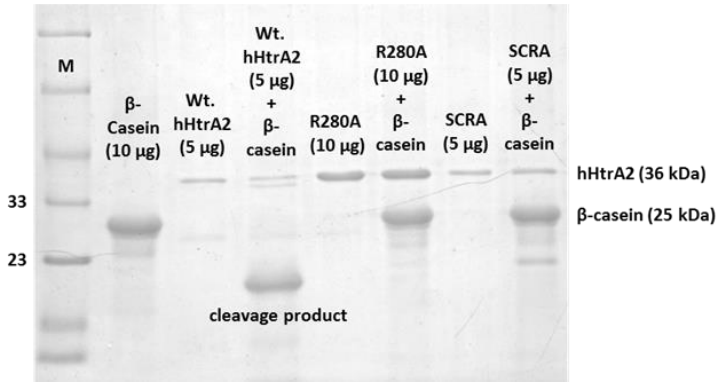

Figure 3.4. Effect of conserved L3 loop residues (S276 and R280) on protease activity A) 12% SDS gel showing in vitro (gel based) β-casein (substrate) cleavage assay for hHtrA2S276A, (B) In vitro (fluorescence based) protease assay for hHtrA2S276A; here hHtrA2S306A (negative) and wild type hHtrA2 (positive) are used as controls (C) In vitro (gel based) β-casein cleavage assay for hHtrA2R280A. Abbreviations: SCRA (S276C + R280A) double mutant. Loss of activity was observed in hHtrA2S276A and hHtrA2R280A mutants at given enzyme concentrations.

	V_{max} (M/s)	K_m (µM)	k_{cat} (s^{-1})	Hills coefficient (n)	k_{cat}/K_m ($M^{-1}s^{-1}$)
Wild type hHtrA2	$2.9x10^{-11}$	6.5815	$5.9x10^{-6}$	2.1185	$8.96x10^{-7}$

Table 3.2: Kinetic parameters for wild type hHtrA2

With an aim at understanding the importance of loop L3 (on which S276 is located) for protease activity, the residues of the loop were scanned and the conserved residues were identified. Amongst some of the previously identified residues, Arginine 280 was found to be highly conserved across species. Crystal structure of liganded and unliganded DegS and hHtrA1 (*3, 4*) demonstrate that upon substrate binding, this conserved arginine residue interacts with residues in LD* leading to conformational changes at and around the active site making it more conducive for substrate binding. To understand the importance of this arginine residue in hHtrA2, we mutated it to alanine in wild type hHtrA2 as well as in hHtrA2S276C (double mutant). The protease activity using substrate β-casein was monitored as a function of enzyme concentration. For all the concentrations of hHtrA2R280A and hHtrA2 (R280A, S276C), no activity was observed compared to wild type hHtrA2 as shown in **Figure 3.4C,** suggesting R280 is important for hHtrA2 activity and the

structural determinants on loop L3 that modulate HtrA activity might be overall conserved between DegS, hHtrA1 and hHtrA2.

X-ray crystallographic structure determination and refinement

Crystallization trials of hHtrA2S306A were carried out side-by-side along with hHtrA2S276C for structural comparison under similar crystallization conditions. Both the protein crystals were of good quality and diffraction data were collected to 2.05Å resolution. The R_{merge} for hHtrA2S276C in the highest resolution shell was 74.8%, the Mean I/ sigma (I) and the completeness in the highest resolution shell were 2.0 and 99.6%, respectively; therefore, the data were processed to 2.05 Å resolution.

Processing of the diffraction data using **X**-ray **D**etector **S**oftware (XDS) (*70*) showed that the crystal belonged to space group H3, with unit-cell parameters (in Å) a = b = 84.38, c = 127.84, $\alpha = \beta = 90^{o}$, $\gamma = 120^{o}$. Calculation of the Matthews coefficient showed the presence of one molecule (considering the molecular weight of 36 kDa) in the asymmetric unit, with a VM (Matthews, 1968) of 2.48 $Å^3$ Da^{-1} and a solvent content of 50.36%. Data were indexed and integrated using software XDS and were subsequently scaled using the software AIMLESS from the CCP4 suite (*60*). Analysis of diffraction data revealed that the crystals were twinned with the twin law (h, -h-k, -l). Molecular replacement and phasing were carried out using Phenix software (*71*) with the coordinates of the inactive form of hHtrA2 (hHtrA2S306A) (PDB code 1LCY, Li et al, 2002) as the search model. A test set composed of 5% of the total reflections, assigned at random, was excluded from refinement to allow calculation of the free R factor. The final twinned R_{work} and R_{free} were found to be 15.72% and 18.82% respectively. No density was obtained for a part of L3 loop (residues 281-291) as well as the hinge region that connects protease to PDZ

domain (344-358) and therefore they have not been included in the final model. However, the S276C mutant residue is visible in the crystal structure.

	hHtrA2S306A	**hHtrA2S276C**	**hHtrA2S306A**
PDB entry	-	5WYN	1LCY
Data collection and processing			
Beamline	ESRF, BM30 (FIP)	PX-BL21, Indus-2	X12C
Wavelength (Å)	0.979763	0.9792	0.9788
Space group	H3	H3	R3
Unit cell dimensions			
a, b, c (Å)	85.96, 85.96, 126.97	84.28, 84.38, 127.84	-
α, β, γ (°)	90, 90, 120	90, 90, 120	90, 90, 120
Diffraction data			
Resolution range [Å] (highest resolution shell)	43.0 - 1.84 (1.95 – 1.84)	48.08-2.05 (2.11-2.05)	-
Unique reflections	30244	21668	23,282
R_{merge} [%] (highest resolution shell)	7.8 (78.1)	6.4 (74)	5.8 (10)
Completeness (%) (highest resolution shell)	99.9 (99.6)	99.8 (99.6)	99.4 (99.8)
$CC_{(1/2)}$ (%) (highest resolution shell)	99.8 (58.2)	99.8 (99.9)	-
I/sigma (I) (highest resolution shell)	14.89 (2.04)	16.4 (2.0)	17.5(-)
Refinement			
Resolution (A˚)	42.98 – 2.01	42.823 - 2.05	20 – 2.0
R_{work}/R_{free} (%)	16.51/22.05	15.72/18.82	21.5/24.1
MolProbity statistics			
Outliers (%)	1.72	0.00	-
Allowed (%)	2.76	4.18	-
Favored (%)	95.52	95.82	-
Rotamer outliers (%)	0.00	0.00	-

Table 3.3 summarizes the data collection and refinement statistics for both the crystal structures

Structural basis of inactivation of hHtrA2S276C mutant:

In overall conformation of all the serine proteases, the foundation of the structure called as catalytic triad in such a way that it is sufficiently close for electron transfer from Aspartate to Serine through Histidine is essential for formation of a catalytically active enzyme (*20*). In mature hHtrA2 (PDB: 1LCY), catalytic triad comprises His198, Asp225 and Ser306 (*1*)**.** Structural comparison of the both the crystal structures 1LCY and 5WYN showed that hHtrA2S276C maintains proper hydrogen bonding distances. For example, the atomic distances between the nitrogen (ε) atom of His198 and the oxygen (γ) of Ser306 has been found to be 3.2Å and that between the nitrogen (δ) of His198 and the oxygen (δ) of Asp228 for this structure was 2.8 Å. However, presence of C276 in L3 loop might have adversely affected the activity of the protease due to significant reduction in the number of water molecules as observed **(Figure 3.5A)** in the crystal structures of the two proteins (hHtrA2S306A PDB: 1LCY & hHtrA2S276C PDB: 5WYN) **(Table 3.4).**

PDB ID	Resolution (Å)	Space group	Total no. of water molecules	Reference
1LCY	2.01	H3	301	Li et al 2002
5WYN	2.05	H3	190	-
-	2.01	H3	305	

Table 3.4: Comparison of number of structural water molecules of crystal structures

Water (W) molecule no. 377, forms an interaction between side chains of S276 and I270* (distance 4.1Å) of the adjacent molecule **(Figure 3.5B-D).** However, in case of the mutant hHtrA2S276C, where highly hydrophobic cysteine residue (CH2-SH) replaces the serine, W377 is absent suggesting abrogation of this water-mediated interaction might have adversely affected its activity. To eliminate the possibility of this observation being an artifact (as a consequence of different crystallization conditions), active site mutant hHtrA2S306A was crystallized under identical crystallization conditions as hHtrA2S276C. Superimposition of the structures of hHtrA2S306A and 1LCY (277 Cα atoms with RMSD value of 0.242Å) confirm that the same water molecule (W3777 in case of 1LCY) is present in the hHtrA2S306A as well with a stable *b-factor* (*temperature factor*) of 18.68 $Å^2$ thus highlighting its functional relevance **(Figure 3.5E).**

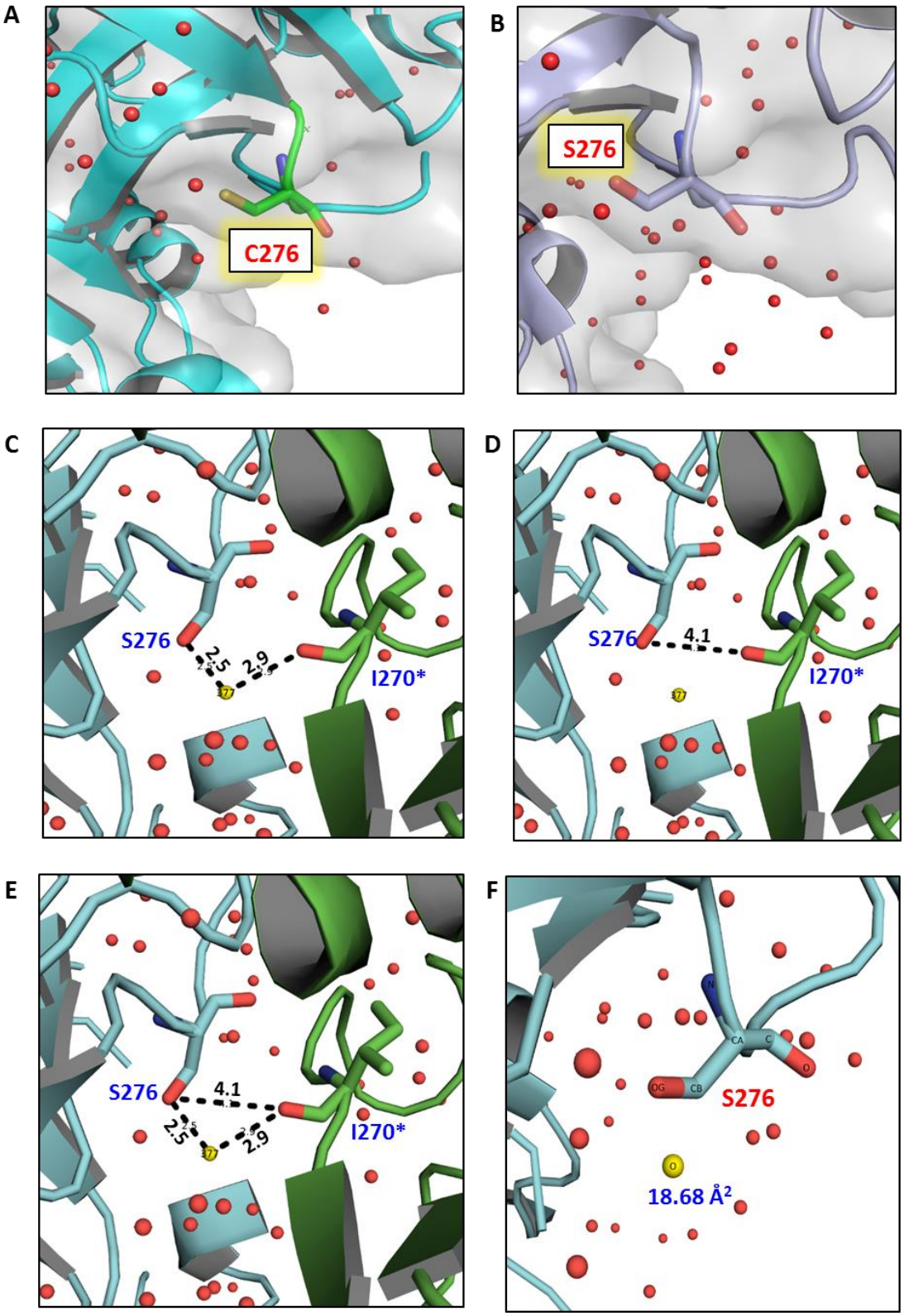
A
C276
B
S276
C
S276
2.5
2.9
I270*
D
S276
4.1
I270*
E
S276
4.1
2.5
2.9
I270*
F
N
CA
C
O
OG
CB
S276
O
18.68 Å²

Figure 3.5. Monitoring water molecule and its interaction around cysteine 276 in hHtrA2S276C structure (A) hHtrA2S276C in cyan (PDB: 5WYN) depicting significantly less water molecules around C276 (indicated in green; stick model) as compared to (B) hHtrA2S306A (PDB: 1LCY) crystal structure (light blue). (C) Water molecule (W377) involve in strong H2 bonding between S276 and I270*, (D & E) Atomic distance between –OH of serine and =CO (main chain) of I270* is 4.1Å, which in presence of W377 is forming strong hydrogen bond. Positions of the ordered water (solvent) molecules are shown as red crosses. W377 water molecule is shown by yellow non bonded (nb) _spheres, (F) W377 molecule (yellow colored) with its *b-factor*

Characterization of water-mediated stability using Molecular Dynamics Simulation (MDS):

To further validate the importance of W377 molecule in stabilizing the protease structure in the dynamic loop region, MDS was performed. The coordinates of the structures used were the crystal structure of hHtrA2S306A (PDB: 1LCY) (*1*) and modeled structure of S276C created on the same template for further MDS analysis for 10 ns. Upon analyzing the trajectories visually, and using water mediated hydrogen bonds with important residues, we observed that in case of hHtrA2S276C, there is no water mediated hydrogen bonding with the cysteine residue **(Figure 3.6A, Video file 1A)** On the other hand, in hHtrA2S306A there is a stable water mediated hydrogen bonding interaction with the serine residue **(Figure 3.6B, Video file 1B)** thus reiterating the importance of the water molecule (W377) in its activity.

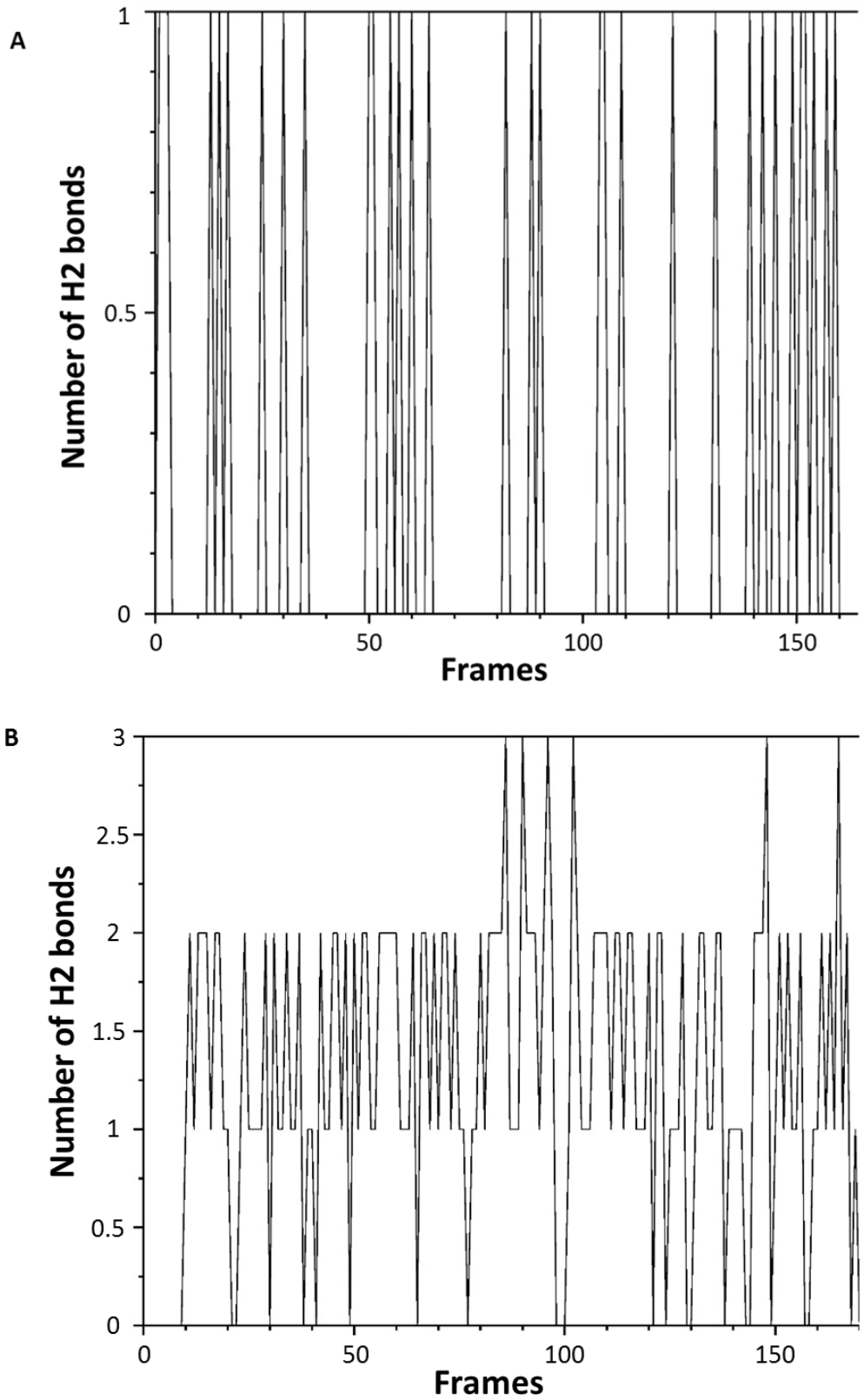
A
Number of H2 bonds
1
0.5
0
0
50
100
150
Frames
B
Number of H2 bonds
3
2.5
2
1.5
1
0.5
0
0
50
100
150
Frames

Figure 3.6. MD simulation and analysis using GROMACS suite, trajectories were analyzed visually using water-mediated hydrogen bonds with important residues. The transient hydrogen bond that was observed in hHtrA2S276C (A), was observed with the residue C276, which was absent in case of (B) wild type hHtrA2

Summary and conclusion:

The regulatory loops (mainly L3 & LD) that play critical roles in the transmission of allosteric signal and formation of activation cluster have been elaborately studied in DegS, HtrA1 and more recently in *E. coli* DegP proteases (*72*) . It has been found that subtle structural differences define their substrate specificity as well as their distinct mechanisms of activation, which in turn determine the explicit functions they perform within the cell. However, although the structure of hHtrA2 has been solved, intricate dissection of the loop regions with identification of critical residues involved in regulating its dynamic allosteric behavior is yet to be delineated.

Therefore, to understand the structural basis of inactivity in human counterpart (hHtrA2S276C) of mnd2 mouse mutant, high resolution crystal structure was solved followed by elucidation of its biophysical properties. Although, the mutant showed no overall secondary structural changes, conformational stability (T_m value ~74°C) or conformational changes (RMSD: 0.244Å) compared to the wild type, a significant reduction in the number of hydrating water molecules in the mutant was observed in the crystal structure. A close look at the H2O molecules from structures, hHtrA2S306A and hHtrA2S276C (PDB ID: 5WYN) show absence of a critical water molecule that mediates interaction between side chains of S276 and I270* [Water (W) molecule no. 377]. This observation was validated by solving structure of hHtrA2S306A under identical crystallization conditions as S276C mutant. It is well established that the contribution of water molecules to a protein's three dimensional structure is phenomenal. Hydration of protein structure is very important for maintaining its overall tertiary/quaternary structure (*73*) as well as its biological functions (*74-76*) On the contrary, disturbance in the protein–water interactions has been found to be associated with unfavorable alterations in stability or dynamics of the protein (*75, 76*) Depending upon the nature of the amino acids, water molecules form a network of interaction with

the side chains. Side chains of hydrophobic amino acids tend to repel water molecules thereby interfering with its biological activity by abolishing the water mediated ionic interactions. Therefore, replacement of polar serine with a more hydrophobic cysteine residue (*77*) might have led to shielding of the surrounding region with respect to polar water molecules thus leading to abrogation of the water-mediated interaction in hHtrA2S276C.

hHtrA2, along with 7 α-helices and 19 anti-parallel β-strands, is comprised of several long loop regions (LD, LA, L1, L2 and L3) (*78*), **(Table 3.5)** which play an important role in regulation of its catalytic activity (*20, 79, 80*).

Loop Name	Residues involved	function
LA	170-174	-
LD	259-273	Activation loop
L3	275-295	Sensor loop
L1	302-306	composed of oxyanion hole residues and catalytic serine
L2	323-329	substrate specificity function

Table 3.5: Regulatory loops, residues involved and their function in hHtrA2

Upon substrate binding, conformational changes in the sensor loop L3 in several HtrA proteins have been identified that allows them to interact with residues from LD* followed by L1* leading to a coordinated relay of information from L3 to L1* via LD*. This series of events enables the active-site to switch to a 'proteolytically ON' state (*20, 79*). Using molecular dynamics simulation, we have earlier demonstrated that in a catalytically active hHtrA2, regulatory loops (L1, LD and

L3) shift from disordered to an ordered state (*79*) during the process of activation. This corroborates with the current structural data that demonstrates a water-mediated H-2 bond between S276 on L3 and I270 from LD*, which might be an important component of this allosteric pathway. Similar mechanism of water-mediated conformational transition to a functional state has been demonstrated in hemoglobin that allosterically regulates binding of oxygen (*81*). Using structural biology and functional enzymology studies, we have provided insight into the role of a critical water molecule in conformational selection in hHtrA2 protease. Overall, the crystallographic data helped in deciphering the structural basis of hHtrA2S276C inactivity and its mechanism of action.

Significance of the study:

It is the first extensive study carried out for HtrA2 where we solved the crystal structure of hHtrA2 S276C at 2Å resolution with its intact catalytic triad unlike S306A HtrA2 structure (PDB: 1LCY). We delineated the cause behind inactivation of this point mutation, which led to mnd2 pathogenesis in mice. It would be of interest to further investigate whether mutations in HtrA2 could be found in patients with neurodegenerative disorders. Moreover, it has also provided a basic understanding of intricate mechanism of action that governs HtrA2 catalytic activity.

CHAPTER 4:

HtrA2 and Parkinson's disease

1. Introduction

Parkinson's disease (PD) is the most common movement disorder and the second most predominant neurodegenerative disease which affects about 2% of people over the age of 65 (*82*) and about 5% above the age group of 80 years (*83*). In India, the prevalence rate of PD has been reported to be 53 per 100,000 (*84*). It is described by symptoms include tremor, rigidity, bradykinesia, depression, anxiety and cognitive impairment due to severe loss of dopamine producing neurons (*85, 86*). Though the etiology of PD remains unclear, approximately 5–10% of the patients have been found to be affected by genetic factors. The majority of cases of PD appear to be sporadic in nature**,** in recent years, (Alpha-synuclein) (*87*)**,** *UCHL1* (Ubiquitin C-Terminal Hydrolase L1) (*88*), and *LRRK2* (Leucine rich repeat kinase 2) (*40*) have been identified to be associated with autosomal dominant PD, while *ATP13A2* (Probable cation-transporting ATPase 13A2) (*42*) *DJ-1* (Protein deglycase DJ-1) (*38*)**,** *PINK1* (PTEN-induced kinase-1) (*89*), *PLA2G6* (85/88 kDa calcium-independent phospholipase A2, Group VI phospholipase A2) (*90*) found to be in both familial and non-familial PD (*91*). Defects reported in other genes, including *PINK1* and *HTRA2*, are less frequent. A large number of studies have been reported to understand the functional role of *HTRA2/OMI* in PD pathogenesis due to its association which has been reported to be linked to the autosomal recessive form of familial PD. HTRA2 mutant mice present an advanced neurodegenerative phenotype with features resembling Parkinson's disease (*46*). A subsequent genetic study on PD patients from Germany and Belgium found that heterozygous mutations of HtrA2, Gly399Ser and Arg404Trp respectively, is associated with the development of PD (*5, 92*). To date, the functional role for HtrA2 risk variants in neuronal death is still unclear. Therefore, to explicate the impact of HtrA2 in PD, we examined HTRA2 mutations in PD patients of Indian origin. We sequenced all the eight exons of HTRA2 in 170 Indian PD cases and 160

controls. We also led in vitro functional assays to study the potential toxic effect of found variants on mitochondria.

Experimental procedures:

Recombinant protein production and purification –

Mature (Δ133) Wild type HtrA2 and its variants T109M (aka T242M), T109E (aka T242E) with C-terminal 6x His-tag in pET-20b (Addgene, Cambridge, MA, USA) were expressed and purified as described previously (*6*). The PD associated mutant (T109M) was made by SDM using PCR, and were expressed in *E. coli* strain BL21 (DE3). Cells were grown at 37°C till the OD_{600} reaches 0.6-0.8 and was then induced with 0.2 mM IPTG. Cells were further cultured at 16°C for 16hrs post induction. Mutant proteins were purified by affinity chromatography using Nickel-Nitrilo triacetic acid (Ni-NTA) resin (Novagen, MA, USA) in buffer 20 mM Na_2HPO_4/NaH_2PO_4, pH 8.0 containing 100 mM NaCl.

Protein crystallization

FPLC purified HtrA2 T242M protein at a concentration of 17 mg/ml was used for setting up crystallization trials. Crystallization trials were set using commercially available crystallization kits (Hampton Research, Inc) using hanging drop method. Unbound HtrA2 T242M crystals were observed using crystal buffer (0.1M MES pH 6.5 (buffer), 2M NaCl (Precipitant), 0.1M KH_2PO_4 and 0.1M NaH_2PO_4) from Crystal Screen 21 (Hampton research).

In vitro enzyme activity assay

Protease activity of bacterially-expressed 6x histidine tagged WT HtrA2 and HtrA2 T242M in pET20b vector were determined according to the manufacturer's instructions. Purified proteins were incubated with β-casein (Sigma) in protease cleavage buffer (20 mM HEPES (pH 8.0), 100mM NaCl). For each 30µl reaction mixture, 2ug of respective protein was incubated with 6ug of β-casein at 37°C for 60mins, and results were analyzed by SDS-PAGE. For all quantitative studies, fluorescein isothiocyanate (FITC)-casein (Sigma) was used, and assays were performed as described previously (18). The fluorescent substrate cleavage was measured by incubating respective concentration of enzymes (Wt and mutant) with increasing concentrations (0 – 20 µM) of β-casein at 37°C in cleavage buffer (20 mM Na_2HPO_4/NaH_2PO_4, pH 8.0 containing 100 mM NaCl, 0.1 mM DTT). FITC-fluorescence was monitored in a multi-well plate reader (Berthold Technologies, TN, USA) using excitation wavelength of 485 nm and emission at 545 nm. Reaction rates (v_0) were calculated using linear regression analysis equation:

$$Velocity = Basal + \frac{Max}{1 + \left[\frac{Kact}{substrate}\right] n}$$

where 'K_{act}' is half maximal activation constant and 'n' is the Hill constant (*55*). The steady-state kinetic parameters were calculated from the reaction rates by fitting the data to Hill form of Michaelis-Menten equation,

$$Velocity = Vmax/(1 + \left(\frac{K0.5}{[substrate]}\right) n)$$

, where 'V_{max}' is the maximum velocity and $K_{0.5}$ is substrate concentration at half maximal velocity using KaleidaGraph (Synergy software). All the experiments were done independently in triplicate and the mean ± S.E.M. values are shown in the plots.

Structure Solution of HtrA2 T242M

Crystal structure of the HtrA2 T242M was solved by Molecular Replacement (MR) using Phaser program (*61*). The HtrA2 S306A structure (PDB-1LCY) was acquired from the Protein Data Bank, and was processed for removal of water and ligand molecules from the coordinate file, and was thereafter used as the search model (*62*). The rotational and translation searches were carried out using PHASER software (*63*) and the MR solution was further refined by REFMAC 5 of CCP4 suite (*57, 64*). Initially the model was refined as rigid body, and later rounds were of restrained refinement (*64*).

Polymerase chain reaction amplification, and molecular analysis

Exon-specific intronic primers were designed **(Table 4.1)** to cover full length of exon, keeping the amplicon size appropriate for genetic analyzer (ABI 3500 × L) using oligoanalyser (Bioinformatics tool). Primers got synthesized by commercial oligo synthesizer (MWG Biotech, India). PCR amplification was carried out in a 20µl of reaction volume. Sequence alignment was carried out by Variant Reporter Software (ABI***).***

Name of the primer	Sequence	Amplicon size (kb)	Annealing temperature (°C)
HTRA2 1F	TTGGGAAGGCGGAGTCTT	882	62
HTRA2 1R	CTGAAATGGAGGGAAAGCAC		
HTRA2 2+3F	GCAGATGTGGTGGAGAAGAC	650	60
HTRA2 2+3R	CCTCCCCCATCATTTGTCAT		
HTRA2 4+5F	GGGGAGTTTGTTGTTGCCAT	826	62
HTRA2 4+5R	GCTACATCCTTCCTTCCCTG		
HTRA2 5+6F	GGTGAGTGAGACATCCTTCC	692	62
HTRA2 5+6R	TACAAAGTGGAGTGGGATAA		
HTRA2 7+8F	GAAGACAGAAAGTGAGTTGC	570	60
HTRA2 7+8R	CATTTAACCCTCTGTCTCGG		

Table 4.1: Details of the primer sequences and annealing temperatures

Patients study

Patients enrolled in neurology department of various hospitals of north Karnataka state of India with the symptoms of the PD were included in the study (*93*). With the signed informed consent, 170 early and late onset PD patients (males 68%, females 32%) belonging to both rural and urban areas of north Karnataka were included. All the subjects (330) were interviewed with the help of a structured pre-tested questionnaire. This was followed by clinical examination and relevant laboratory investigations. Standard definitions were used to measure the physical activity, tremor, rigidity, bradykinesia, and akinesia (*94*). Along with the patients, age, gender and ethnically matched 160 healthy individuals were selected as control. These controls were selected on the condition that each control should not have the family history of PD or similar clinical features. The controls were recruited for the study to rule out any possible population specific single nucleotide polymorphisms (SNPs), which may not be involved in causing PD.

HTRA2 Genotyping

Genomic DNA (gDNA) from PD patients and healthy control individuals was extracted from peripheral blood samples using Qiagen QIAamp DNA Mini Kit (Cat#51304). HTRA2 mutation analysis was performed by direct sequencing of all eight exons. For this, gDNA was amplified in a 25µl PCR reaction volume containing 5µl gDNA (20ng/µl), 0.5µl of each Forward & Reverse primers (10pmol), 1µl deoxynucleotide triphosphate (2.5mmol), 0.5µl Taq Polymerase (2U/µl - Thermo Scientific), 2.5µl Taq Buffer (10X) and the total volume was adjusted to 25µl using

molecular biology grade water. Primers for PCR were designed using Oligo Explorer-1.5 **(Table 4.1)**. PCR amplification was carried out under following conditions: an initial denaturation at 95°C for 5 mins, followed by 35 cycles of denaturation at 95°C for 45 sec, primer annealing at specific annealing temperature for each primer set for 45 sec, Primer extension at 72°C for 45 sec followed by final extension at 72°C for 5 min.

PCR products were confirmed for their respective amplicon size by 1% Agarose gel electrophoresis with standard 100-bp molecular weight marker (digested Lambda Phage DNA-SD Prodigy). Purification of PCR products was done using ExoSAP IT (USB Products, Affimetrix). Sanger Sequencing was performed using BigDyes Terminator Cycle Sequencing kit v3.1 (Applied Biosystems) on ABI 3500 & 3730 DNA Sequencer (Applied Biosystems) and electropherograms were analyzed by chromas lite version 2.6.4.

Cell cultures and transfections

HEK293T and human dopaminergic neuroblastoma cell line (SHSY5Y) was grown in Dulbecco's modified Eagle's medium (DMEM; Invitrogen). Media was supplemented with 10% (v/v) fetal bovine serum, 1% penicillin and streptomycin (PAN, www.pan-biotech.com). Cells were maintained at 37°C in a humidified atmosphere of 5% (v/v) CO_2 in air. Cells were seeded 24hrs prior to the transfection on poly-L-lysine coated multiwall plates. Cells were transiently transfected with the respective expression constructs using Lipofectamine 2000 (Invitrogen, Italy) according to the manufacturer's protocol. All the cell culture media and reagents were from Invitrogen (Carlsbad, CA). For serum withdrawal, cells were cultured in medium without 10% heat-

inactivated fetal bovine serum. GSK-3 inhibitor SB415286 were purchased from Selleckchem (St. Louis, MO) and dissolved in dimethyl sulfoxide (Me2SO).

Plasmids

Expression plasmid (pCDNA3-WT type HtrA2/ HtrA2 S306A-Flag) was a kind gift from Dr. L.M. Martins (Leicester). The PD associated mutant of HtrA2, HtrA2 T242M was obtained using Quick-change site-directed mutagenesis kit (Stratagene, Italy) according to the manufacturer's instructions. The following primers were used: 5' TAAGGAGCCTCTCCCC**ATG**CTGCCTC-3' as forward primer and 5'-GAGGCAGCATGGGGAGAGGCTCCTTA-3' as reverse primer. Polymerase chain reaction (PCR) was carried out as described earlier (*2*). The presence of the desired mutation was confirmed by plasmid sequencing.

Etoposide-Induced Apoptosis.

Cells were exposed to 150 μmol/L of etoposide (Sigma), added from a 2 mmol/L stock solution in DMSO.

MTT (Cell Viability) Assay

Cell viability was quantified by its ability to reduce tetrazolium salt 3-(4,5- dimethylthiazole-2ϒ)-2,5-diphenyl tetrasodium bromide (MTT) to colored formazan products (Sigma# m-2128) as per manufacturer’s protocol. MTT reagent (5mg/ml in PBS) was added to the cells at 1/10th volume of the medium to stain only viable cells and incubated at 37°C for 4hrs. MTT solubilisation buffer

(0.01M HCl, 10% SDS) of two fold volume was added to cells, followed by incubation in the dark at 37°C for 24hrs. The absorbance was measured at 570nm with Spectrostar Nano-Biotek, Lab Tech plate Reader. Cell viability was expressed as the percentage of absorbance obtained in control cultures.

Antibodies and Immunoblotting

Cell extracts were prepared by lysing cells for 20 mins on ice in 50 mM Tris-HCl, pH 7.4, 250 mM NaCl, 0.1% Nonidet NP-40, 5 mM EDTA, 50 mM NaF in the presence of protease inhibit cocktail comprised of aprotinin, leupeptine and phenyl-methyl-sulfonyl-fluoride (PMSF). Insoluble material was pelleted at 14,000 × *g* for 30 mins at 4°C and the protein concentration was determined using Bradford reagent (Sigma). A 50μg weight of total cellular proteins was separated on 12% SDS-PAGE and electrotransferred to Nitrocellulose membrane (Millipore, Italy). Subsequent to electrophoresis and transfer, immunoblotting was carried out by using the following antibodies. The blocking solution for all antibodies was 5% bovine serum albumin (BSA) in TBST [10 mM Tris, pH 8.0, 150 mM NaCl, 0.5% (vol/vol) Tween 20]. Antibodies were diluted as needed in 5% BSA in TBS–Tween-20 0.05% (TBS-T). Anti-BAX mouse monoclonal antibody (Santa Cruz Biotechnology), anti-HtrA2 rabbit polyclonal antibody (Santa Cruz Biotechnology). Antibody binding was revealed using horse raddish peroxidase secondary conjugated antibodies (Santa Cruz Biotechnology) and visualized by enhanced chemiluminescence (ECL; Thermo Fischer, USA).

Flow cytometry

For all flow cytometry measurements, the cells were harvested using phosphate-buffered saline (PBS) with 2mM EDTA and washed once with PBS after which they were stained with appropriate dyes. After 48hrs of transient transfection, adherent and detached SHSY5Y cells were combined, washed twice with PBS and resuspended in Annexin-V binding buffer (BD Biosciences) and incubated with required amount of Annexin-V-FITC/Propidium Iodide (PI) (BD Biosciences) in dark for 20 minutes at room temperature followed by acquisition on FL-1 channel of FACS caliber flow cytometer and data was analyzed on Cell Quest software. To measure the levels of mitochondrial superoxide, the cells were stained with 5μM MitoSox Red (Invitrogen) in PBS for 15mins at 37°C. The cells were then washed once with PBS and resuspended in PBS. For each sample, ~50,000 cells were measured using the 488 nm argon laser and emission through the PE filter (575 nm).

Apoptotic assay

DNA content was assessed by staining ethanol fixed cells with propidium iodide and monitoring by FACScan (Becton-Dickinson). Numbers of PI-positive cells with sub-G1 DNA content were determined with a MODFIT LT program.

Assessment of mitochondrial membrane potential (ΔΨm)

To study the effect of HtrA2 T242M on the mitochondrial membrane potential (ΔΨm), we employed 5,5′,6,6′-tetrachloro-1,1′,3,3′ tetraethylbenzimidazolylcarbocyanine iodide (JC-1) dye

(eBiosciences, San Diego, CA, USA), a cationic cell permeable dye and selectively accumulates in mitochondria in a potential dependent manner. Mitochondrial membrane polarization leads to the reversible formation of J-aggregates which causes a shift in the fluorescence emission from 530nm (corresponding to JC-1 monomers which emits green fluorescence) to 590nm (corresponding to J-aggregates which emits red-orange fluorescence). Cells growing in confocal dishes were incubated with 10µM JC-1 dye for 30mins. The cells were then washed with PBS, replenished with fresh medium and observed under a fluorescence microscope.

Transmission electron microscopy

Briefly, the WT HtrA2 and HtrA2 T242M transfected neuronal (SHSY5Y) and HEK293T cells were harvested by trypsinization and fxed with 3% glutaraldehyde at 4°C for 3–4hrs followed by washing with 0.1M sodium cacodylate buffer. The cell pellets were then fixed in Osmium tetroxide for 1hr at 4°C in dark, subjected to dehydration by passing through different grades of alcohol and then mounted with Araldite resin. The ultrathin sections (~60–70 nm) were mounted on formvar coated copper grids. These sections were stained with uranyl acetate solution and counterstained with lead citrate. Electron micrographs were captured on a Jeol 100-CXII electron microscope (Jeol, UK) using Olympus camera and iTEM software.

Immunofluorescence and confocal microscopy

To check the effect of WT and HtrA2 T242M on mitochondrial membrane potential (MMP) live cell imaging has been carried out. Cells were cultured in confocal dishes and stained with 10 µM JC-1 dye. For immunofluorescence staining, cells growing on coverslips were fixed with 4% paraformaldehyde followed by permeabilization with 0.5% triton X-100. Blocking was done in

5% BSA for 1hr. The cells were then incubated with primary antibody specific for the desired protein for 1hr at room temperature (RT) followed by detection with appropriate secondary antibody with 1hr incubation at RT in dark. Nuclei were counterstained with 4′,6-diamidino-2-phenylindole (DAPI). The slides were observed under laser confocal microscope.

Co-Immunoprecipitation

For immunoprecipitation in HEK293T cells overexpressing HtrA2-Flag, lysates were made with an immunoprecipitation lysis buffer (50 mM HEPES [pH 7.5], 10 mM KCl, 50 mM NaCl, 1 mM EDTA, 0.5 mM EGTA, 1.5 mM MgCl2, 10% glycerol, 0.5% NP-40, 10 mM NaF, 1 mM Na2VO5, 10 mM b-glycerophosphate and 1x protease inhibitor cocktail (Sigma, P2714) and were incubated with anti-FLAG agarose beads (Sigma) overnight at 4°C. After 5 washes with lysis buffer the immunocomplexes were separated on SDS PAGE and were analyzed by Western Blot analysis.

Crystallization, Data Collection, and Processing

Crystals of the HtrA2 T242M were obtained at 22°C by the hanging-drop vapor diffusion method. The reservoir solution contained 0.1M MES pH 6.5 (buffer), 2M NaCl (Precipitant), 0.1M KH_2PO_4 and 0.1M NaH_2PO_4. The protein was at 25mg/ml concentration, in a buffer containing 10 mM HEPES (pH 8.0), 100 mM NaCl. Crystals in the shape of hexagonal cubes generally appeared in 1 week, and took about around 10-12 days to grow to full size. The crystals were transferred in a few steps to the cryoprotectant buffer (30% glycerol), and flash-frozen in liquid nitrogen.

X-ray diffraction data to 2.5 A˚ were collected at 100 K using CuK_{α} radiation generated by a Rigaku Micromax 007HF generator equipped with R-Axis IV++ detector at the Protein Crystallography Facility, IIT Bombay, India. Data were indexed and integrated using software **X**-ray **D**etector **S**oftware (XDS) and were subsequently scaled using the software AIMLESS from the CCP4 suite (*60, 70*). The crystal is isomorphous to that of the wild-type, belonging to space group R3H and with one molecule in the asymmetric unit.

Results

Mutation analysis of HTRA2 gene

Of the 170 PD patients, five were with positive family history for PD, with one first-degree relative suffering from PD. A total of 38 PD patients were without any family history, hence they have been treated as sporadic PD. A total of 57 patients were identified as idiopathic PD, where no known cause was observed and no family history of PD was found**.** Among all the PD patients recruited for study, 15 (9 males and 6 females) belonged to age group of 40-49, 24 (16 males and

eight females) patients belonged to age group 50-59, 34 (25 males and 9 females) PD patients belonged to the age group of 61-70, 27 (17 males and 10 females) PD patients belonged to age group of 70-79, and 8 (6 males and 2 females) belonged to the age group of 80-89.

All the eight exons of HTRA2 gene both for the forward and reverse primer amplicons were analyzed for mutations or any other possible molecular alteration in comparison with the reference sequence and control sample sequence.

HTRA2 mutation screening

To determine the frequency of HTRA2 mutations as a cause of familial Parkinsonism and to identify novel mutations in the gene, all 8 exons of HTRA2 gene from 170 (early and late onset) Parkinson disease cases and 160 normal individual s were sequenced. Sanger sequencing under the conditions shown in **Table 4.2** led to the detection of three exonic (c.421G>T, c.725C>T and c.1195G>A) sequence variations. The exonic sequence variations c.421G>T in exon 1 (leading to p.A141S) in a total of 2 PD patients (1.17%) and 3 neurologically normal control individuals (1.87%) and c.1195G>A in exon 7 (leading to p.G399S), in a total of 2 PD patients (1.17%) and 4 neurologically normal control individuals (2.5%) both were previously identified as a mutation associated with PD by Strauss et al (*5*).

Exon	Variant	% in cases	% in controls	Odds Ratio	95% CI	P value
1	p.A141S c.421 G>T	2/170 (1.17%)	3/160 (1.87%)	0.623	0.102-3.778	0.606
3	**p.T242M c.725 C>T**	1/170 (0.58%)	0/160 (0%)	2.840	0.114-70.2	0.52
7	p.G399S c.1195 G>A	2/170 (1.17%)	4/160 (2.5%)	0.464	0.083-2.570	0.379

Table 4.2: Data Statistics for identified HtrA2 variants

The c.725C>T variant, located in exon 3 and which affects the second base of the codon results in the substitution of a Methionine for a Threonine (T242M), was found in one patient (0.58%), but was not observed in any control chromosomes **(Figure 4.1 A & B).** This amino acid (Threonine 242) position is found to be evolutionary conserved across species **(Figure 4.1C).**

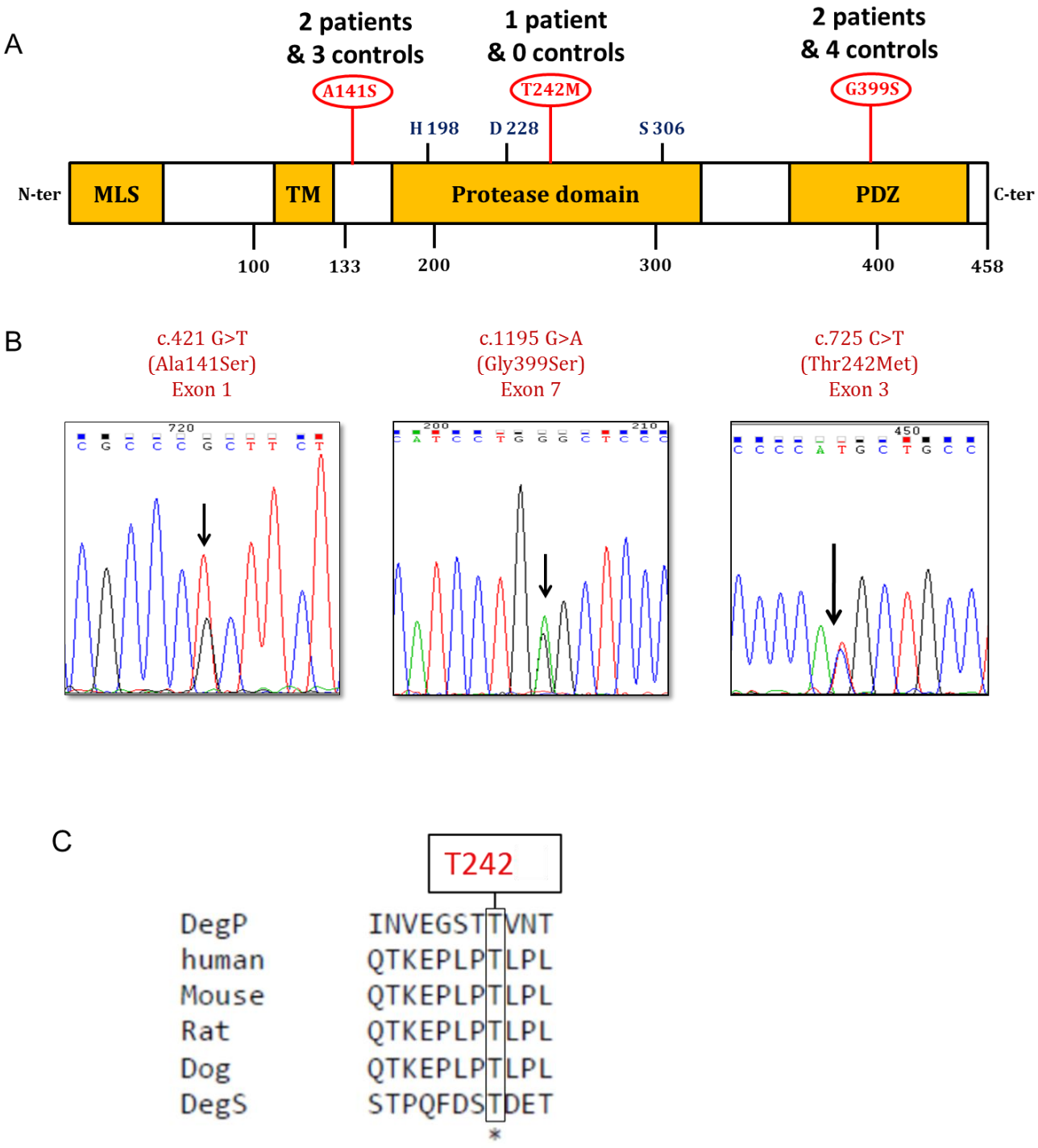

Figure 4.1. HTRA2 variants identified in Indian PD patients. A) The mutated residue, A141S, is found N-terminal domain. T242M in the protease domain; G399S in the PDZ domain. MLS mitochondrial localizing sequence. **B)** Direct sequencing of HTRA2 showing

one novel and two earlier identified substitution changes: c.725 C>T, c.421 G>T and c.1195 G>A respectively. **C)** p.T242M variant occurs in conserved position in its homologues.

Clinical result

The case carrying the c.725 C>T (p.T242M) variant was a 77-year-old woman. Patient's parents were from Karnataka region with no known consanguinity and no family history of Parkinsonism. Patient had modified Hoehn Yahr Scale of 3.0 that literally means having a mild to moderate bilateral disease, some postural instability and physical independency. She had difficulty performing his working activities. There was also psychological disturbance, particularly anxiety. At the same time, sleep disturbances started and the patient felt depressed. Three months after the initial manifestation of the disease, the patient developed speech difficulties, especially with pronunciation.

In vitro functional assay of *HTRA2* Thr242Met variant

Effects of HtrA2 T242M on the serine protease activity in vitro

Protease activity of the WT and T242M HtrA2 was measured both qualitatively and quantitatively using β-casein as substrate. In the gel based protease assay (qualitative) at different concentrations of T242M HtrA2, there was no significant difference in the enzyme activity **(Figure 4.2A)**. However, after comparison, quantitative fluorescence based in vitro protease (enzyme (T242M HtrA2) – substrate (FITC-β-casein)) assay, significant decrease (~1.8 fold) in the reaction rates (K_{cat}/K_m) were measured as compared to WT HtrA2 **(Figure 4.2B)**. Our results also indicate that

T242M HtrA2 has similar $k_{0.5}$ value suggesting, substrate binding is not affected and on the similar line, both the enzymes showed positive co-operativity.

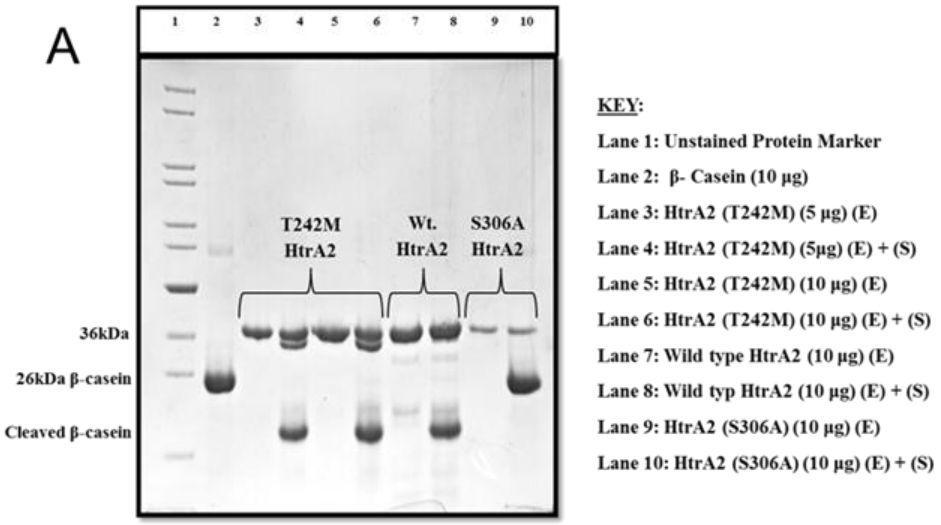

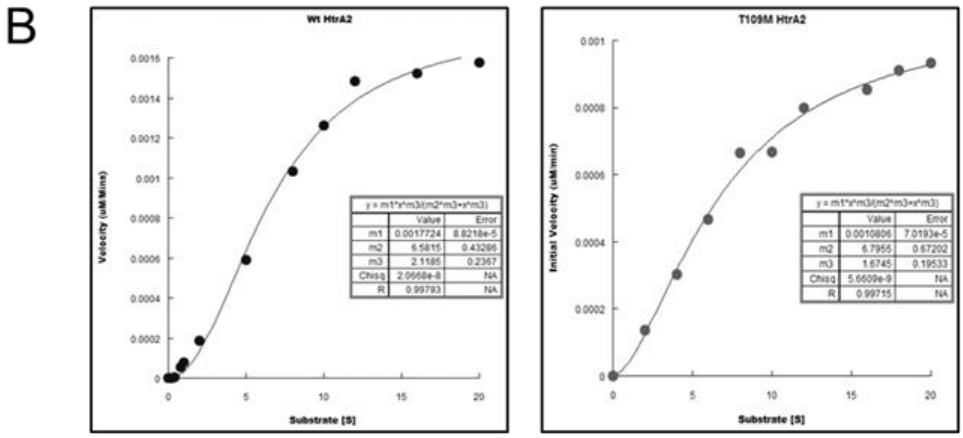

HtrA2 protein	Vmax (M/sec)	Km (uM)	kcat (S^{-1})	Hills coefficient	kcat/Km ($M^{-1}s^{-1}$)
Wild type	$2.9x10^{-11}$	6.5815	$5.9x10^{-6}$	2.1185	**$8.96x10^{-7}$**
T242M	$1.8x10^{-11}$	6.7955	$3.6x10^{-6}$	1.6745	**$5.30x10^{-7}$**

Table: Values are the mean +/- SEM and are generated from data points obtained from at least three independent experiments

Figure 4.2. Effect of HtrA2 T242M on the serine protease activity in vitro A) 12% SDS gel showing in vitro (gel based) β-casein (substrate) cleavage assay for T242M

HtrA2, (B) In vitro (fluorescence based) protease assay or quantitative enzyme substrate cleavage assay.

T242M HtrA2 does not interfere in trimer formation

According to the crystal structure of HtrA2 (*7*), Threonine 242 is located in the serine protease domain placed in the loop region in between β6 (harbor residue from catalytic triad; Aspartate 228) & β7 structure (that harbor residue responsible for trimerisation) **(Figure 4.3A).**

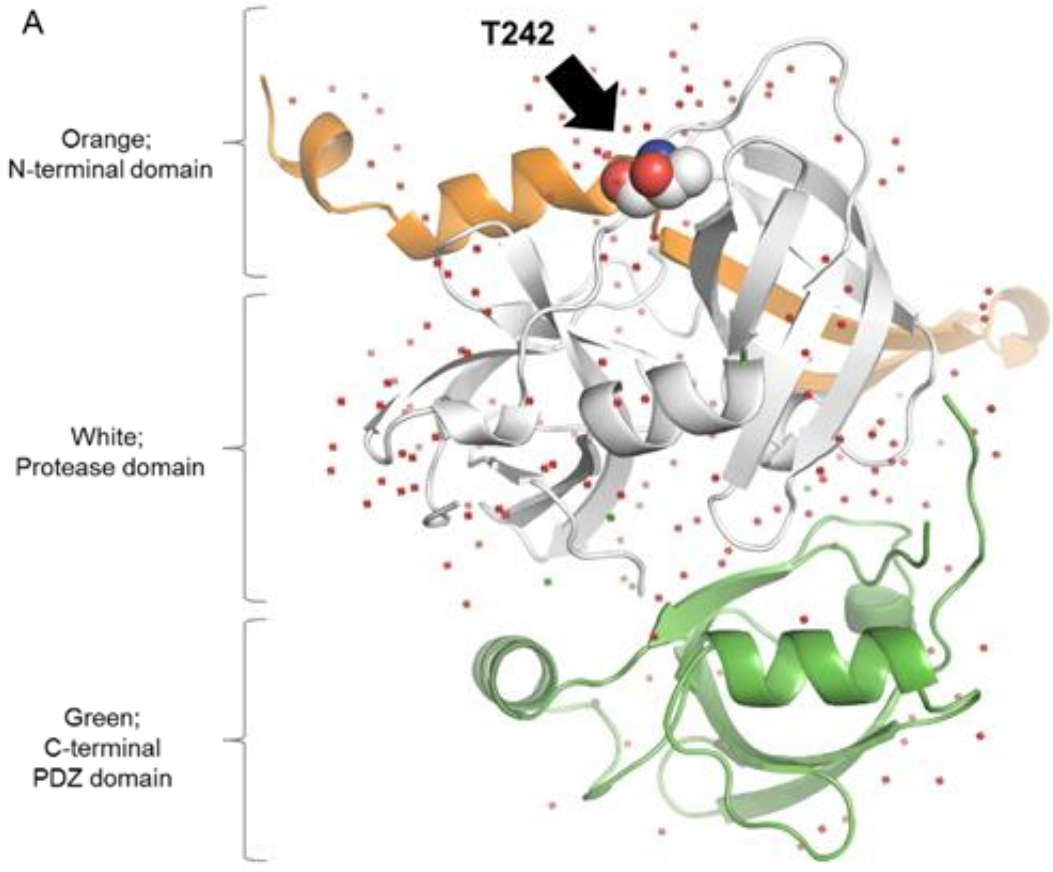

Figure 4.3. **Position of HTRA2 variants identified in Indian PD patients.**

Therefore to evaluate for possible effects of the T242M HtrA2 protein on trimer formation, size exclusion chromatography has been carried out. We observed T242M HtrA2 were eluted as single peaks as detected at ~73.9ml of elution volume **(Figure 4.3B**), similar oligomeric status for WT type HtrA2 has also been observed previously (*2*), suggesting the mutation does not affect the oligomeric property of HtrA2 protein. Thus, we could say variant retain the ability to form homotrimerisation.

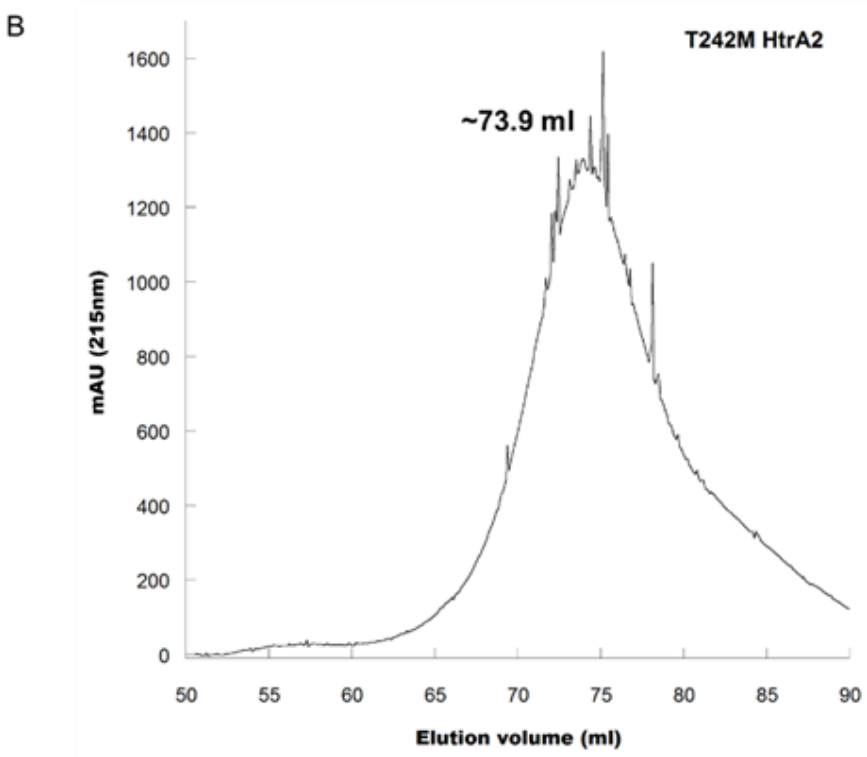

Figure 4.3 B) Direct sequencing of HTRA2 showing one novel and two earlier identified substitution changes: c.725 C>T, c.421 G>T and c.1195 G>A respectively, arrows indicate the positions of the changes.

T242M HtrA2 mediates caspase dependent cell death in neuronal cells

To investigate whether T242M mediates cell death via the canonical caspase-dependent pathway, we transiently transfected SHSY5Y (thrice cloned subline of the neuroblastoma cell line SK-N-SH) cells with HtrA2 (T242M) and assessed caspase activation by western blotting after 48hrs. Presence of activated (cleaved) caspase-3 in HtrA2 (T242M)-transfected neurons indicates caspase-dependent cell death **(Figure 4.4A).** This was further supported by the MTT assay results showing significant time dependent reduction in the cell viability in HtrA2 (T242M) transfected neurons compared to WT transfected neurons **(Figure 4.4B).** Analysis of neuronal cell death by flow cytometry revealed there is a significant ~2 fold increase in Annexin V/PI (dual) positive cells in the HtrA2 (T242M) treated population as compared to WT and vehicle control population **(Figure 4.4C).** Also, SHSY5Y cells transfected to HtrA2 (T242M) showed an increase in the number of cells with sub-G1 DNA content compared with cells expressing WT HtrA2 and empty vector **(Figure 4.4D).** All these observations point towards a caspase dependent apoptotic form of cell death induced by T242M HtrA2 in dopamine producing neuronal cells. This underscores the toxic effect of the T242M mutation in terms of mitochondrial dysfunction and cell death.

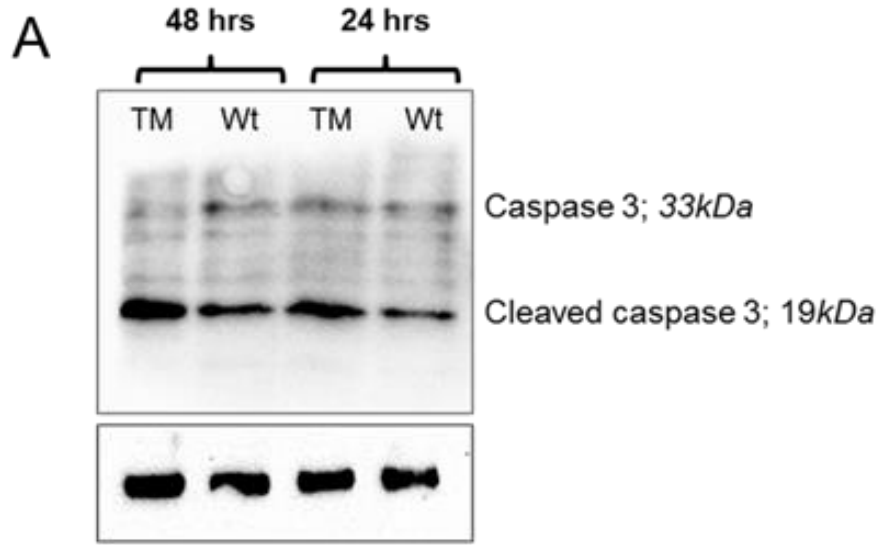
A
48 hrs
24 hrs
TM
Wt
TM
Wt
Caspase 3; 33kDa
Cleaved caspase 3; 19kDa

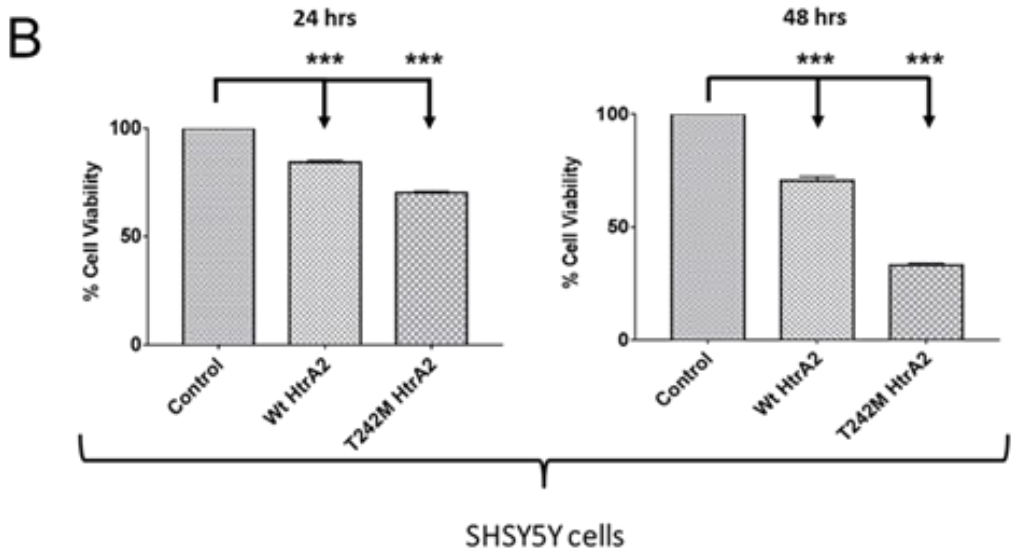
B
24 hrs
48 hrs
***
***
***
***
100
50
0
% Cell Viability
Control
Wt HtrA2
T242M HtrA2
SHSY5Y cells

C

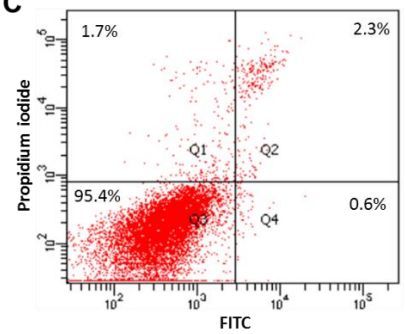

Control HEK293 cells after 48hrs.

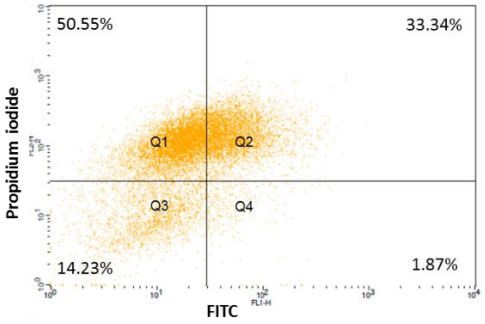

Wt. HtrA2 transfected HEK293 cells after 48 hrs.

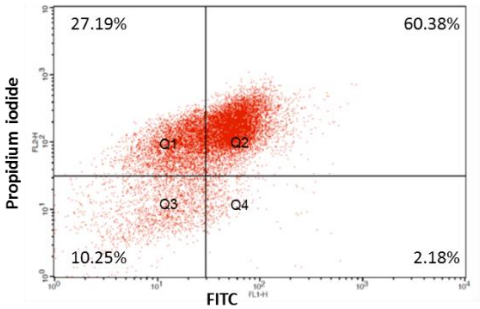

T242M HtrA2 transfected HEK293 cells after 48 hrs.

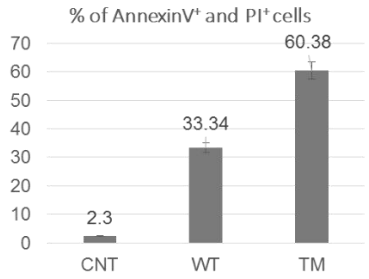

D

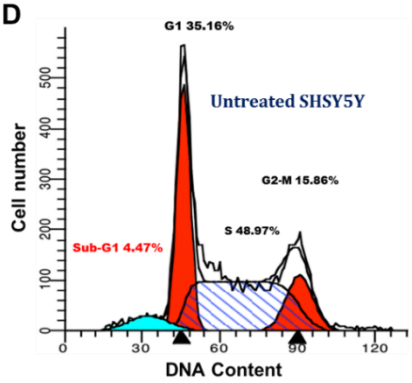

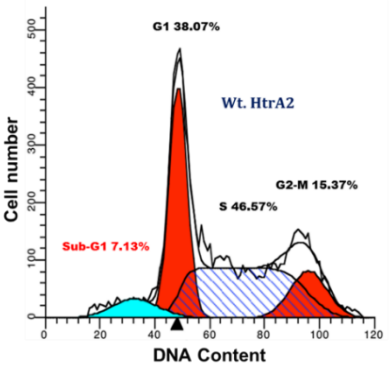

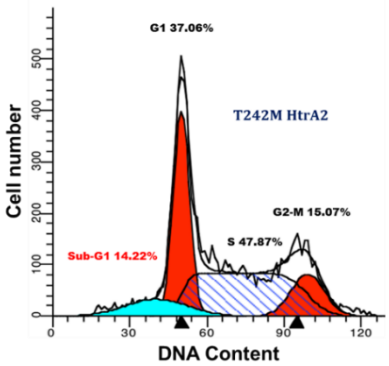

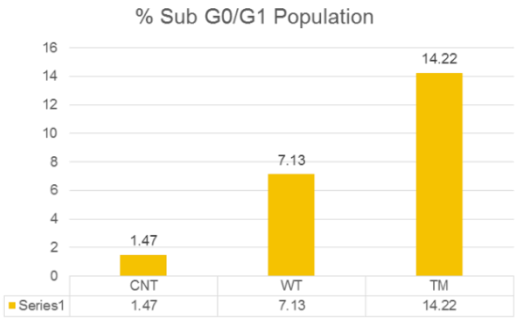

Figure 4.4. T242M HtrA2 mediates caspase dependent cell death in neuronal cells

A) Presence of activated (cleaved) caspase-3 in T242M HtrA2 transfected neurons indicate a caspase dependent cell death, **B)** MTT assay results showing significant time dependent reduction in the cell viability in T242M HtrA2 transfected neurons compared to WT transfected neurons, **C)** a significant ~2 fold increase in Annexin V/PI (dual) positive cells in the T242M HtrA2 treated population as compared to WT and vehicle control population, **D)** DNA content frequency histogram of SHSY5Y cells (1 x 10^5) transfected with T242M HtrA2; The cells were stained with propidium iodide and measured by flow cytometry. Note that the position of apoptotic cells was shifted to lower DNA content values, suggestive of DNA extraction from these cells.

BAX up regulation induces increased cell death in T242M HtrA2 cells

A number of molecular factors such as Bcl-2 family members; Bad and Bax play key roles in the execution of apoptosis. We therefore investigated their expression pattern in SHSY5Y cells overexpressing HtrA2 (T242M). The Bcl-2 family of genes plays an important role in the regulation of apoptosis. Thus, in order to understand the molecular mechanism by which HtrA2 (T242M) induces caspase dependent apoptotic cell death, we evaluated the expression levels of Bad and Bax proteins using western blotting. It has been reported that under apoptotic stress, HtrA2 migrate to the nucleus and cleaves p73α (a structural and functional homologue of the p53 tumor suppressor protein) in the C-terminal portion, enabling the protein to increase its transactivation activity on the apoptotic gene BAX (*95*).

We observed a significant up-regulation in the expression of Bax protein in the HtrA2 (T242M)-transfected SHSY5Y cells as compared to vehicle control and WT HtrA2 cells. This observation

indicates that over-expression of the mutant HtrA2 leads to increase in pro-apoptotic Bax level in the cell, which is significantly higher compared to its expression when mature HtrA2 is overexpressed **(Figure 4.5)**.

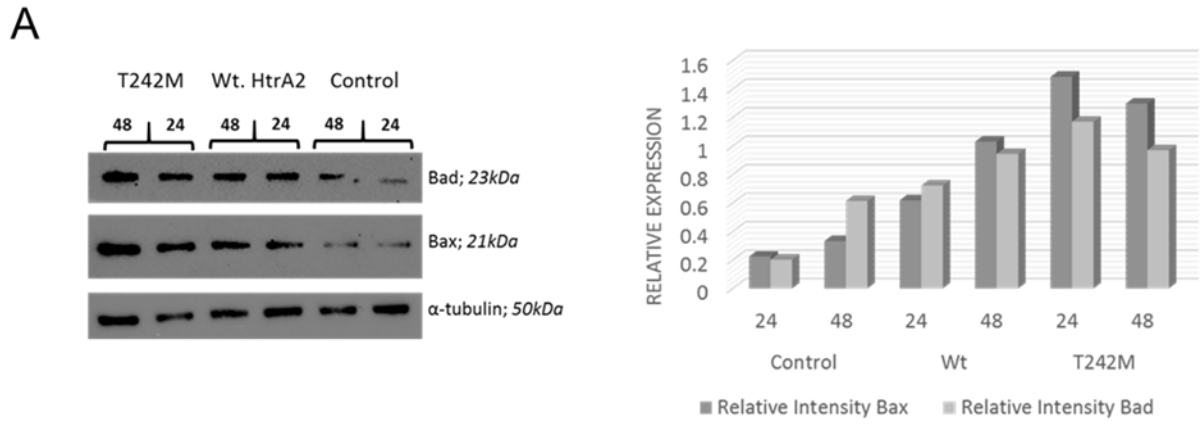

Figure 4.5. BAX up regulation induces increased cell death in T242M HtrA2 cells. A significant up-regulation in the expression of the Bax protein in the T242M HtrA2 transfected SHSY5Y cells compared to vehicle control and WT HtrA2 cells.

Ultra structural changes induced by T242M HtrA2

Since mitochondrial dysfunction has been shown to be an integral part of both sporadic and familial PD (*96*), we examined the morphology of HEK293T and SH-SY5Y cells overexpressing WT and HtrA2-T242M using electron microscopy, at the ultra-structural level. We have identified characteristic changes of mitochondria in a subset of cells. When compared with neurons overexpressing WT HtrA2 **(Figure 4.6A-D)**, we observed abnormal mitochondrial morphology with disorganized cristae that were more pronounced in cells overexpressing HtrA2-T242M **(Figure 4.6E-H)**. Some of these mitochondria were filled with dense, lamellar structures. Numerous autophagic vesicles containing electron dense materials, protein inclusions and

degenerating cellular organelles were readily visible throughout the cytoplasm. In our studies, observation of co-localization of mitochondria and lysosomes suggested autophagy as a plausible mechanism of cell death in those cells. Extensive cytoplasmic vacuolation was also apparent and intact mitochondria were not readily detectable. On the contrary, control cells exhibited numerous mitochondria (with intact inner and outer membranes and distinct cristae) and few cytoplasmic vacuoles. **(Figure 4.6H-K)**.

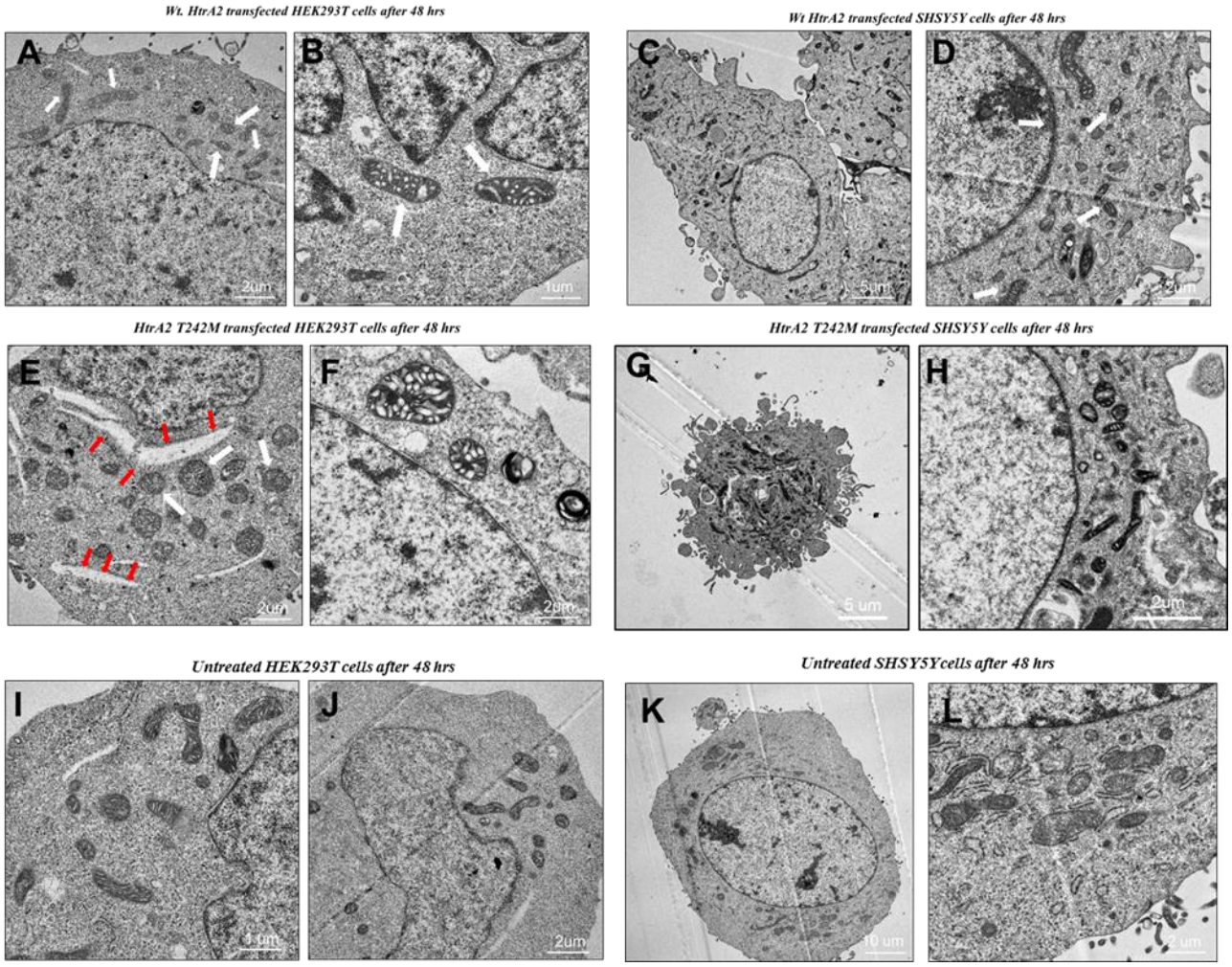

Figure 4.6. Ultra-structural changes induced by T242M HtrA2.

HtrA2 (T242M) induces mitochondrial membrane depolarization in neurons

To correlate the observed morphological alterations with mitochondrial functions if any, we next examined the effects of HtrA2-T242M overexpression on mitochondrial membrane potential (ΔΨm) by fluorescence microscopy using JC-1 dye. Mitochondrial membrane potential is considered to be a sensitive marker for mitochondrial health. As compared to the vehicle control, HtrA2-T242M transfected SH-SY5Y cells induced depolarization of the mitochondrial membrane. This is reflected by a significant increase in green to red fluorescence ratio of JC-1 dye. Increase in green fluorescence of JC-1 dye (due to JC-1 monomers) indicates a drop in ΔΨm, whereas increased red fluorescence (due to JC-1 aggregates) corresponds to stable ΔΨm, which is indicative of a healthy functional mitochondria. After treatment with 150 μmol/L Etoposide (apoptotic inducer by different mechanisms including loss of mitochondrial transmembrane potential) for 6h(*8*), the mitochondrial membrane potential was decreased in all the samples investigated. However, this effect was more pronounced in cells overexpressing HtrA2-T242M compared to WT HtrA2 **(Figure 4.7A)**. We also investigated whether HtrA2-T242M induces ROS (Reactive Oxygen Species) accumulation in mitochondria using Mito SOX Red dye. Mito SOX Red dye specifically accumulates in mitochondria, which upon oxidation by superoxide radicals exhibits red fluorescence. We observed increased ROS production by flow cytometry as compared to the WT-HtrA2, which was depicted by an increased proportion of Mito SOX Red positive HtrA2-T242M treated neurons **(Figure 4.7B).** Therefore, these studies implicate role of HtrA2-T242M mutation in mitochondrial dysfunction and morphological aberrations.

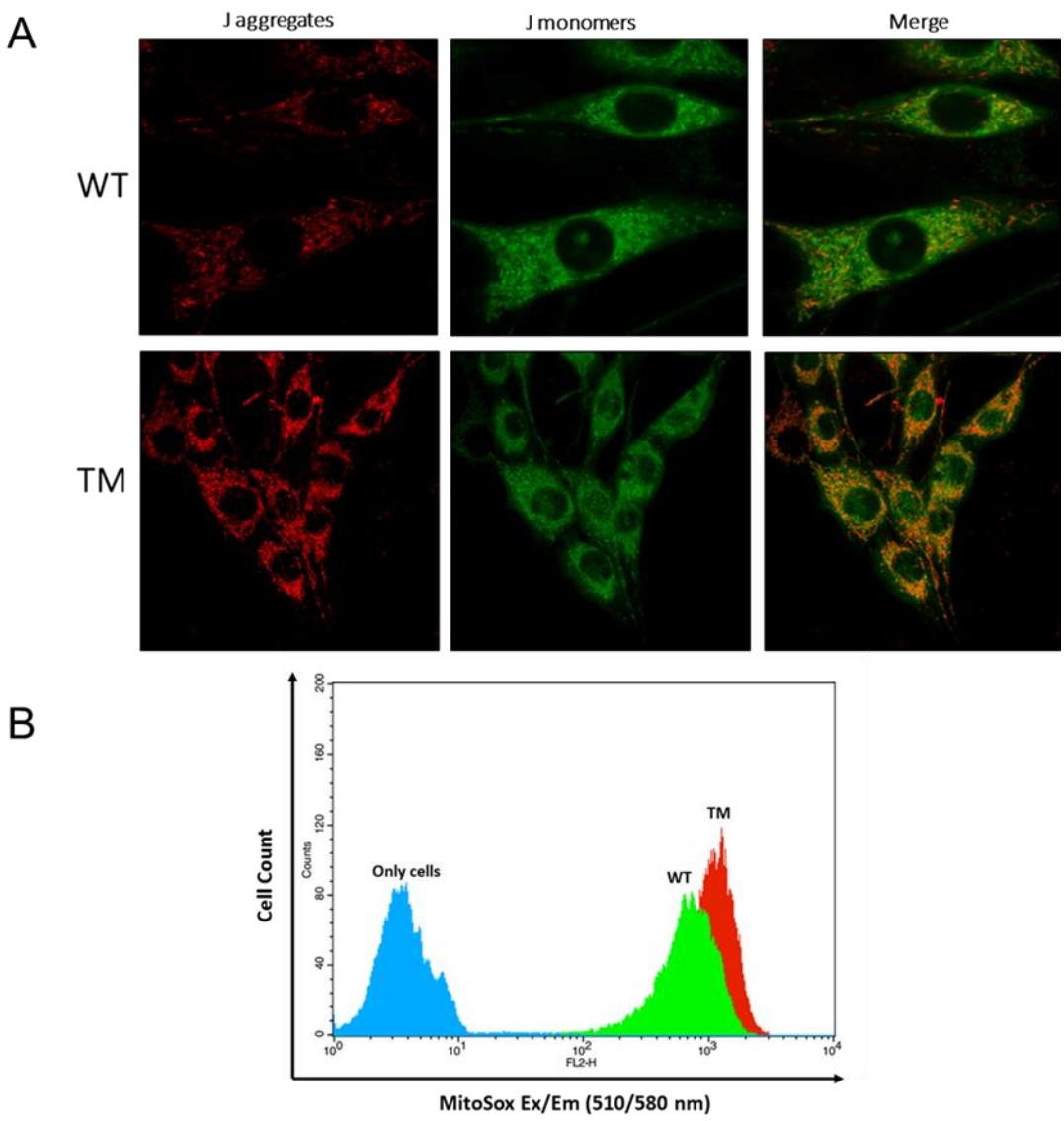

Figure 4.7. **T242M HtrA2 brings oxidative stress and membrane depolarization in the mitochondria of SHSY5Y cells**. **A)** T242M HtrAA2 and Wt. HtrA2 treated SHSY5Y cells were stained with JC-1 dye. **B)** SHSY5Y cells ($1x10^5$) were treated with T242M HtrA2 or Wt HtrA2 for 48 hours. The cells were stained with 5 µM MitoSOX Red dye and the amount of ROS accumulation in mitochondria was measured by flow cytometry on FL2 channel. The blue curve on extreme left indicate unstained cells, the green and red

curves represent Wt. HtrA2 and T242M HtrA2 treated cells respectively. The histogram plots are representative of three independent experiments.

GSK3β physically interacts and phosphorylates HtrA2

Using *Phosphositeplus* (*97*) *(*https://www.phosphosite.org*)*, we identified that Thr242 in the protease domain of HtrA2 is the potential phosphorylation site. To determine whether HtrA2 phosphorylation is likely to affect its proteolytic activity, we produced Thr242Glu (T242E), a phospho-mimetic HtrA2 mutant and compared its protease activity with that of the wild-type enzyme by using a previously described assay (*2*, *7*). Interestingly, we observed that phosphomimic mutant of HtrA2 completely lack the basal ability to cleave its generic substrate β-casein at variable concentrations **(Figure 4.8A)**.

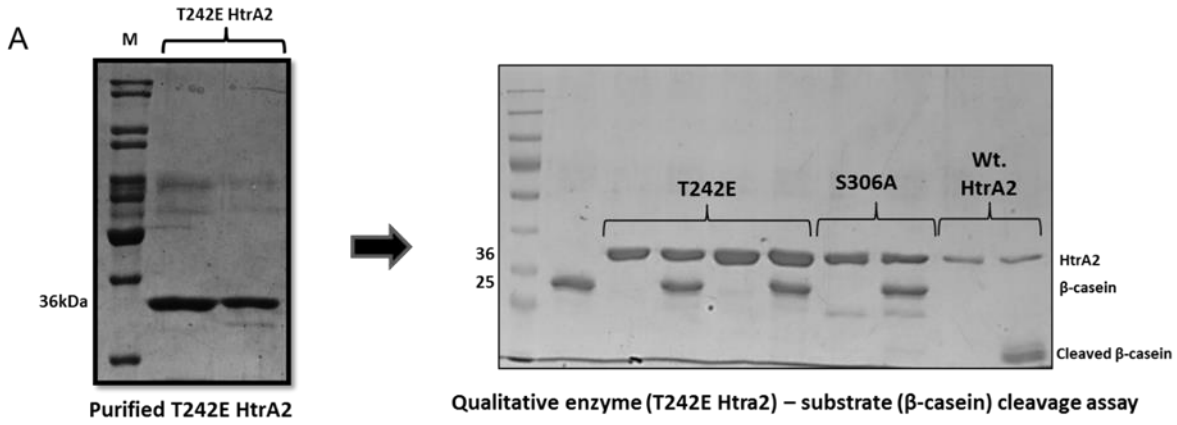

Later, the same residue was additionally mutated to alanine: T242A and as expected it showed protease activity just as wild type and T242M HtrA2. Also, alignment of HtrA2 homologues of different species shows that Threonine 242 is conserved in human, rodent, bacteria and canine. Threonine being a post translational modification site (Phosphorylation), we further wanted to investigate the nature of the kinase phosphorylating HtrA2 on Thr242 in intact cells. An analysis

with the *Scansite algorithm (98) (*http://scansite.mit.edu*) and NetPhos 3.1 server* (*99*) *(*http://www.cbs.dtu.dk/services/NetPhos/*)* showed that Threonine 242, is a putative phosphorylation site for proline directed serine/threonine kinases and it is located in the phosphorylation consensus site within its protease domain which is phosphorylated by glycogen synthase kinase 3β (GSK3β). Since these findings were indicative of a functional relation between HtrA2 and GSK3β, we investigated a physical interaction between these two proteins. Therefore, a carboxy-terminally FLAG tagged version of HtrA2 was expressed in HEK-293T cells, in order to recover and purification of tagged HtrA2 along with interacting proteins. We observed a direct interaction of overexpressed FLAG-tagged HtrA2 protein with endogenous GSK3β protein in co-immunoprecipitation experiments using HEK293T cells **(Figure 4.8B).** Moreover, to determine whether GSK3β phosphorylation could target HtrA2 or if GSK3β is a bona fide kinase for HtrA2, we performed an ADP-Glo kinase assay (https://www.promega.com/products/cell-signaling/kinase-assays/kinase-profiling-simplified/adp_glo-kinase-assay/), a type of *in vitro* kinase assay using T242M and Wt HtrA2. The assay works by measuring the amount of ADP generated after the kinase reaction **(Figure 4.8C)**. Collectively, we established that GSK3β interacts, phosphorylates and attenuates HtrA2 serine protease activity.

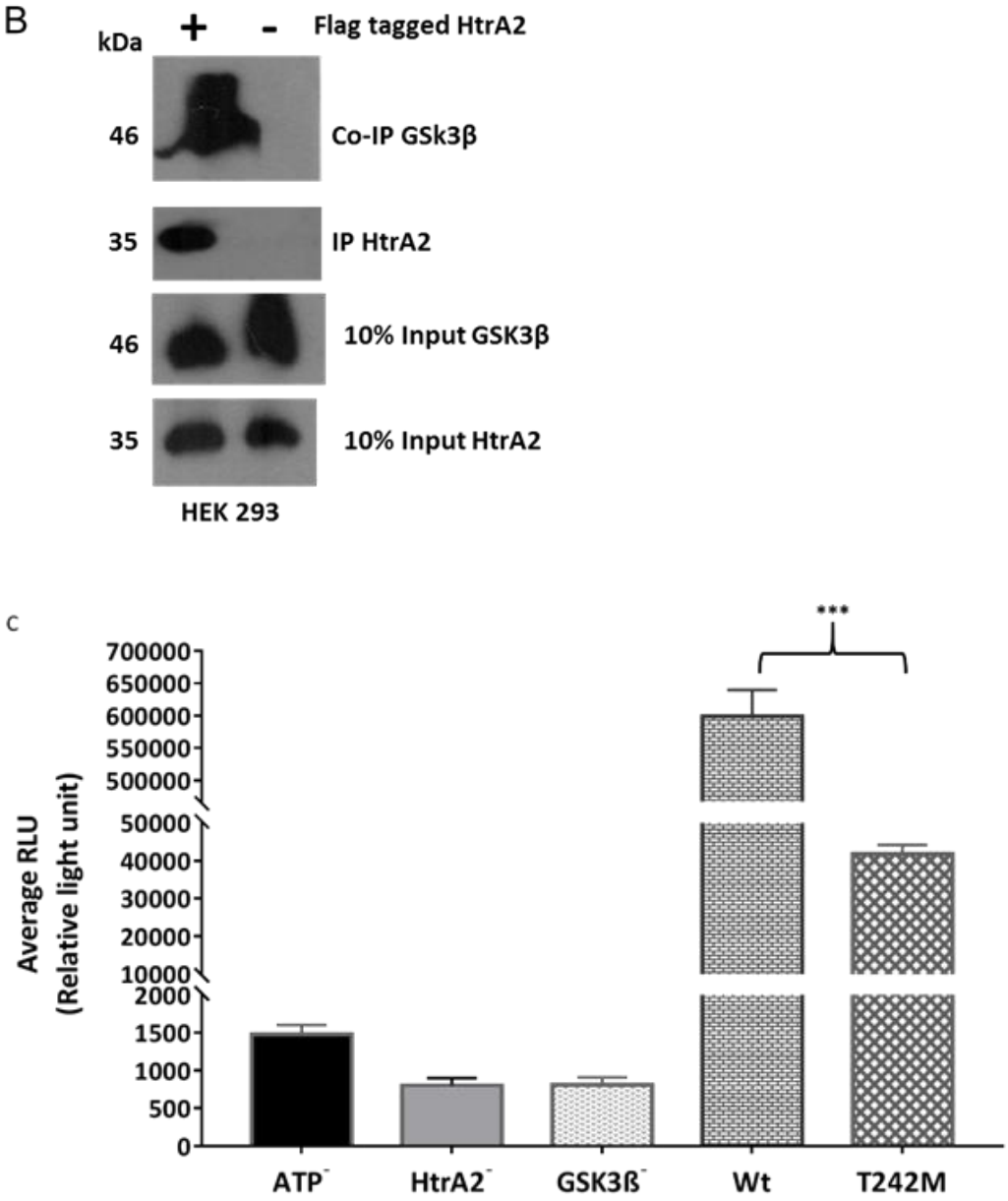

Figure 4.8. A) **Phosphorylation of HtrA2 decreases its proteolytic activity**; Protease activity of wild-type HtrA2 and the T242E phospho-mimetic mutants; 12% SDS PAGE was performed, β-casein used as a substrate, S306A HtrA2 (catalytically inactive mutant) used as a negative control B) **HtrA2 interacts with GSK3β.** HEK293T cells were

transfected with FLAG-tagged HtrA2 (+) while untransfected cells (-) were used as controls. Lysates were subjected to Western blot analysis directly (inputs) or after incubation overnight with anti-FLAG coupled agarose. Immunoblot were probed with anti-GSK3β and anti-HtrA2 as indicated. C) **In vitro kinase assay.** ADP Glo™ kinase assay showing Wt. HtrA2 phosphorylation; X axis, ATP^- (reaction without ATP), $HtrA2^-$ (reaction without HtrA2 as a substrate), $GSK3\beta^-$ (reaction without GSK3β as an enzyme) all these three acted as a negative controls. The plots are representative of three independent experiments.

GSK3β Inhibits HtrA2 Serine Protease Activity and pro-apoptotic function through a Phosphorylation-dependent Manner

Since mature/functional HtrA2 plays an important role in inducing the programmed cell death at post-mitochondrial level (*9, 10*) (*11, 12*), we next examined whether GSK3β anti-apoptotic function is mediated by phosphorylation of HtrA2. Therefore, to investigate the role we transfected SHSY5Y cells (5×10^5) with phosphomimic mutant (T242E) of HtrA2 and analyze the cell cycle using PI staining followed by flow cytometry. Interestingly, we detected remarkable increase in the survival of T242E transfected neurons (decreased sub G0/G1 population) relative to Wt and HtrA2 (T242M) transfected neurons **(Figure 4.9)**.

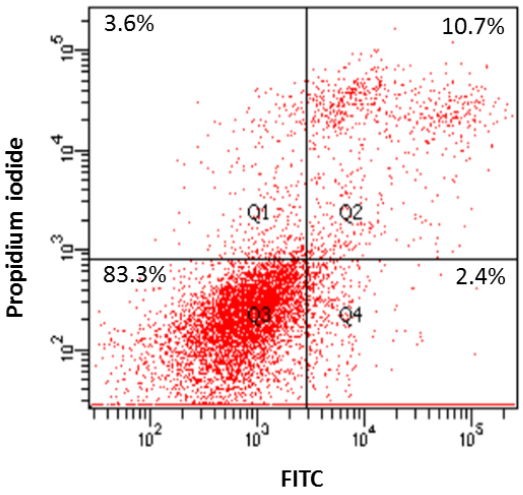

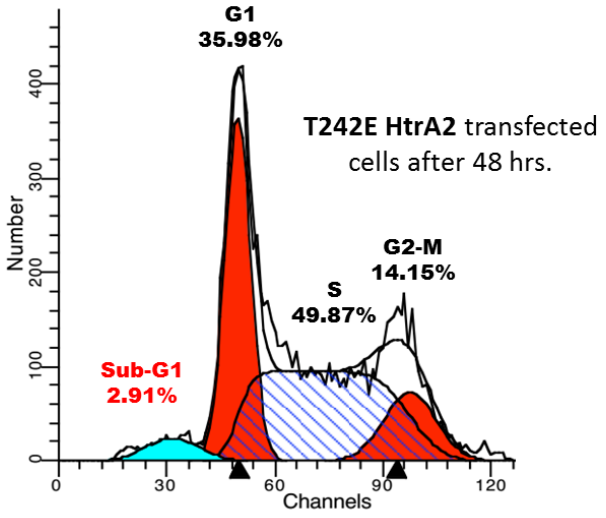

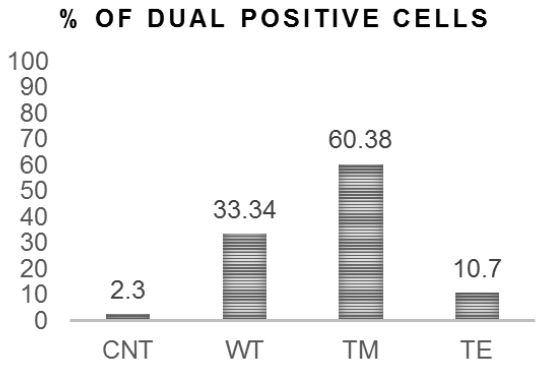

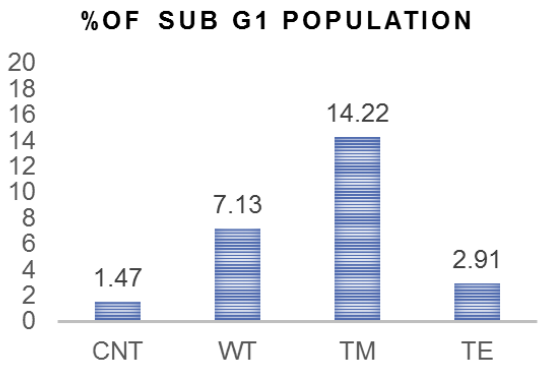

GSK-3β is essential for HtrA2 T242 phosphorylation with Apoptotic Stimuli

Growth factor withdrawal activates GSK-3 after inactivation of PI-3K/Akt pathway (*13, 14*). We employed flow cytometry to verify the involvement of GSK-3β signaling in SHSH5Y cells. Prior to that, to investigate the role of GSK-3β in phosphorylation-dependent HtrA2 inactivation, we inhibited GSK-3 by using a well-known potent inhibitor *SB415286* (Selleckchem Inc.). We transfected SHSY5Y cells (1 x 10^5) with T242M and WT HtrA2 with and without the inhibitor and subsequent serum withdrawal for 6hrs (so as to activate GSK-3β) and analyzed the cell death using Annexin V/PI staining followed by flow cytometry. Interestingly, our flow cytometry data

indicated that in presence of inhibitor, there is increase in cell death in both mutant and wild type HtrA2-transfected neurons as opposed to cells without inhibitor **(Figure 4.10A)**. In order to show inhibition by the specific inhibitor used, stability of β-catenin (Wnt signaling) was checked using western blotting **(Figure 4.10B)**. It is well known that in presence of inhibitor, GSK-3β-mediated destabilization of β-catenin was found to be inhibited.

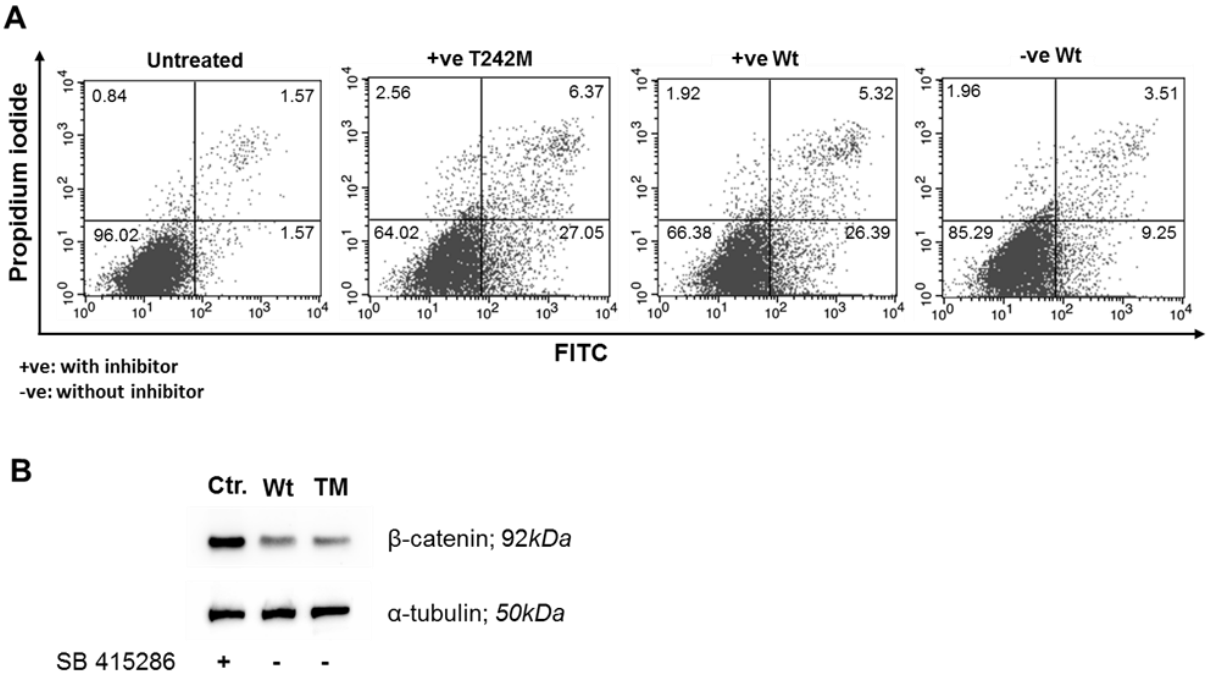

Figure 4.10. Characterization of GSK-3β mediated HtrA2 T242 phosphorylation under apoptotic Stimuli; A) SHSY5Y cells ($1x10^5$) were cultured under serum withdrawal (6hrs) or normal culture conditions transfected with Wt. and T242M HtrA2 for 36 h. percentage of apoptotic cells (early and late) were determined using Annexin V/PI staining and then flow cytometry. B) SHSY5Y cells ($1x10^5$) were transfected with Wt and T242M and treated with inhibitor and kept under serum withdrawal for 6hrs. We used Western blotting to determine the protein expression of β-catenin.

Structure of the T242M Mutant of HtrA2

To elucidate the three-dimensional structural details at the molecular level, structure of catalytically inactive T42M i.e. (T242M/S306A) HtrA2 using X-ray crystallography was solved at 2.5 Å resolution. Interestingly, the overall structure of the trimeric mutant was found to be similar to HtrA2 (S306A)(*1, 7*), with root-mean-square deviation (rmsd) of 0.2 Å between their equivalent Cα atoms **(Figure 4.11A-C)**. Structural analysis of T242M mutant show that the trimer contains α/β fold that is conserved among members of the HtrA superfamily, with 19β-strands and 7α-helices. The mutation site, T242 on the surface of the trimer is located in the loop connecting β6 and β7, and far from the catalytic serine residue. This loop exhibits low thermal or B factor (~23Å^2) suggesting less dynamic changes in that region in both the WT (PDB: 1LCY) (*1*) and the mutant structures. Therefore, the structural data suggest no significant structural alteration has been found in the mutant protein.

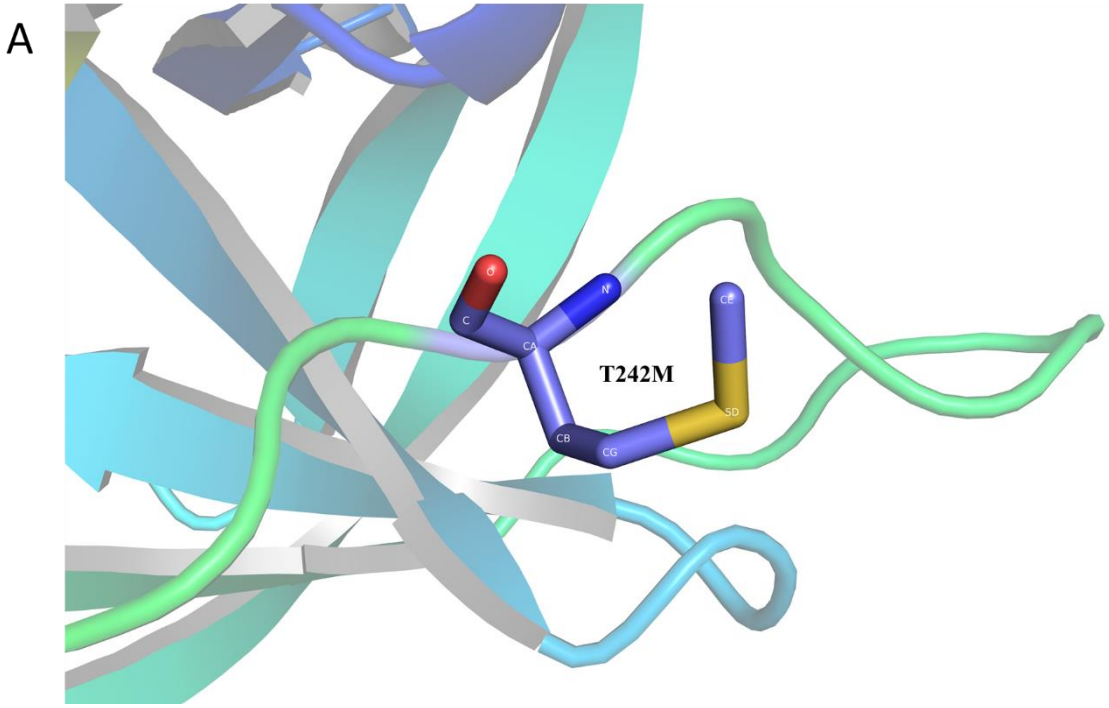

B

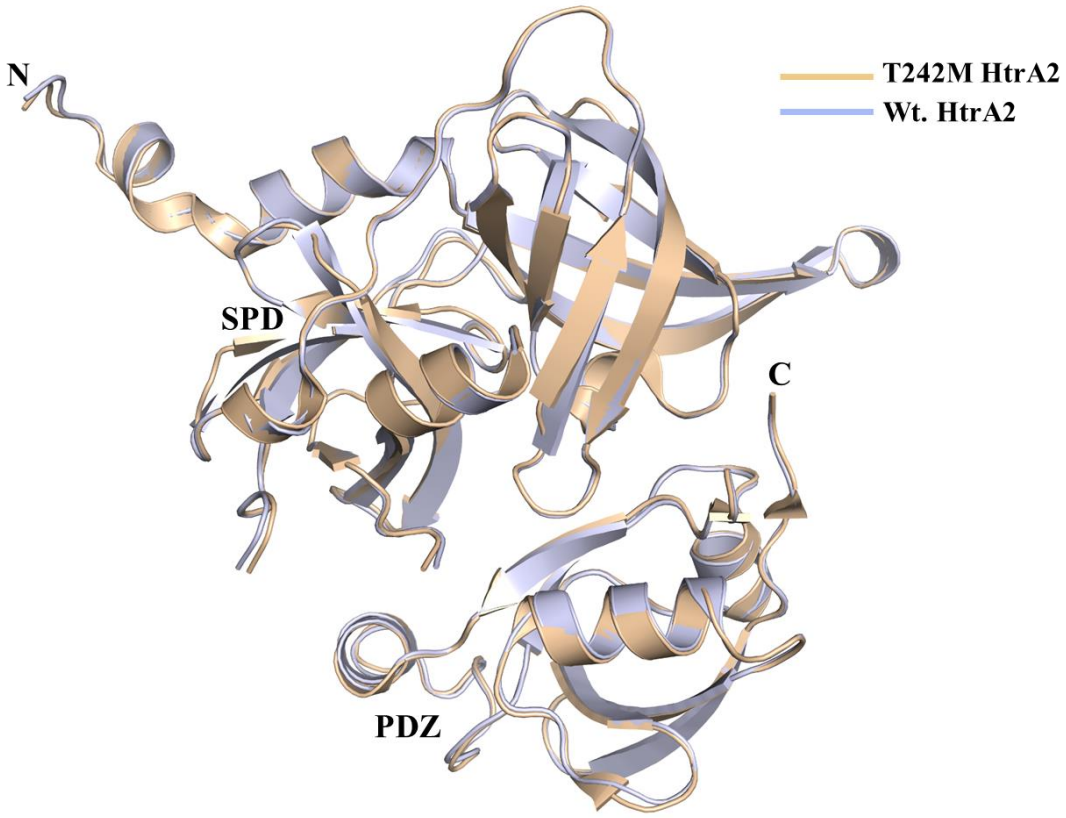
N
T242M HtrA2
Wt. HtrA2
SPD
C
PDZ

C

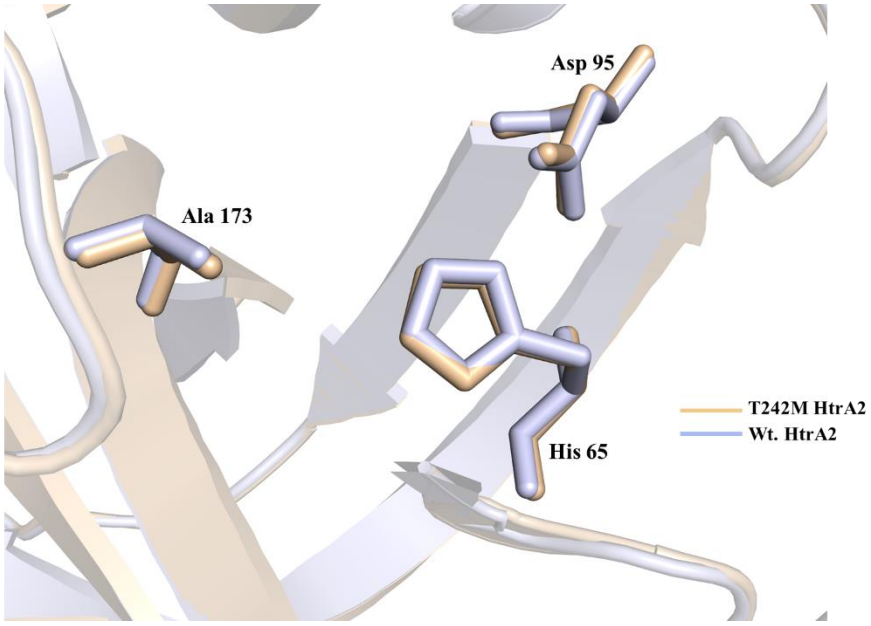
Asp 95
Ala 173
His 65
T242M HtrA2
Wt. HtrA2

Figure 4.11. Crystal Structure of the HtrA2 T242M solved at 2.5Å. A) The side chains of residue 242 are shown as stick model. Produced with PyMOL (DeLano Scientific, Palo Alto, CA, USA). B) Schematic drawing of the alignment of crystal structures of Wt. HtrA2 (PDB accession number 1LCY) and HtrA2 T242M. T242M monomer is colored in yellow and the Wt HtrA2 in light purple. Abbreviations: N: N terminal, C: C terminal, SPD: Serine protease domain, C) Stick diagram of the alignment of catalytic triad between the two structures.

Data collection and processing	T242M HtrA2	Wt. HtrA2 (1LCY)
Space group	R3H (146)	R3H
Unit cell dimensions		
a, b, c (Å)	85.9, 85.9, 126.9	-
α, β, γ (°)	90, 90, 120	90,90,120
Diffraction data		
Resolution range [Å] (highest resolution shell)	42,980 – 2.542 (2.608 – 2.542)	-
Unique reflections	30241	23,282
R_{merge} [%] (highest resolution shell)	7.8 (78.17)	5.8 (10)
Completeness (%) (highest resolution shell)	99.9 (99.65)	99.4 (99.8)
$CC_{(1/2)}$ (%) (highest resolution shell)	99.8 (58.23)	-
I/sigma (I) (highest resolution shell)	14.8 (2.0)	17.5
Refinement		
R_{work}/R_{free} (%)	18.6/23.2	21.5/24.1
MolProbity statistics		
Outliers (%)	1.38	-
Allowed (%)	3.10	-
Favored (%)	95.52	-

Table 4.3. Data analysis and statistics for T242M and Wt. HtrA2 (1LCY)

Summary and conclusion

1. We carried out extensive sequencing of HTRA2/PARK13 gene (*10, 15, 16*) in a cohort of 170 early and late onset Indian PD patients and identified a novel, non-synonymous, heterozygous, substitution at position 242 in the protease domain.
2. Here, we provide evidence that the c.725 C>T; p.T242M variant is causative of an autosomal recessive form of late onset PD by genetic and functional data and may be a pathogenic mutation.
3. We demonstrate that the c.725C>T substitution is a rare polymorphism because in a total of 340 alleles of early and late onset PD patients, only our homozygous index patient carried this substitution.
4. Based on the functional studies, our observation provides compelling evidence to support our finding that the T242M variant is detrimental for proper functioning of the protease as it disrupts mitochondrial function
5. Based on our findings on the molecular details of interaction between HtrA2 and GSK-3β, we speculate a general role for HtrA2 in cellular survival pathway under stress conditions. Our study opens up new areas of investigation on the role of HtrA2 in cellular homeostasis.
6. We know that growth factors directly and/or indirectly associated with the PI3-kinase/Akt pathway and then activates GSK-3β (*13, 14*). Just like many other proteases, the proteolytic activity of HtrA2 is tightly regulated to prevent unwanted proteolysis. Our studies indicates that GSK-3β phosphorylates HtrA2 thereby regulates its protease activity and play a role in neuronal survival **(Figure 4.12)**.

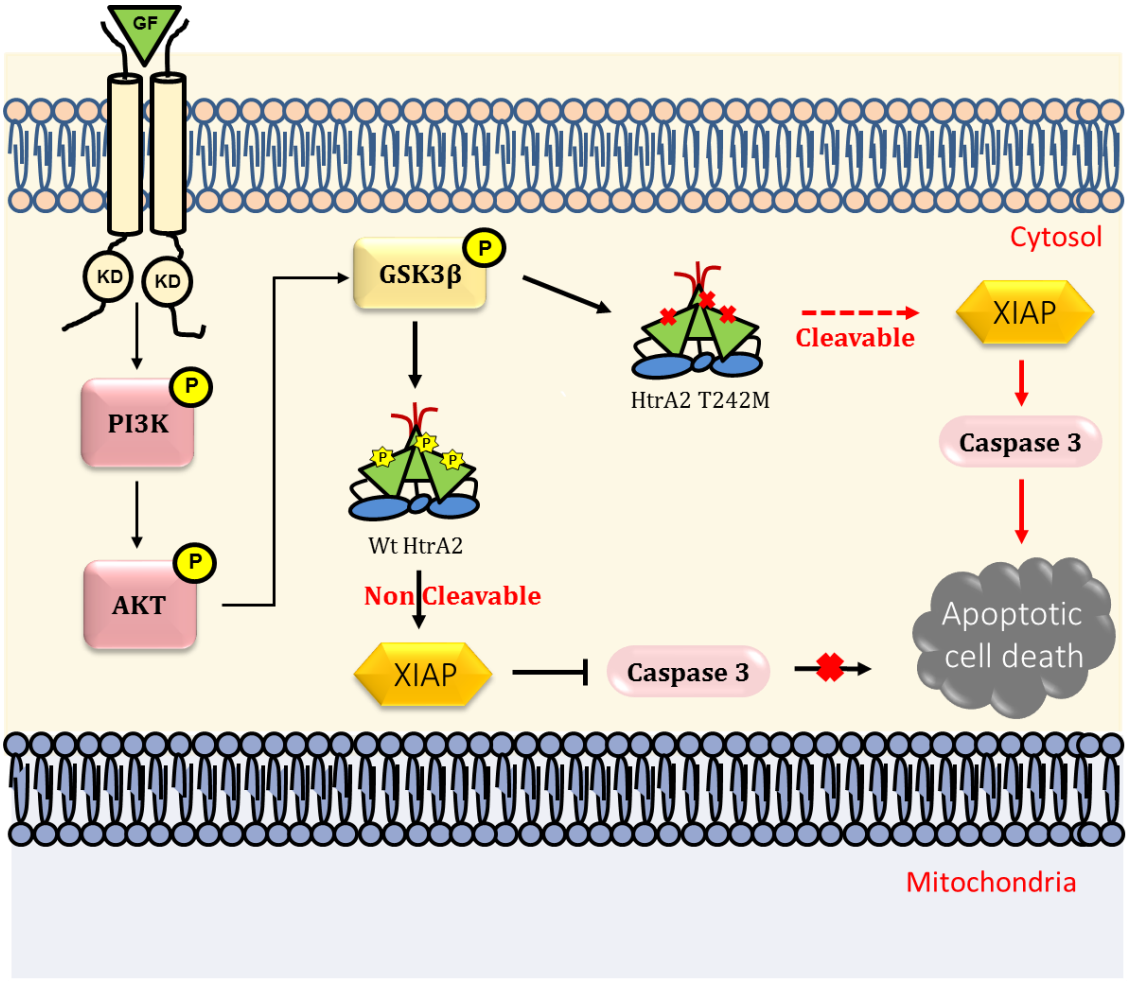

Figure 4.12. Schematic illustration of GSk3β regulation of HtrA2. GSK3β, Glycogen synthase kinase 3, β-isoform, XIAP X-linked inhibitor of apoptosis; PI3K, Phosphatidylinositol-4, 5-bisphosphate 3-kinase; Akt, Protein kinase B.

Significance of the study:

For the first time we have reported a novel mutation (c.725C>T, p.T242M) in HtrA2 from Indian Parkinson's disease patients. We have characterized the mutant both structurally as well as functionally and established a model signifying HtrA2's mechanism of regulation through phosphorylation at a site present in protease domain. Identification of this regulation control switch will open up avenues for modulating HtrA2 function favorably for therapeutic intervention. This study gives a definitive indication for the role of HtrA2 in Parkinson's disease.

References

References:

1. W. Li *et al.*, Structural insights into the pro-apoptotic function of mitochondrial serine protease HtrA2/Omi. *Nature structural biology* **9**, 436-441 (2002).
2. L. K. Chaganti, R. R. Kuppili, K. Bose, Intricate structural coordination and domain plasticity regulate activity of serine protease HtrA2. *FASEB journal : official publication of the Federation of American Societies for Experimental Biology* **27**, 3054-3066 (2013).
3. K. Zeth, Structural analysis of DegS, a stress sensor of the bacterial periplasm. *FEBS letters* **569**, 351-358 (2004).
4. C. Eigenbrot *et al.*, Structural and functional analysis of HtrA1 and its subdomains. *Structure* **20**, 1040-1050 (2012).
5. K. M. Strauss *et al.*, Loss of function mutations in the gene encoding Omi/HtrA2 in Parkinson's disease. *Human molecular genetics* **14**, 2099-2111 (2005).
6. P. R. Bejugam *et al.*, Allosteric regulation of serine protease HtrA2 through novel non-canonical substrate binding pocket. *PloS one* **8**, e55416 (2013).
7. A. R. Wagh, K. Bose, Structural Basis of Inactivation of Human Counterpart of Mouse Motor Neuron Degeneration 2 Mutant in Serine Protease HtrA2. *Bioscience reports*, (2018).
8. S. Jamil, I. Lam, M. Majd, S. H. Tsai, V. Duronio, Etoposide induces cell death via mitochondrial-dependent actions of p53. *Cancer cell international* **15**, 79 (2015).
9. Y. Suzuki *et al.*, A serine protease, HtrA2, is released from the mitochondria and interacts with XIAP, inducing cell death. *Molecular cell* **8**, 613-621 (2001).
10. A. M. Verhagen *et al.*, HtrA2 promotes cell death through its serine protease activity and its ability to antagonize inhibitor of apoptosis proteins. *The Journal of biological chemistry* **277**, 445-454 (2002).
11. L. Cilenti *et al.*, Characterization of a novel and specific inhibitor for the pro-apoptotic protease Omi/HtrA2. *The Journal of biological chemistry* **278**, 11489-11494 (2003).
12. R. Hegde *et al.*, Identification of Omi/HtrA2 as a mitochondrial apoptotic serine protease that disrupts inhibitor of apoptosis protein-caspase interaction. *The Journal of biological chemistry* **277**, 432-438 (2002).
13. U. Maurer, C. Charvet, A. S. Wagman, E. Dejardin, D. R. Green, Glycogen synthase kinase-3 regulates mitochondrial outer membrane permeabilization and apoptosis by destabilization of MCL-1. *Molecular cell* **21**, 749-760 (2006).
14. R. Mishra *et al.*, Glycogen synthase kinase-3beta induces neuronal cell death via direct phosphorylation of mixed lineage kinase 3. *The Journal of biological chemistry* **282**, 30393-30405 (2007).
15. C. W. Gray *et al.*, Characterization of human HtrA2, a novel serine protease involved in the mammalian cellular stress response. *European journal of biochemistry / FEBS* **267**, 5699-5710 (2000).
16. S. Krick *et al.*, Mpv17l protects against mitochondrial oxidative stress and apoptosis by activation of Omi/HtrA2 protease. *Proceedings of the National Academy of Sciences of the United States of America* **105**, 14106-14111 (2008).
17. S. Wickner, M. R. Maurizi, S. Gottesman, Posttranslational quality control: folding, refolding, and degrading proteins. *Science* **286**, 1888-1893 (1999).
18. L. M. Martins *et al.*, The serine protease Omi/HtrA2 regulates apoptosis by binding XIAP through a reaper-like motif. *The Journal of biological chemistry* **277**, 439-444 (2002).
19. L. Faccio *et al.*, Characterization of a novel human serine protease that has extensive homology to bacterial heat shock endoprotease HtrA and is regulated by kidney ischemia. *The Journal of biological chemistry* **275**, 2581-2588 (2000).

20. T. Clausen, C. Southan, M. Ehrmann, The HtrA family of proteases: implications for protein composition and cell fate. *Molecular cell* **10**, 443-455 (2002).
21. G. Y. Nie, A. Hampton, Y. Li, J. K. Findlay, L. A. Salamonsen, Identification and cloning of two isoforms of human high-temperature requirement factor A3 (HtrA3), characterization of its genomic structure and comparison of its tissue distribution with HtrA1 and HtrA2. *The Biochemical journal* **371**, 39-48 (2003).
22. S. I. Hu *et al.*, Human HtrA, an evolutionarily conserved serine protease identified as a differentially expressed gene product in osteoarthritic cartilage. *The Journal of biological chemistry* **273**, 34406-34412 (1998).
23. T. Krojer, M. Garrido-Franco, R. Huber, M. Ehrmann, T. Clausen, Crystal structure of DegP (HtrA) reveals a new protease-chaperone machine. *Nature* **416**, 455-459 (2002).
24. B. Lipinska, M. Zylicz, C. Georgopoulos, The HtrA (DegP) protein, essential for Escherichia coli survival at high temperatures, is an endopeptidase. *Journal of bacteriology* **172**, 1791-1797 (1990).
25. J. Skorko-Glonek *et al.*, The Escherichia coli heat shock protease HtrA participates in defense against oxidative stress. *Molecular & general genetics : MGG* **262**, 342-350 (1999).
26. C. Spiess, A. Beil, M. Ehrmann, A temperature-dependent switch from chaperone to protease in a widely conserved heat shock protein. *Cell* **97**, 339-347 (1999).
27. L. M. Martins *et al.*, Binding specificity and regulation of the serine protease and PDZ domains of HtrA2/Omi. *The Journal of biological chemistry* **278**, 49417-49427 (2003).
28. K. Jellinger, New developments in the pathology of Parkinson's disease. *Advances in neurology* **53**, 1-16 (1990).
29. S. Gandhi, N. W. Wood, Molecular pathogenesis of Parkinson's disease. *Human molecular genetics* **14**, 2749-2755 (2005).
30. S. Przedborski, Pathogenesis of nigral cell death in Parkinson's disease. *Parkinsonism & related disorders* **11 Suppl 1**, S3-7 (2005).
31. D. Sulzer, Multiple hit hypotheses for dopamine neuron loss in Parkinson's disease. *Trends in neurosciences* **30**, 244-250 (2007).
32. M. J. Farrer, Genetics of Parkinson disease: paradigm shifts and future prospects. *Nature reviews. Genetics* **7**, 306-318 (2006).
33. J. Hardy, P. Lewis, T. Revesz, A. Lees, C. Paisan-Ruiz, The genetics of Parkinson's syndromes: a critical review. *Current opinion in genetics & development* **19**, 254-265 (2009).
34. I. Martin, V. L. Dawson, T. M. Dawson, Recent advances in the genetics of Parkinson's disease. *Annual review of genomics and human genetics* **12**, 301-325 (2011).
35. T. Kitada *et al.*, Mutations in the parkin gene cause autosomal recessive juvenile parkinsonism. *Nature* **392**, 605-608 (1998).
36. A. B. Singleton *et al.*, alpha-Synuclein locus triplication causes Parkinson's disease. *Science* **302**, 841 (2003).
37. M. H. Polymeropoulos *et al.*, Mutation in the alpha-synuclein gene identified in families with Parkinson's disease. *Science* **276**, 2045-2047 (1997).
38. V. Bonifati *et al.*, Mutations in the DJ-1 gene associated with autosomal recessive early-onset parkinsonism. *Science* **299**, 256-259 (2003).
39. C. Paisan-Ruiz *et al.*, Cloning of the gene containing mutations that cause PARK8-linked Parkinson's disease. *Neuron* **44**, 595-600 (2004).
40. A. Zimprich *et al.*, Mutations in LRRK2 cause autosomal-dominant parkinsonism with pleomorphic pathology. *Neuron* **44**, 601-607 (2004).
41. J. T. Greenamyre, T. G. Hastings, Biomedicine. Parkinson's--divergent causes, convergent mechanisms. *Science* **304**, 1120-1122 (2004).

42. A. Ramirez *et al.*, Hereditary parkinsonism with dementia is caused by mutations in ATP13A2, encoding a lysosomal type 5 P-type ATPase. *Nature genetics* **38**, 1184-1191 (2006).
43. L. Egger *et al.*, Serine proteases mediate apoptosis-like cell death and phagocytosis under caspase-inhibiting conditions. *Cell death and differentiation* **10**, 1188-1203 (2003).
44. M. Okada *et al.*, A novel mechanism for imatinib mesylate-induced cell death of BCR-ABL-positive human leukemic cells: caspase-independent, necrosis-like programmed cell death mediated by serine protease activity. *Blood* **103**, 2299-2307 (2004).
45. D. L. Vaux, J. Silke, HtrA2/Omi, a sheep in wolf's clothing. *Cell* **115**, 251-253 (2003).
46. J. M. Jones *et al.*, Loss of Omi mitochondrial protease activity causes the neuromuscular disorder of mnd2 mutant mice. *Nature* **425**, 721-727 (2003).
47. L. M. Martins *et al.*, Neuroprotective role of the Reaper-related serine protease HtrA2/Omi revealed by targeted deletion in mice. *Molecular and cellular biology* **24**, 9848-9862 (2004).
48. A. Molgaard, S. Larsen, Crystal packing in two pH-dependent crystal forms of rhamnogalacturonan acetylesterase. *Acta crystallographica. Section D, Biological crystallography* **60**, 472-478 (2004).
49. A. D'arcy, C. Elmore, M. Stihle, J. Johnston, A novel approach to crystallising proteins under oil. *Journal of crystal growth* **168**, 175-180 (1996).
50. N. E. Chayen, P. Shaw Stewart, D. Maeder, D. Blow, An automated system for micro-batch protein crystallization and screening. *Journal of applied crystallography* **23**, 297-302 (1990).
51. M. Zeppezauer, H. Eklund, E. S. Zeppezauer, Micro diffusion cells for the growth of single protein crystals by means of equilibrium dialysis. *Archives of biochemistry and biophysics* **126**, 564-573 (1968).
52. J. M. Jones *et al.*, mnd2: a new mouse model of inherited motor neuron disease. *Genomics* **16**, 669-677 (1993).
53. J. S. Weber *et al.*, High-resolution genetic, physical, and transcript map of the mnd2 region of mouse chromosome 6. *Genomics* **54**, 107-115 (1998).
54. S. M. Kelly, T. J. Jess, N. C. Price, How to study proteins by circular dichroism. *Biochimica et biophysica acta* **1751**, 119-139 (2005).
55. J. Sohn, R. Sauer, OMP peptides modulate the activity of DegS protease by differential binding to active and inactive conformations. *Mol Cell* **33**, 64-74. (2009).
56. A. Leslie, Recent changes to the MOSFLM package for processing film and image plate data. (1992).
57. M. D. Winn *et al.*, Overview of the CCP4 suite and current developments. *Acta Crystallographica Section D: Biological Crystallography* **67**, 235-242 (2011).
58. B. W. Matthews, Solvent content of protein crystals. *Journal of molecular biology* **33**, 491-497 (1968).
59. A. Kumar *et al.*, Protein crystallography beamline (PX-BL21) at Indus-2 synchrotron. *Journal of synchrotron radiation* **23**, 629-634 (2016).
60. M. D. Winn *et al.*, Overview of the CCP4 suite and current developments. *Acta crystallographica. Section D, Biological crystallography* **67**, 235-242 (2011).
61. M. G. Rossmann, The molecular replacement method. *Acta Crystallographica Section A: Foundations of Crystallography* **46**, 73-82 (1990).
62. J. A. Clapperton *et al.*, Structure and mechanism of BRCA1 BRCT domain recognition of phosphorylated BACH1 with implications for cancer. *Nature structural & molecular biology* **11**, 512-518 (2004).
63. A. J. McCoy *et al.*, Phaser crystallographic software. *Journal of applied crystallography* **40**, 658-674 (2007).

64. A. W. Schuttelkopf, D. M. Van Aalten, PRODRG: a tool for high-throughput crystallography of protein-ligand complexes. *Acta Crystallographica Section D: Biological Crystallography* **60**, 1355-1363 (2004).
65. H. M. Berman *et al.*, The Protein Data Bank. *Acta crystallographica. Section D, Biological crystallography* **58**, 899-907 (2002).
66. S. Pronk *et al.*, GROMACS 4.5: a high-throughput and highly parallel open source molecular simulation toolkit. *Bioinformatics* **29**, 845-854 (2013).
67. B. Hess, C. Kutzner, D. van der Spoel, E. Lindahl, GROMACS 4: Algorithms for Highly Efficient, Load-Balanced, and Scalable Molecular Simulation. *Journal of chemical theory and computation* **4**, 435-447 (2008).
68. D. Van Der Spoel *et al.*, GROMACS: fast, flexible, and free. *Journal of computational chemistry* **26**, 1701-1718 (2005).
69. D. Zurawa-Janicka *et al.*, Temperature-induced changes of HtrA2(Omi) protease activity and structure. *Cell stress & chaperones* **18**, 35-51 (2013).
70. W. Kabsch, Xds. *Acta crystallographica. Section D, Biological crystallography* **66**, 125-132 (2010).
71. P. D. Adams *et al.*, The Phenix software for automated determination of macromolecular structures. *Methods* **55**, 94-106 (2011).
72. D. Figaj *et al.*, The LD loop as an important structural element required for transmission of the allosteric signal in the HtrA (DegP) protease from Escherichia coli. *The FEBS journal* **283**, 3471-3487 (2016).
73. P. L. Privalov, C. Crane-Robinson, Role of water in the formation of macromolecular structures. *European biophysics journal : EBJ* **46**, 203-224 (2017).
74. F. Franks, Protein stability: the value of 'old literature'. *Biophysical chemistry* **96**, 117-127 (2002).
75. M. Chaplin, Do we underestimate the importance of water in cell biology? *Nature reviews. Molecular cell biology* **7**, 861-866 (2006).
76. L. Zhang *et al.*, Mapping hydration dynamics around a protein surface. *Proceedings of the National Academy of Sciences of the United States of America* **104**, 18461-18466 (2007).
77. N. Nagano, M. Ota, K. Nishikawa, Strong hydrophobic nature of cysteine residues in proteins. *FEBS letters* **458**, 69-71 (1999).
78. N. Singh, R. R. Kuppili, K. Bose, The structural basis of mode of activation and functional diversity: a case study with HtrA family of serine proteases. *Archives of biochemistry and biophysics* **516**, 85-96 (2011).
79. N. Singh, A. D'Souza, A. Cholleti, G. M. Sastry, K. Bose, Dual regulatory switch confers tighter control on HtrA2 proteolytic activity. *The FEBS journal* **281**, 2456-2470 (2014).
80. A. K. de Regt *et al.*, A conserved activation cluster is required for allosteric communication in HtrA-family proteases. *Structure* **23**, 517-526 (2015).
81. M. F. Colombo, D. C. Rau, V. A. Parsegian, Protein solvation in allosteric regulation: a water effect on hemoglobin. *Science* **256**, 655-659 (1992).
82. M. C. de Rijk *et al.*, Prevalence of Parkinson's disease in Europe: A collaborative study of population-based cohorts. Neurologic Diseases in the Elderly Research Group. *Neurology* **54**, S21-23 (2000).
83. M. C. de Rijk *et al.*, Prevalence of parkinsonism and Parkinson's disease in Europe: the EUROPARKINSON Collaborative Study. European Community Concerted Action on the Epidemiology of Parkinson's disease. *Journal of neurology, neurosurgery, and psychiatry* **62**, 10-15 (1997).
84. S. K. Das *et al.*, Epidemiology of Parkinson disease in the city of Kolkata, India: a community-based study. *Neurology* **75**, 1362-1369 (2010).

85. L. S. Forno, Neuropathology of Parkinson's disease. *Journal of neuropathology and experimental neurology* **55**, 259-272 (1996).
86. A. Toulouse, A. M. Sullivan, Progress in Parkinson's disease-where do we stand? *Progress in neurobiology* **85**, 376-392 (2008).
87. S. Higuchi *et al.*, Mutation in the alpha-synuclein gene and sporadic Parkinson's disease, Alzheimer's disease, and dementia with lewy bodies. *Experimental neurology* **153**, 164-166 (1998).
88. C. Das *et al.*, Structural basis for conformational plasticity of the Parkinson's disease-associated ubiquitin hydrolase UCH-L1. *Proceedings of the National Academy of Sciences of the United States of America* **103**, 4675-4680 (2006).
89. E. M. Valente *et al.*, Hereditary early-onset Parkinson's disease caused by mutations in PINK1. *Science* **304**, 1158-1160 (2004).
90. N. V. Morgan *et al.*, PLA2G6, encoding a phospholipase A2, is mutated in neurodegenerative disorders with high brain iron. *Nature genetics* **38**, 752-754 (2006).
91. S. Lesage, A. Brice, Parkinson's disease: from monogenic forms to genetic susceptibility factors. *Human molecular genetics* **18**, R48-59 (2009).
92. V. Bogaerts *et al.*, Genetic variability in the mitochondrial serine protease HTRA2 contributes to risk for Parkinson disease. *Human mutation* **29**, 832-840 (2008).
93. G. S. Kadakol, S. S. Kulkarni, G. M. Wali, P. B. Gai, Molecular analysis of alpha-synuclein gene in Parkinson's disease in North Karnataka, India. *Neurology India* **62**, 149-152 (2014).
94. M. Karimi *et al.*, Subthalamic nucleus stimulation-induced regional blood flow responses correlate with improvement of motor signs in Parkinson disease. *Brain : a journal of neurology* **131**, 2710-2719 (2008).
95. M. Marabese, M. Mazzoletti, F. Vikhanskaya, M. Broggini, HtrA2 enhances the apoptotic functions of p73 on bax. *Cell death and differentiation* **15**, 849-858 (2008).
96. J. S. Park, R. L. Davis, C. M. Sue, Mitochondrial Dysfunction in Parkinson's Disease: New Mechanistic Insights and Therapeutic Perspectives. *Current neurology and neuroscience reports* **18**, 21 (2018).
97. P. V. Hornbeck *et al.*, PhosphoSitePlus: a comprehensive resource for investigating the structure and function of experimentally determined post-translational modifications in man and mouse. *Nucleic acids research* **40**, D261-270 (2012).
98. J. C. Obenauer, L. C. Cantley, M. B. Yaffe, Scansite 2.0: Proteome-wide prediction of cell signaling interactions using short sequence motifs. *Nucleic acids research* **31**, 3635-3641 (2003).
99. N. Blom, T. Sicheritz-Ponten, R. Gupta, S. Gammeltoft, S. Brunak, Prediction of post-translational glycosylation and phosphorylation of proteins from the amino acid sequence. *Proteomics* **4**, 1633-1649 (2004).

Publication reprints

Bioscience Reports (2018) **38** BSR20181072
https://doi.org/10.1042/BSR20181072

PORTLAND PRESS

Research Article

Structural basis of inactivation of human counterpart of mouse motor neuron degeneration 2 mutant in serine protease HtrA2

Ajay R. Wagh[1,2] and Kakoli Bose[1,2]

[1]Advanced Centre for Treatment, Research and Education in Cancer (ACTREC), Tata Memorial Centre, Kharghar, Navi Mumbai 410210, India; [2]Homi Bhabha National Institute, Training School Complex, Anushaktinagar, Mumbai 400094, India

Correspondence: Kakoli Bose (kbose@actrec.gov.in)

Serine protease high temperature requirement protease A2 (HtrA2) is involved in apoptosis and protein quality control. However, one of its murine inactive mutants (S276C aka mnd2) is associated with motor neuron degeneration 2. Similarly, this conserved mutation in human HtrA2 (hHtrA2) also renders the protease inactive, implicating pathogenicity. However, the structural determinants for its inactivation have not yet been elucidated. Here, using multidisciplinary approach, we studied the structural basis of inactivity associated with this mutation in hHtrA2. Characterization of secondary and tertiary structural properties, protein stability, oligomeric properties, and enzyme activity for both wild-type and mutant has been performed using biophysical and functional enzymology studies. The structural comparison at atomic resolution has been carried out using X-ray crystallography. While enzyme kinetics showed inactivity, spectroscopic probes did not identify any significant secondary structural changes in the mutant. X-ray crystallographic analysis of the mutant protein at 2 Å resolution highlighted the significance of a water molecule that plays important role in mediating intermolecular interactions for maintaining the functional ensemble of the protease. Overall, the crystallographic data along with biophysical and enzymology studies helped decipher the structural basis of inactivity of hHtrA2S276C, which might pave way toward further investigating its correlation with aberration of normal cellular functions, hence pathogenicity.

Introduction

HtrA2 belongs to the high temperature requirement factor A (HtrA) family of serine proteases, which are conserved from prokaryotes to humans. HtrA was originally identified as a heat-shock-induced serine protease in *Escherichia coli* that degraded misfolded/unfolded proteins formed during excessive stress conditions [1]. The members of the HtrA family share common domain arrangement such as chymotrypsin-like serine protease domain and at least one or two C-terminal PDZ [postsynaptic density protein (PSD95), *Drosophila* disc large tumor suppressor (Dlg1), and zonula occludens-1 protein (zo-1)] or protein–protein interaction domain(s) [2]. Once these regulatory PDZ domains recognize misfolded/damaged proteins or any other interacting partner with a specific function, a series of conformational changes with concomitant activation of the protease take place [3].

The members of HtrA family are found to be associated with several critical biological functions, as well as pathogenicity, such as protein quality control, unfolded protein response, cell growth, apoptosis, and disorders including Alzheimer's, Parkinson's, arthritis and cancer [3-5]. Human HtrA2, the most well-known among the four human HtrA family members (HtrA1–4), has been found to exhibit proapoptotic activity with the ability to stimulate apoptosis through multiple pathways [3]. While hHtrA2 predominantly resides in the intermembrane space of the mitochondria, it has also been reported to be present

Received: 28 June 2018
Revised: 23 July 2018
Accepted: 31 July 2018

Accepted Manuscript Online: 01 August 2018
Version of Record published: 05 October 2018

Bioscience Reports (2018) **38** BSR20181072
https://doi.org/10.1042/BSR20181072

in the endoplasmic reticulum (ER) and Golgi bodies [6]. Human HtrA2 is synthesized as a 458 amino acid precursor protein, comprising a short N-terminal region, a serine protease, and a C-terminal PDZ domain. The protease undergoes maturation upon removal of first 133 residues that encompass a transmembrane (TM) region and a mitochondrial localization signal (MLS). This cleavage exposes an inhibitor of apoptosis protein (IAP) recognizing tetra-peptide motif (AVPS), which is unique to this member of the HtrA family. Under apoptotic stimulation, a mature processed form of hHtrA2 (Δ133) is released into the cytosol where it binds to the cytosolic IAPs and negates their caspase-inhibitory activity [7] by direct proteolytic cleavage [5]. The mature protein has also been found to stimulate apoptosis-like morphological changes and extensive cell death that are not blocked by caspase inhibitors [5], suggesting it can induce cell death through multiple pathways.

Structurally, mature hHtrA2 exists as a homotrimer with pyramidal architecture where the core serine protease domains are surrounded by C-terminal PDZ domains that reside at the base. The short N-terminal regions that form the top of the pyramid involve in packing of the three monomers primarily through van der Waals interactions thus creating an extremely buried active-site milieu. HtrA2 consists of 7 α-helices and 19 β-strands, which together form well-defined domains along with several functionally important loop structures [8]. Among these loops, the active site serine residue (S306) resides in Loop 1 (L1; 302-306), while Loop 3 (L3; 275-285) harbors the mnd2 mutation. Apart from rendering flexibility to the trimeric protease ensemble, these loops that together form the activation domain have also been implicated in allosteric modulation of serine protease activity of hHtrA2 [3,9]. A close look at its bacterial counterpart, DegP, shows that it exhibits major rearrangement upon ligand binding in the sensor loop L3. This results in its interaction with the activation loop LD of a neighboring subunit (referred to here as LD*), thereby inducing disorder-to-order transition of the activation domain [3]. The structural signature as well as the dynamics associated with this mechanism of activation is conserved in the HtrA family including hHtrA2 that requires a coordinated action of the regulatory loops. The PDZ domain in hHtrA2 is connected to the protease domain via a flexible linker sequence and has a peptide binding groove (YIGV, a variation of GLGF motif) formed by β14 and α7 structures. The peptide-binding pocket of the PDZ domain is buried at the interface between the PDZ and the protease domains suggesting requirement of a significant conformational change for binding of the C-terminal interacting partners.

Recently, increasing evidences have linked hHtrA2 to neurodegeneration and the cellular protein quality control system. Motor neuron degeneration 2 (mnd2) homozygous mice, in which the missense mutation S276C leads to a remarkable loss of murine HtrA2's protease activity, showed severe neurodegeneration in the striatum and less severe neurodegeneration in the brain stem and spinal cord [10]. Interestingly, several missense mutations, in the gene coding for hHtrA2, were reported to be associated with Parkinson's disease (PD) [11]. In consonance with these reports, hHtrA2 has also been found in neurons and glial cells in brains with α-synucleinopathies [12] as well as in Lewy bodies [11]. Similar to mnd2 mice, hHtrA2 knockout mice showed loss of a population of neurons in the striatum, with PD phenotype leading to death within 30 days of birth [13]. Additionally, many other neurodegenerative disease proteins, such as presenilin-1 [14,15] and amyloid precursor protein, [16] have been reported to be associated with hHtrA2. Furthermore, loss of hHtrA2 activity in non-neuronal tissues has recently been shown to cause premature aging [17].

However, apart from the mouse model study, no further mechanistic characterization has been done on S276C mutant to delineate the structural basis of its inactivation. Therefore, the aim of the present work is to understand how S276C point mutation that resides away from the catalytic triad completely abolishes the protease activity, which would indirectly shed light on hHtrA2 mechanism of action. In HtrA family, it is known that the sensory loop L3 (that harbors S276), upon substrate binding, rearranges and carries out intermolecular interactions, which ultimately leads to enzyme activation [3]. Similarly, sensory loops have been found to play crucial functional roles in hHtrA2 as well [9,18]. Therefore, mutation of serine 276 to a cysteine in hHtrA2 might destabilize the intermolecular interaction networks involving loop L3 and adjoining residues and loops. The present study reports the crystal structure of hHtrA2S276C protease at 2 Å resolution with intact catalytic triad. Comparison with hHtrA2 structure suggests that the absence of a critical water-mediated intermolecular interaction between side chains of S276 of L3 and I270 from LD* (of adjoining monomer) might abrogate the relay of signal towards loop L1*, which include residues of oxyanion hole and catalytic triad thus resulting in an inactive variant of the protease.

Materials and methods

Sub cloning, protein expression, and purification

Recombinant mature (Δ133) hHtrA2 with C-terminal 6X-Histidine tag in pET-20b (Addgene, Cambridge, MA, U.S.A.) vector was expressed and purified as described previously [19]. To introduce mutations (S276C, S276A,

R280A, and S306A), site-directed mutagenesis (SDM) (Stratagene, TX, U.S.A.) was performed. Primers used for SDM are shown in Supplementary Table S1. Mutations were confirmed by Sanger DNA sequencing.

Recombinant proteins (wild-type [wt] and hHtrA2S276C, S276A, R280A, and S306A) were expressed in *E. coli* strain Rosetta (DE3) (Novagen, Billerica, MA, U.S.A.). Cells were grown at 37°C until OD_{600} of 0.6 was reached and then induced with 0.25 mM IPTG. Cells were further cultured at 16°C for 20 h postinduction. Proteins with the 6X-His tag were purified by affinity chromatography using nickel–nitrilotriacetic acid matrix (Ni-NTA) (Novagen), in 20 mM Na_2HPO_4/NaH_2PO_4 (pH 8.0) buffer containing 100 mM NaCl (referred to as buffer-A hereafter). Mutant hHtrA2 proteins were further purified through a gel filtration column (Superdex® 200 10/300 GL; GE AKTA purifier) as a part of a two-step purification. The purity of the eluted fractions was checked on 12% SDS–PAGE. During the procedure of crystallization of hHtrA2S276C and S306A, proteins were concentrated using an Amicon ultra centrifugation unit (Millipore, molecular-weight cutoff 10kDa) to get a maximum concentration of 25 mg/ml.

In vitro protease activity assays

Protease activity of mature wt hHtrA2 and its mutants (S276C, S276A, and R280A) was measured by in-gel as well as continuous fluorescence-based protease assays. The in-gel protease assay was carried out as described previously [20,21]. Protease activity of all the hHtrA2 variants was determined using substrate β-casein (Sigma Chemicals, St Louis, MO, U.S.A.) and compared with the wt hHtrA2 (used as a positive control) and catalytically inactive mutant (S306A) of hHtrA2 (used as a negative control). For each 20 µl of reaction mixture, mutant protein was incubated with 10 µg of β-casein in buffer-A at 37°C for 60 min and results were analyzed by SDS–PAGE. For all quantitative studies, FITC β-casein (Sigma) was used as described earlier [20]. Reaction rates (V_o) at different substrate concentrations were calculated using linear regression analysis. Steady state kinetic parameters were determined by fitting the data to the Hill form of the Michaelis–Menten equation:

$$\text{Velocity } (V) = \frac{V_{\max}}{\left[1 + \left(\frac{K_{0.5}}{[\text{substrate}]}\right) n\right]}$$

where $V_{\max}$ is the maximum velocity, 'n' is the Hill constant, and $K_{0.5}$ is the substrate concentration at half maximal velocity using KaleidaGraph (Synergy Software, Reading, PA, U.S.A.) as previously mentioned [9,20].

Native-PAGE assay

Purified proteins (wt and hHtrA2S276C) in native-PAGE sample buffer (62.5 mM Tris-Cl, pH 6.8, 15% glycerol, and 0.01% bromophenol blue) were separated on a 7.5% native-PAGE. Samples were run along with the standard protein ladder of molecular weight (MW) (NativeMark™ Unstained Protein Standard, Thermo Fisher Scientific, Inc.) ranging from 40 to 150 kDa.

Gel filtration chromatography

Gel filtration chromatography was performed in a buffer comprising 10 mM HEPES (pH 8.0), 100 mM NaCl referred to as buffer-B hereafter. Highly concentrated (∼20 mg/ml) purified mutant proteins (S276C and S306A) were separately applied to a Superdex S200 HR 10/300 column (GE Healthcare, Uppsala, Sweden) that was pre-equilibrated in buffer-B. Proteins were then eluted in the same buffer at a flow rate of 0.2 ml/min. The standards used for calibration were as follows: BSA 66 kDa, alcohol dehydrogenase 150 kDa, and β-amylase 200 kDa. Elution volume (V_e)/void volume (V_0) compared with log of molecular masses of standards was plotted to generate the calibration curve from which MWs of hHtrA2 and its variants were calculated as described earlier [20].

Dynamic light scattering

The dynamic light scattering (DLS) measurements were performed using the DynaPro-MS800 instrument (Protein Solutions Inc., VA, U.S.A.). The mutant hHtrA2S276C protein and buffer solutions were filtered (0.22 µm pore size) and degassed prior to measurement. Protein (3 mg/ml) in buffer-A was loaded into a 45 µl quartz cuvette. Experiments were performed at 25°C and at least 20–30 measurements each of a 10-s duration were collected. The refractive index and viscosity values were taken for water as provided by the software. Histogram analyses of DLS results were carried out using the software DYNAMICS version 6.0. The molecular size estimation in the present work was done using Wyatt technology DynaPro particle size analyzer. From the correlation function, the diffusion coefficients (D_T) of the molecules were calculated by fitting the data. Finally the hydrodynamic radius (R_h) of the particles and

Bioscience Reports (2018) **38** BSR20181072
https://doi.org/10.1042/BSR20181072

molecules were determined:

$$D = \frac{kT}{6\pi\,\eta_0 R_{\mathrm{h}}} \tag{1}$$

$$R_{\mathrm{h}} = \frac{kT}{6\pi\,\eta_0 R_{\mathrm{h}}} \tag{2}$$

Here, k is the Boltzmann constant, T is temperature in Kelvin, and η_0 is viscosity of solvent.

Far-UV circular dichroism spectroscopy

Far-UV circular dichroism (CD) measurements were made using a JASCO J-815 spectropolarimeter (JASCO, Easton, MD, U.S.A.) with a 1 mm cell at 25°C in a thermostatted cell holder at a concentration of 10 μM in buffer-A. CD spectra of wt hHtrA2 and purified hHtrA2S276C were recorded in the far-UV region (260–195 nm). All spectra were recorded at least thrice and the average is plotted. The mean residue ellipticity [θ] mrw, λ (deg · cm^2 · $dmol^{-1}$) is given by

$$[\theta]\,\mathrm{mrw},\ \lambda = \frac{\mathrm{MRW}\theta}{10d.c} \tag{3}$$

where θ is the observed ellipticity (degrees), d is the path length (cm), λ is the wavelength (nm), and c is the concentration (g/ml).For thermal denaturation studies, far-UV CD experiments were performed between 25 and 100°C at 2°C intervals. Thermal denaturation studies were performed to measure melting point temperatures (T_{m}) of wt and hHtrA2S276C. Far-UV CD signals were recorded between 20 and 85°C at 2°C intervals at 208 nm. The mean residue ellipticity was computed as reported previously [22].

Protein crystallization

Concentrated protein samples of hHtrA2S276C and S306A (∼25 mg/ml) were used for crystallization. Initial crystallization trials were performed by hanging-drop vapor-diffusion method in 48-well crystallization plates (Hampton Research, Laguna Niguel, California, U.S.A.) utilizing the commercial crystallization screens: Screen 1 and Screen 2 (Hampton Research). Drops prepared by mixing 2 μl of protein solution with an equal volume of crystallization buffer were equilibrated against 500 μl of crystallization buffers.

Initially, crystal-like particles were observed in one of the wells containing formulation number 21 (0.1 M MES pH 6.5 (buffer), 2 M NaCl (Precipitant), 0.1 M KH_2PO_4, and 0.1 M NaH_2PO_4) from Crystal Screen 2 (Hampton research) postincubation at 295K for 2 weeks. For the crystallization of hHtrA2S306A, the same condition was followed. Further finer optimization of crystallization conditions led to the formation of larger crystals. Finally, equilibration of a mixture of 2μl of protein solution with 1μl of precipitant solution against reservoir solution at 295K for 15days produced diffraction-quality crystals, with a biggest dimension of 0.3 × 0.2 × 0.2 mm. The crystals were cryo-protected using ultrapure glycerol (Hampton Research).

X-ray diffraction data collection and processing

The single-crystal diffraction experiments on hHtrA2S276C mutant protein crystals were carried out on the protein crystallography beam line (PX-BL21) at the 2.5GeV Indus-2 synchrotron radiation facility RRCAT, Indore, India [23]. The crystals were soaked in a cryo-protectant solution (reservoir/well solution with 30% glycerol). A total of 131 diffraction images for S276C crystals were collected on a MAR225 CCD (Rayonix) detector from a cryo-cooled crystal (100 K) by using 1° oscillation and X-rays of wavelength 0.97947 Å.

For hHtrA2S306A, multiwavelength X-ray data were collected at the beamline BM30 (FIP), ESRF, and Grenoble. All data sets were collected using the single, flash-frozen crystal of hHtrA2 S306A of size 0.35 × 0.45 × 0.2 mm. Data were indexed and integrated using software **X**-ray **D**etector **S**oftware (XDS) and were subsequently scaled using the software AIMLESS from the CCP4 suite [24].

MD simulation and analysis

The coordinates of the initial structure used in the present study are from the crystal structure of hHtrA2S306A (1LCY) [8] obtained from the protein data bank (PDB) [25]. The crystal structure (1LCY) has missing N-terminal residues (AVPSP) and two flexible regions (^{344}RGEKKNSSSGISGSQ^{358} and ^{282}ARDLGLPQT^{290}); therefore, we modeled and refined the missing loop regions using Prime 3.0 (Schrodinger, LLC, New York, 2011).

Accordingly, we created S276C on the same template for our further MDS studies. We subjected both the proteins, wt hHtrA2 and hHtrA2S276C), to molecular dynamics simulation (MDS) run for 10 ns each using GROMACS suite [26-28]. For each structure, all water molecules within 3.0 Å of a nitrogen or an oxygen atom were included in the search. All calculations were run under periodic boundary conditions using an orthorhombic (minimum distance between protein and cell faces was initially set to 10 Å) cell geometry.

Results

Determining oligomeric property of hHtrA2S276C

The crystal structure of catalytically inactive mutant (Ser306Ala) of hHtrA2 (PDB: 1LCY) demonstrates that Serine 276 is located near one of the residues involved in trimerisation (Phe 256), as shown in Supplementary Figure S1 [8]. To investigate whether S276C mutation affects the trimeric structure of the protein, we determined its apparent MW using native-PAGE, size exclusion chromatography (SEC) and DLS.

In the native-PAGE, comparison of mobility of both the bands (wt and mutant) with the standard markers depicted that the proteins are of equal MW (Figure 1A). However, native-PAGE separates proteins depending upon the charge they have and wt hHtrA2 bands displaced slightly down relative to wt hHtrA2. Furthermore, to validate the results of native-PAGE experiment, quantitative approaches have been used such as SEC and DLS. In SEC, both the wt and mutant hHtrA2 were eluted, and detected as single peaks at approximately 70 ml of elution volume (Figure 1B), similar oligomeric status for wt hHtrA2 has been observed previously [20], suggesting that the mutation does not affect the oligomeric property of hHtrA2 protein. Our DLS data also showed that mutation did not affect the overall conformation as the hydrodynamic radii of both wt hHtrA2 and hHtrA2S276C were found to be very similar [18]. Furthermore, DLS analysis also provided average polydispersity of 12.5% at 25°C for hHtrA2S276C indicating its homogeneity (Supplementary Figure S2).

Secondary structural organization and thermal stability of hHtrA2S276C protein

To investigate whether S276C mutation results in alteration in the overall secondary structural organization of the protein or its stability, far-UV CD spectroscopy was performed on purified wt and hHtrA2S276C as observed in Figure 1C. The recorded spectra that are typical for proteins with α-helical and β-stranded structure [20] overlap on each other suggesting no significant secondary structural changes have occurred upon mutation. To determine whether S276C mutation has affected thermal stability of hHtrA2, both wt and the mutant were subjected to thermal denaturation conditions between 20 and 85°C to obtain the melting temperature. Change in ellipticity at 208 nm as a function of temperature has been represented in Figure 1D, which show a T_m value of hHtrA2S276C to be 74°C, which is comparable to that of wt hHtrA2 as reported earlier [20]. The present study indicates that hHtrA2 retains its stability upon S276C mutation and it caused neither destabilizing nor stabilizing effect on the overall structure of protein.

Important L3 loop residues in hHtrA2 activity

To understand the importance of the serine residue at position 276 toward hHtrA2 activity, SDM was performed to replace it with a smaller and hydrophobic alanine residue. *In vitro* substrate cleavage assay using β-casein (both gel-based and fluorescence-based) showed no activity in hHtrA2S276A (Figure 2A,B), suggesting that the serine on loop L3 might be important for positively regulating the activity of the protease. Since both the mutants (hHtrA2S276C and S276A) were found to be inactive, we could not calculate the reaction rate of catalysis; however, we have presented the kinetic parameters for the wt hHtrA2 as shown in Supplementary Table S2, which is comparable to previous literature reports [20].

With an aim at understanding the importance of loop L3 (on which S276 is located) for protease activity, the residues of the loop were scanned and the conserved residues were identified. Among some of the previously identified residues, Arginine 280 was found to be highly conserved across species. Crystal structure of liganded and unliganded DegS and hHtrA1 [29,30] demonstrate that upon substrate binding, this conserved arginine residue interacts with residues in LD* leading to conformational changes at and around the active site making it more conducive for substrate binding. To understand the importance of this arginine residue in hHtrA2, we mutated it to alanine in wt hHtrA2 as well as in hHtrA2S276C (double mutant). The protease activity using substrate β-casein was monitored as a function of enzyme concentration. For all the concentrations of hHtrA2R280A and hHtrA2 (R280A, S276C), no activity was observed compared with wt hHtrA2 as shown in Figure 2C, suggesting that R280 is important for hHtrA2

Bioscience Reports (2018) **38** BSR20181072
https://doi.org/10.1042/BSR20181072

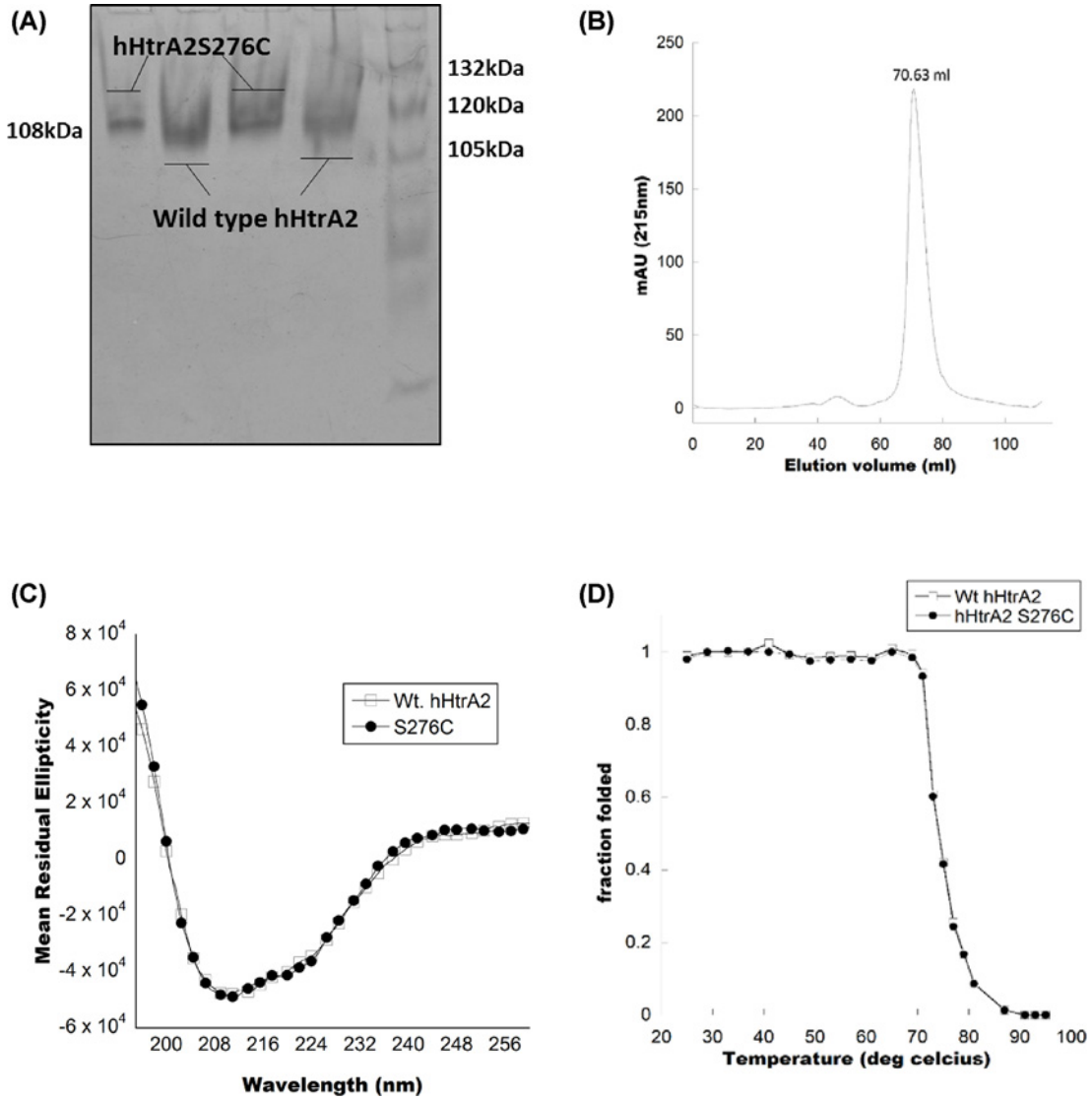

Figure 1. Effect of S276C mutation on the overall conformation of hHtrA2 protease

(**A**) A 7.5% native-PAGE resolving gel visualized by staining with coomassie brilliant blue shows similar band size for both the proteins. (**B**) SEC showing elution peak of hHtrA2S276C at approximately 70 ml that corresponds to approximately 108 kDa as described under 'Materials and methods' section. (**C**) CD analysis of hHtrA2S276C protein. The far-UV CD spectra of wt hHtrA2 and hHtrA2S276C between 195 and 260 nm show very similar secondary structural architecture. The plots are average of data obtained from experiments done in triplicate. (**D**) Thermal denaturation experiment of wt hHtrA2 and hHtrA2S276C using far-UV CD spectroscopy within the temperature range of 20–100°C.

activity, and the structural determinants on loop L3 that modulate HtrA activity might be overall conserved between DegS, hHtrA1, and hHtrA2.

X-ray crystallographic structure determination and refinement

Crystallization trials of hHtrA2S306A were carried out side-by-side along with hHtrA2S276C for structural comparison under similar crystallization conditions. Both the protein crystals were of good quality and diffraction data were collected to 2.05 Å resolution. The R_{merge} for hHtrA2S276C in the highest resolution shell was 74.8%, the mean (I) or sigma(I) and the completeness in the highest resolution shell were 2.0 and 99.6%, respectively; therefore, the data were processed to 2.05 Å resolution.

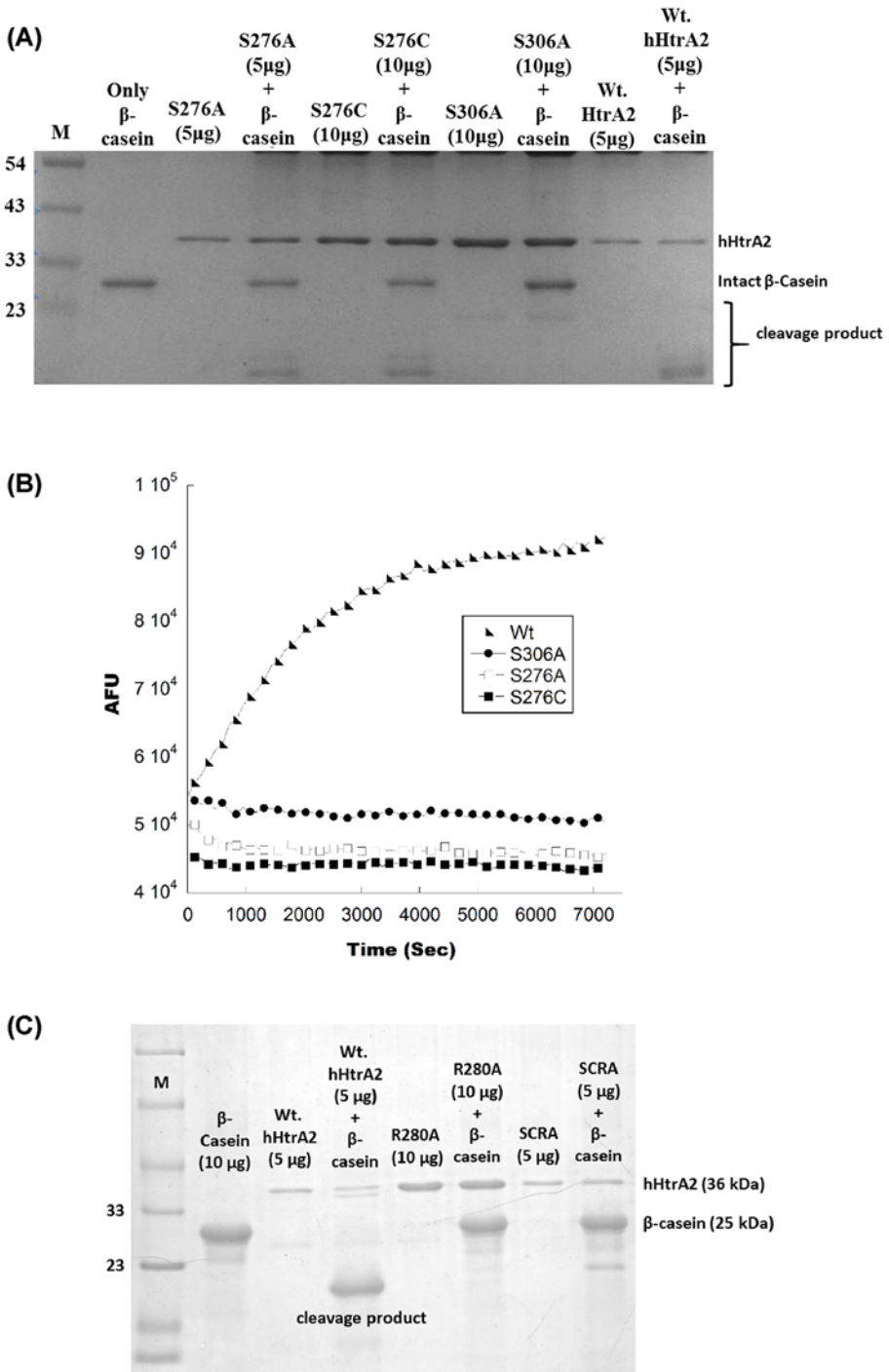

Figure 2. Effect of conserved L3 loop residues (S276 and R280) on protease activity

(**A**) A 12% SDS gel showing *in vitro* (gel based) β-casein (substrate) cleavage assay for hHtrA2S276A. (**B**) *In vitro* (fluorescence based) protease assay for hHtrA2S276A; here hHtrA2S306A (negative) and wt hHtrA2 (positive) are used as controls. (**C**) *In vitro* (gel based) β-casein cleavage assay for hHtrA2R280A. SCRA: S276C + R280A double mutant. Loss of activity was observed in hHtrA2S276A and hHtrA2R280A mutants at given enzyme concentrations.

Bioscience Reports (2018) **38** BSR20181072
https://doi.org/10.1042/BSR20181072

Table 1 Comparison of number of structural water molecules of crystal structures

PDB	Resolution (Å)	Space group	Total number of water molecules	Reference
1LCY	2.01	H3	301	Li et al., 2002 [8]
5WYN	2.05	H3	190	–
–	2.01	H3	305	

Processing of the diffraction data using XDS [31] showed that the crystal belonged to space group H3, with unit-cell parameters (in Å) $a = b = 84.38$, $c = 127.84$, $\alpha = \beta = 90^\circ$, and $\gamma = 120^\circ$. Calculation of the Matthews coefficient showed the presence of one molecule (considering the MW of 36 kDa) in the asymmetric unit, with a VM (Matthews, 1968) of 2.48 $Å^3Da^{-1}$ and a solvent content of 50.36%. Data were indexed and integrated using software XDS and were subsequently scaled using the software AIMLESS from the CCP4 suite [24]. Analysis of diffraction data revealed that the crystals were twinned with the twin law (h, -h-k, -l). Molecular replacement and phasing were carried out using Phenix software [32] with the coordinates of the inactive form of hHtrA2 (hHtrA2S306A) (PDB: 1LCY, Li et al., 2002) as the search model. A test set composed of 5% of the total reflections, assigned at random, was excluded from refinement to allow calculation of the free *R* factor. The final twinned R_{work} and R_{free} were found to be 15.72 and 18.82%, respectively. No density was obtained for a part of L3 loop (residues 281–291) as well as the hinge region that connects protease to PDZ domain (344–358) and therefore they have not been included in the final model. However, the S276C mutant residue is visible in the crystal structure. Supplementary Table S3 summarizes the data collection and refinement statistics for both the crystal structures.

Structural basis of inactivation of hHtrA2S276C mutant

In serine proteases, the formation of the catalytic triad in an arrangement sufficiently close for electron transfer from aspartate to serine through histidine is a prerequisite for formation of an active enzyme [3]. In mature hHtrA2 (PDB: 1LCY), catalytic triad comprises His198, Asp225, and Ser306 [8]. Structural comparison of both crystal structures 1LCY and 5WYN showed that hHtrA2S276C maintains proper hydrogen bonding distances in the active-site triad residues making it compatible for catalytic activity. For example, the atomic distances between the nitrogen (ε) atom of His198 and the oxygen (γ) of Ser306 has been found to be 3.2 Å and that between the nitrogen (δ) of His198 and the oxygen (δ) of Asp228 for this structure was 2.8 Å. However, presence of C276 in L3 loop might have adversely affected the activity of the protease due to significant reduction in the number of water molecules as observed (Figure 3A) in the crystal structures of the two proteins (hHtrA2S306A PDB: 1LCY and hHtrA2S276C PDB: 5WYN) (Table 1).

A careful inspection of water molecules in the X-ray structure of hHtrA2 (PDB: 1LCY) indicates that water (W) molecule number 377 forms an interaction between side chains of S276 and I270* (distance 4.1 Å) of the adjacent molecule (Figure 3B–D). However, in case of the mutant hHtrA2S276C, where highly hydrophobic cysteine residue (CH2-SH) replaces the serine, W377 is absent suggesting abrogation of this water-mediated interaction might have adversely affected its activity. To eliminate the possibility of this observation being an artifact (as a consequence of different crystallization conditions), active site mutant hHtrA2S306A was crystallized under identical crystallization conditions as hHtrA2S276C. Superimposition of the structures of hHtrA2S306A and 1LCY (277 Cα atoms with RMSD value of 0.242 Å) confirm that the same water molecule (W3777 in case of 1LCY) is present in the hHtrA2S306A as well with a stable b-factor (temperature factor) of 18.68 $Å^2$, thus highlighting its functional relevance (Figure 3E).

Characterization of water-mediated stability using MDS

To further validate the importance of W377 molecule in stabilizing the protease structure in the dynamic loop region, MDS was performed. The coordinates of the structures used were the crystal structure of hHtrA2S306A (PDB: 1LCY) [8] and modeled structure of S276C created on the same template for further MDS analysis for 10 ns. Upon analyzing the trajectories visually and using water-mediated hydrogen bonds with important residues, we observed that in case of hHtrA2S276C, there is no water-mediated hydrogen bonding with the cysteine residue (supplementary Figure S3A and supplementary Video S1A). On the other hand, in hHtrA2S306A, there is a stable water-mediated hydrogen bonding interaction with the serine residue (supplementary Figure S3B and supplementary Video S1B), thus reiterating the importance of the water molecule (W377) in its activity.

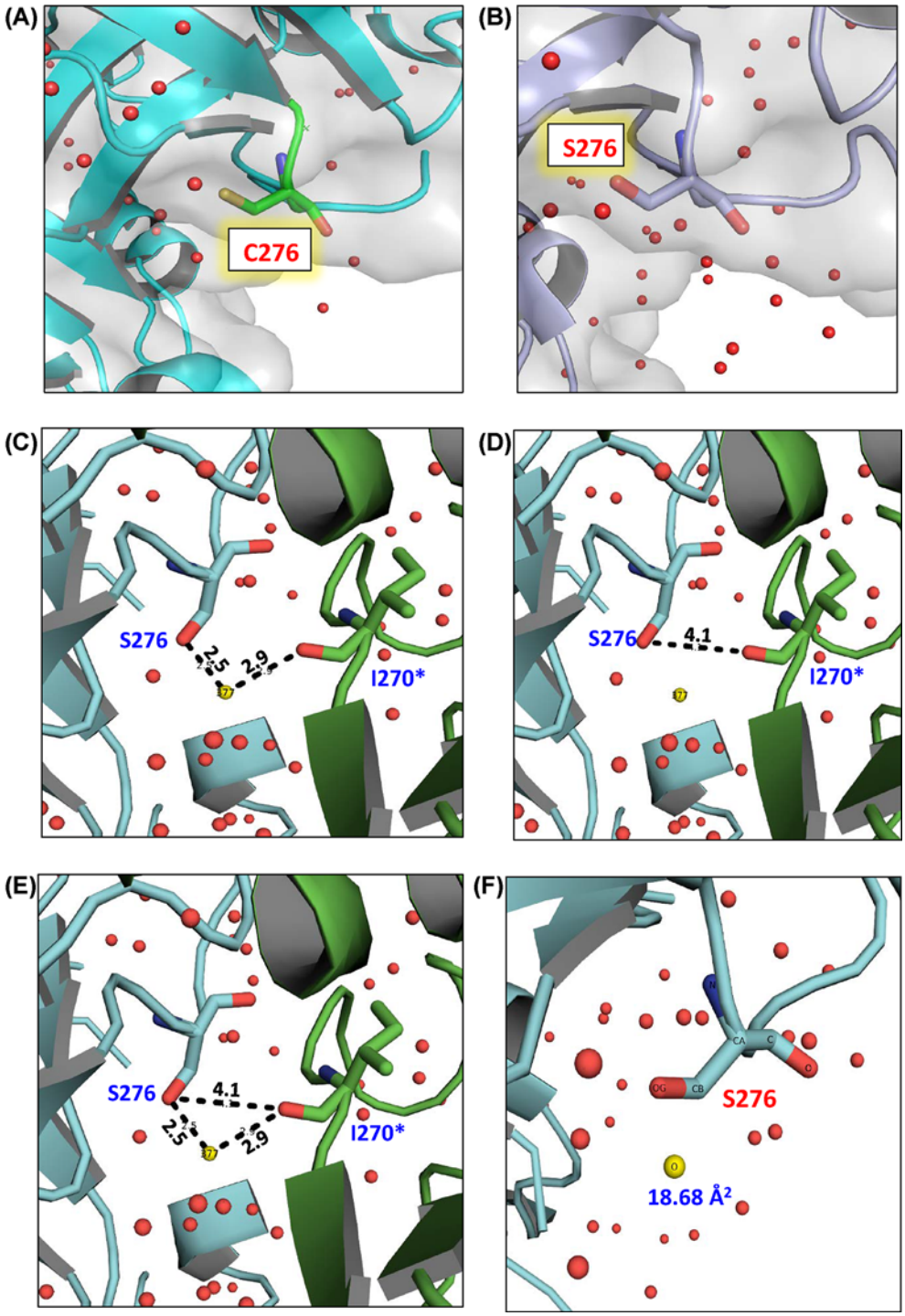

Figure 3. Monitoring water molecule and its interaction around cysteine 276 in hHtrA2S276C structure

(**A**) hHtrA2S276C in cyan (PDB: 5WYN) depicting significantly less water molecules around C276 (indicated in green; stick model) as compared with (**B**) hHtrA2S306A (PDB: 1LCY) crystal structure (light blue). (**C**) Water molecule (W377) involve in strong H2 bonding between S276 and I270*. (**D** and **E**) Atomic distance between –OH of serine and =CO (main chain) of I270* is 4.1 Å, which in presence of W377 is forming strong hydrogen bonds. Positions of the ordered water (solvent) molecules are shown as red crosses. W377 water molecule is shown by yellow non-bonded (nb) _spheres, (**F**) W377 molecule (yellow colored) with its b-factor.

Bioscience Reports (2018) **38** BSR20181072
https://doi.org/10.1042/BSR20181072

Discussion

The regulatory loops (mainly L3 and LD) that play critical roles in the transmission of allosteric signal and formation of activation cluster have been elaborately studied in DegS, HtrA1 and more recently in *E. coli* DegP proteases [33]. It has been found that subtle structural differences define their substrate specificity as well as their distinct mechanisms of activation, which in turn determine the explicit functions they perform within the cell. However, although the structure of hHtrA2 has been solved, intricate dissection of the loop regions with identification of critical residues involved in regulating its dynamic allosteric behavior is yet to be delineated.

Therefore, to understand the structural basis of inactivity in human counterpart (hHtrA2S276C) of mnd2 mouse mutant, high resolution crystal structure was solved followed by elucidation of its biophysical properties. Although, the mutant showed no overall secondary structural changes, conformational stability (T_m value ∼74°C) or conformational changes (RMSD: 0.244Å) compared with the wt, a significant reduction in the number of hydrating water molecules in the mutant was observed in the crystal structure. A close look at the structural water molecules in the X-ray structures of hHtrA2S306A (PDB: 1LCY) and hHtrA2S276C (PDB: 5WYN) show absence of a critical water molecule that mediates interaction between side chains of S276 and I270* [Water (W) molecule no. 377]. This observation was validated by solving structure of hHtrA2S306A under identical crystallization conditions as S276C mutant. It is well established that the contribution of water molecules to a protein's three dimensional structure is phenomenal. Hydration of protein structure is very important for maintaining its overall tertiary/quaternary structure [34] as well as its biological functions [35-37]. On the contrary, disturbance in the protein–water interactions has been found to be associated with unfavorable alterations in stability or dynamics of the protein [36,37]. Depending upon the nature of the amino acids, water molecules form a network of interaction with the side chains. Side chains of hydrophobic amino acids tend to repel water molecules thereby interfering with its biological activity by abolishing the water-mediated ionic interactions. Therefore, replacement of polar serine with a more hydrophobic cysteine residue [38] might have led to shielding of the surrounding region with respect to polar water molecules thus leading to abrogation of the water-mediated interaction in hHtrA2S276C.

Human HtrA2, along with 7 α-helices and 19 anti-parallel β-strands, comprises several long loop regions (LD, LA, L1, L2, and L3) [21] (Supplementary Table S4), which play an important role in regulation of its catalytic activity [3,9,39]. Upon substrate binding, conformational changes in the sensor loop L3 in several HtrA proteins have been identified that allows them to interact with residues from LD* followed by L1* leading to a coordinated relay of information from L3 to L1* via LD*. This series of events enables the active-site to switch to a 'proteolytically ON' state [3,9]. Using MDS, we have earlier demonstrated that in a catalytically active hHtrA2, regulatory loops (L1, LD, and L3) shift from disordered to an ordered state [9] during the process of activation. This corroborates with the current structural data that demonstrates a water-mediated H-2 bond between S276 on L3 and I270 from LD*, which might be an important component of this allosteric pathway. Similar mechanism of water-mediated conformational transition to a functional state has been demonstrated in hemoglobin that allosterically regulates binding of oxygen [40]. Using structural biology and functional enzymology studies, we have provided insight into the role of a critical water molecule in conformational selection in hHtrA2 protease. Overall, the crystallographic data helped in deciphering the structural basis of hHtrA2S276C inactivity and its mechanism of action.

Acknowledgments

We thank European Synchrotron Radiation Facility (ESRF) at Grenoble, France and Department of Atomic Energy (Government of India), RRCAT, India. We are also thankful to the PX-BL-21 beamline scientists Dr R. Makde, Dr B. Ghosh, and Mr A. Kumar from RRCAT, Indore for helping us collect the diffraction data. We acknowledge help from Dr Ashok Varma, ACTREC, Mr. Tushar Raskar, and Prof. MV Hosur for providing in-house facility and initial structure analysis. The authors thank Jitesh Doshi (for MDS study), Dr Lalith Chaganti, and Shubhankar Dutta (for their intellectual inputs and critical feedback on the manuscript).

Funding

The project is funded by grant from Department of Biotechnology (DBT), Government of India [grant number BT/PR10552/BRB/10/606/2008].

Competing interests

The authors declare that there are no competing interests associated with the manuscript.

Author contribution

A.W. performed the experiments, analyzed the data, and wrote the paper. K.B. conceptualized the idea, designed major part of the experiments, helped in data analysis and interpretation, and wrote the paper.

Abbreviations

CD, circular dichroism; DLS, dynamic light scattering; hHtrA2, human high temperature requirement protease A2; Htra, high temperature requirement factor A; IAP, inhibitor of apoptosis protein; MLS, mitochondrial localization signal; mnd2, motor neuron degeneration 2; PD, Parkinson's disease; PDB, protein data bank; PDZ, postsynaptic density protein (PSD95), Drosophila disc large tumor suppressor (Dlg1), and zonula occludens-1 protein (zo-1); SDM, site-directed mutagenesis; SEC, size exclusion chromatography.

References

1 Pallen, M.J. and Wren, B.W. (1997) The HtrA family of serine proteases. *Mol. Microbiol.* **26**, 209–221, https://doi.org/10.1046/j.1365-2958.1997.5601928.x
2 Clausen, T., Kaiser, M., Huber, R. and Ehrmann, M. (2011) HTRA proteases: regulated proteolysis in protein quality control. *Nat. Rev. Mol. Cell Biol.* **12**, 152–162, https://doi.org/10.1038/nrm3065
3 Clausen, T., Southan, C. and Ehrmann, M. (2002) The HtrA family of proteases: implications for protein composition and cell fate. *Mol. Cell* **10**, 443–455, https://doi.org/10.1016/S1097-2765(02)00658-5
4 Zurawa-Janicka, D., Skorko-Glonek, J. and Lipinska, B. (2010) HtrA proteins as targets in therapy of cancer and other diseases. *Expert Opin. Ther. Targets* **14**, 665–679, https://doi.org/10.1517/14728222.2010.487867
5 Suzuki, Y., Imai, Y., Nakayama, H., Takahashi, K., Takio, K. and Takahashi, R. (2001) A serine protease, HtrA2, is released from the mitochondria and interacts with XIAP, inducing cell death. *Mol. Cell* **8**, 613–621, https://doi.org/10.1016/S1097-2765(01)00341-0
6 Gray, C.W., Ward, R.V., Karran, E., Turconi, S., Rowles, A., Viglienghi, D. et al. (2000) Characterization of human HtrA2, a novel serine protease involved in the mammalian cellular stress response. *Eur. J. Biochem.* **267**, 5699–5710, https://doi.org/10.1046/j.1432-1327.2000.01589.x
7 Martins, L.M., Turk, B.E., Cowling, V., Borg, A., Jarrell, E.T., Cantley, L.C. et al. (2003) Binding specificity and regulation of the serine protease and PDZ domains of HtrA2/Omi. *J. Biol. Chem.* **278**, 49417–49427, https://doi.org/10.1074/jbc.M308659200
8 Li, W., Srinivasula, S.M., Chai, J., Li, P., Wu, J.W., Zhang, Z. et al. (2002) Structural insights into the pro-apoptotic function of mitochondrial serine protease HtrA2/Omi. *Nat. Struct. Biol.* **9**, 436–441, https://doi.org/10.1038/nsb795
9 Singh, N., D'Souza, A., Cholleti, A., Sastry, G.M. and Bose, K. (2014) Dual regulatory switch confers tighter control on HtrA2 proteolytic activity. *FEBS J.* **281**, 2456–2470, https://doi.org/10.1111/febs.12799
10 Jones, J.M., Datta, P., Srinivasula, S.M., Ji, W., Gupta, S., Zhang, Z. et al. (2003) Loss of Omi mitochondrial protease activity causes the neuromuscular disorder of mnd2 mutant mice. *Nature* **425**, 721–727, https://doi.org/10.1038/nature02052
11 Strauss, K.M., Martins, L.M., Plun-Favreau, H., Marx, F.P., Kautzmann, S., Berg, D. et al. (2005) Loss of function mutations in the gene encoding Omi/HtrA2 in Parkinson's disease. *Hum. Mol. Genet.* **14**, 2099–2111, https://doi.org/10.1093/hmg/ddi215
12 Kawamoto, Y., Kobayashi, Y., Suzuki, Y., Inoue, H., Tomimoto, H., Akiguchi, I. et al. (2008) Accumulation of HtrA2/Omi in neuronal and glial inclusions in brains with alpha-synucleinopathies. *J. Neuropathol. Exp. Neurol.* **67**, 984–993, https://doi.org/10.1097/NEN.0b013e31818809f4
13 Martins, L.M., Morrison, A., Klupsch, K., Fedele, V., Moisoi, N., Teismann, P. et al. (2004) Neuroprotective role of the reaper-related serine protease HtrA2/Omi revealed by targeted deletion in mice. *Mol. Cell. Biol.* **24**, 9848–9862, https://doi.org/10.1128/MCB.24.22.9848-9862.2004
14 Komatsu, M., Waguri, S., Chiba, T., Murata, S., Iwata, J., Tanida, I. et al. (2006) Loss of autophagy in the central nervous system causes neurodegeneration in mice. *Nature* **441**, 880–884, https://doi.org/10.1038/nature04723
15 Gupta, S., Singh, R., Datta, P., Zhang, Z., Orr, C., Lu, Z. et al. (2004) The C-terminal tail of presenilin regulates Omi/HtrA2 protease activity. *J. Biol. Chem.* **279**, 45844–45854, https://doi.org/10.1074/jbc.M404940200
16 Park, H.J., Kim, S.S., Seong, Y.M., Kim, K.H., Goo, H.G., Yoon, E.J. et al. (2006) Beta-amyloid precursor protein is a direct cleavage target of HtrA2 serine protease. Implications for the physiological function of HtrA2 in the mitochondria. *J. Biol. Chem.* **281**, 34277–34287, https://doi.org/10.1074/jbc.M603443200
17 Klionsky, D.J., Abeliovich, H., Agostinis, P., Agrawal, D.K., Aliev, G., Askew, D.S. et al. (2008) Guidelines for the use and interpretation of assays for monitoring autophagy in higher eukaryotes. *Autophagy* **4**, 151–175, https://doi.org/10.4161/auto.5338
18 Zurawa-Janicka, D., Jarzab, M., Polit, A., Skorko-Glonek, J., Lesner, A., Gitlin, A. et al. (2013) Temperature-induced changes of HtrA2 (Omi) protease activity and structure. *Cell Stress Chaperones* **18**, 35–51, https://doi.org/10.1007/s12192-012-0355-1
19 Bejugam, P.R., Kuppili, R.R., Singh, N., Gadewal, N., Chaganti, L.K., Sastry, G.M. et al. (2013) Allosteric regulation of serine protease HtrA2 through novel non-canonical substrate binding pocket. *PLoS ONE* **8**, e55416, https://doi.org/10.1371/journal.pone.0055416
20 Chaganti, L.K., Kuppili, R.R. and Bose, K. (2013) Intricate structural coordination and domain plasticity regulate activity of serine protease HtrA2. *FASEB J.* **27**, 3054–3066, https://doi.org/10.1096/fj.13-227256
21 Singh, N., Kuppili, R.R. and Bose, K. (2011) The structural basis of mode of activation and functional diversity: a case study with HtrA family of serine proteases. *Arch. Biochem. Biophys.* **516**, 85–96, https://doi.org/10.1016/j.abb.2011.10.007
22 Kelly, S.M., Jess, T.J. and Price, N.C. (2005) How to study proteins by circular dichroism. *Biochim. Biophys. Acta* **1751**, 119–139, https://doi.org/10.1016/j.bbapap.2005.06.005

23 Kumar, A., Ghosh, B., Poswal, H.K., Pandey, K.K., Jagannath, Hosur MV et al. (2016) Protein crystallography beamline (PX-BL21) at Indus-2 synchrotron. *J. Synchrotron Radiat.* **23**, 629–634, https://doi.org/10.1107/S160057751600076X
24 Winn, M.D., Ballard, C.C., Cowtan, K.D., Dodson, E.J., Emsley, P., Evans, P.R. et al. (2011) Overview of the CCP4 suite and current developments. *Acta Crystallogr. D Biol. Crystallogr.* **67**, 235–242, https://doi.org/10.1107/S0907444910045749
25 Berman, H.M., Battistuz, T., Bhat, T.N., Bluhm, W.F., Bourne, P.E., Burkhardt, K. et al. (2002) The Protein Data Bank. *Acta Crystallogr. D Biol. Crystallogr.* **58**, 899–907, https://doi.org/10.1107/S0907444902003451
26 Pronk, S., Pall, S., Schulz, R., Larsson, P., Bjelkmar, P., Apostolov, R. et al. (2013) GROMACS 4.5: a high-throughput and highly parallel open source molecular simulation toolkit. *Bioinformatics* **29**, 845–854, https://doi.org/10.1093/bioinformatics/btt055
27 Hess, B., Kutzner, C., van der Spoel, D. and Lindahl, E. (2008) GROMACS 4: algorithms for highly efficient, load-balanced, and scalable molecular simulation. *J. Chem. Theory Comput.* **4**, 435–447, https://doi.org/10.1021/ct700301q
28 Van Der Spoel, D., Lindahl, E., Hess, B., Groenhof, G., Mark, A.E. and Berendsen, H.J. (2005) GROMACS: fast, flexible, and free. *J. Comput. Chem.* **26**, 1701–1718, https://doi.org/10.1002/jcc.20291
29 Zeth, K. (2004) Structural analysis of DegS, a stress sensor of the bacterial periplasm. *FEBS Lett.* **569**, 351–358, https://doi.org/10.1016/j.febslet.2004.06.012
30 Eigenbrot, C., Ultsch, M., Lipari, M.T., Moran, P., Lin, S.J., Ganesan, R. et al. (2012) Structural and functional analysis of HtrA1 and its subdomains. *Structure* **20**, 1040–1050, https://doi.org/10.1016/j.str.2012.03.021
31 Kabsch, W. (2010) Xds. *Acta Crystallogr. D Biol. Crystallogr.* **66**, 125–132, https://doi.org/10.1107/S0907444909047337
32 Adams, P.D., Afonine, P.V., Bunkoczi, G., Chen, V.B., Echols, N., Headd, J.J. et al. (2011) The Phenix software for automated determination of macromolecular structures. *Methods* **55**, 94–106, https://doi.org/10.1016/j.ymeth.2011.07.005
33 Figaj, D., Gieldon, A., Bartczak, M., Koper, T., Zarzecka, U., Lesner, A. et al. (2016) The LD loop as an important structural element required for transmission of the allosteric signal in the HtrA (DegP) protease from Escherichia coli. *FEBS J.* **283**, 3471–3487, https://doi.org/10.1111/febs.13822
34 Privalov, P.L. and Crane-Robinson, C. (2017) Role of water in the formation of macromolecular structures. *Eur. Biophysics J.* **46**, 203–224, https://doi.org/10.1007/s00249-016-1161-y
35 Franks, F. (2002) Protein stability: the value of 'old literature'. *Biophys. Chem.* **96**, 117–127, https://doi.org/10.1016/S0301-4622(02)00014-5
36 Chaplin, M. (2006) Do we underestimate the importance of water in cell biology? *Nat. Rev. Mol. Cell Biol.* **7**, 861–866, https://doi.org/10.1038/nrm2021
37 Zhang, L., Wang, L., Kao, Y.T., Qiu, W., Yang, Y., Okobiah, O. et al. (2007) Mapping hydration dynamics around a protein surface. *Proc. Natl. Acad. Sci. U.S.A.* **104**, 18461–18466, https://doi.org/10.1073/pnas.0707647104
38 Nagano, N., Ota, M. and Nishikawa, K. (1999) Strong hydrophobic nature of cysteine residues in proteins. *FEBS Lett.* **458**, 69–71, https://doi.org/10.1016/S0014-5793(99)01122-9
39 de Regt, A.K., Kim, S., Sohn, J., Grant, R.A., Baker, T.A. and Sauer, R.T. (2015) A conserved activation cluster is required for allosteric communication in HtrA-family proteases. *Structure* **23**, 517–526, https://doi.org/10.1016/j.str.2015.01.012
40 Colombo, M.F., Rau, D.C. and Parsegian, V.A. (1992) Protein solvation in allosteric regulation: a water effect on hemoglobin. *Science* **256**, 655–659, https://doi.org/10.1126/science.1585178